

REGULATION OF TRAFFIC INTO AND OUT OF THE YEAST ENDOSOME
BY THE VPS9P CUE DOMAIN AND THE VPS5P PX DOMAIN

APPROVED BY SUPERVISORY COMMITTEE

Michael Roth, Ph.D.

Alfred Gilman, M.D., Ph.D.

Richard Anderson, Ph.D.

Bruce Horazdovsky, Ph.D.

Dedicated to my family and friends
for all of their support

REGULATION OF TRAFFIC INTO AND OUT OF THE YEAST ENDOSOME
BY THE VPS9P CUE DOMAIN AND THE VPS5P PX DOMAIN

by

Brian Andrew Davies

DISSERTATION

Presented to the Faculty of the Graduate School of Biomedical Sciences

The University of Texas Southwestern Medical Center at Dallas

In Partial Fulfillment of the Requirements

For the Degree of

DOCTOR OF PHILOSOPHY

The University of Texas Southwestern Medical Center at Dallas

Dallas, Texas

June, 2003

Acknowledgements

I would like to thank my committee members, Mike Roth, Al Gilman, Dick Anderson and Bruce Horazdovsky for their frank assessments and helpful suggestions. I would also like to thank my scientific collaborators including Gali Prag, James Hurley and other members of the Hurley Lab, Zhijian James Chen and Li Deng at UTSW, and Suk-Hoon Yoon for cloning *VPS5*; the members of the K3 and L3 hallways, too numerous to mention, for their assistance; Steve Nothwehr, Beverly Wendland and Claudio Joazeiro for helpful scientific exchanges; members of the Roth lab, especially Renee Tall; and the members of the Horazdovsky Lab that I have had the pleasure of working with over the past 8 years, with special consideration to Greg Tall and Hiroko Hama, Darren Carney, Imran Alibhai and Justin Topp, as well as Agnel Sfeir for her insights into Vps9p function, Andrew Friedberg, Pam Marshall, Kim Wong and Jeanne Fringer. In addition, Dave Katzmann's expertise as well as the help of the Guggenheim 16th floor crowd has been invaluable since the move to the Mayo Clinic. I almost forgot Mike Anderson, who almost became a part of the lab considering how often we ate at Anderson's. I would also like to thank my very scientifically minded family, the Davies clan, for both moral support, technical assistance (at times), as well as a heck of a lot of good times. I owe Bruce Horazdovsky a huge debt for allowing me to explore the yeast system and being patient with my circuitous path, and also for all of the incredible food.

REGULATION OF TRAFFIC INTO AND OUT OF THE YEAST ENDOSOME
BY THE VPS9P CUE DOMAIN AND THE VPS5P PX DOMAIN

Publication No. _____

Brian Andrew Davies, Ph.D.

The University of Texas Southwestern Medical Center at Dallas, 2003

Supervising Professor: Bruce Frank Horazdovsky Ph.D.

The presence of membrane bound compartments in eukaryotic cells enables the generation of discrete environments in which distinct and sometimes competing chemical reactions occur. The mammalian lysosome represents an example of this principle. The lysosome is an acidic, hydrolase-rich compartment that functions in macromolecular degradation. The delivery of material to the lysosome both from biosynthetic and endocytic pathways is a highly regulated process, and defects in the lysosomal trafficking system have been linked to congenital diseases including mucopolidosis type II (I-cell disease).

An analogous trafficking system functions in the fungi *Saccharomyces cerevisiae* to deliver biosynthetic and endocytic cargo to the yeast vacuole. Genetic and biochemical analyses

of the yeast vacuolar protein sorting pathway have defined the steps in this process and identified more than 40 gene products involved. Soluble vacuolar hydrolases are diverted from the secretory pathway through interaction with a vacuolar protein sorting receptor in the trans-Golgi compartment. This receptor then facilitates transport to the endosome where the biosynthetic and endocytic pathways coincide. The receptor is recycled back to the Golgi while the vacuolar hydrolases and endocytic material are conveyed to their ultimate destination. I have been interested in two aspects of this pathway in yeast, focusing on traffic into and out of the endosome.

The first question addressed is the identification of the cytosolic components that mediate receptor recycling (Chapters 2 and 3). The Sorting Nexin-1 homolog Vps5p is demonstrated to form a complex with Vps17p to mediate this process. Vps5p and Vps17p also interact with Vps26p, Vps29p and Vps35p and the lipid phosphatidylinositol-3-phosphate to recycle the receptor. The significance of these protein-protein interactions and the lipid-protein interaction in Vps5p function is examined.

The second question addressed is the regulation of traffic into the endosome by modulators of the guanine nucleotide exchange factor Vps9p (Chapters 4 and 5). Ubiquitin is identified as one such regulator, and the Vps9p CUE domain is demonstrated to be a new ubiquitin binding motif. The mechanism by which the CUE domain binds ubiquitin is addressed, and the functional relevance of Vps9p ubiquitin binding and ubiquitylation are examined *in vivo*.

Table of Contents

| | |
|--|-----------|
| Dedication | ii |
| Acknowledgements | iv |
| Table of Contents | vii |
| Publications | ix |
| List of Abbreviations | x |
| List of Tables, Figures and Appendices | xiii |
| | |
| Chapter 1. Introduction | 14 |
| Lysosomal Protein Transport | 14 |
| Vacuolar Protein Transport | 16 |
| Carboxypeptidase Y Sorting | 19 |
| Vacuolar Protein Sorting Receptor Recycling | 22 |
| Formation of the Multi-vesicular Body | 24 |
| Endocytosis | 26 |
| Research Aims | 28 |
| | |
| Chapter 2. The yeast Sorting Nexin-1 homolog, Vps5p, forms a complex with Vps17 and is required for recycling the vacuolar protein sorting receptor, Vps10p | 29 |
| Summary | 29 |
| Introduction | 30 |
| Materials and methods | 33 |
| Results | 41 |
| Discussion | 57 |
| | |
| Chapter 3. Characterization of the Vps5p PX domain function in vacuolar protein sorting receptor recycling | 62 |
| Summary | 62 |
| Introduction | 62 |
| Materials and methods | 67 |
| Results | 72 |
| Discussion | 82 |
| | |
| Preface to Chapters IV and V | 88 |
| | |
| Chapter 4. Vps9p CUE domain ubiquitin binding is required for efficient endocytic protein traffic | 89 |
| Summary | 89 |
| Introduction | 89 |
| Materials and methods | 92 |
| Results | 101 |
| Discussion | 112 |

| | |
|---|------------|
| Chapter 5. Structure-function analysis of the Vps9p CUE domain | 116 |
| Summary | 116 |
| Introduction | 117 |
| Materials and methods | 120 |
| Results | 126 |
| Discussion | 144 |
| Chapter 6. Discussion | 149 |
| Vacuolar protein sorting pathway | 149 |
| Role of the sorting nexins in Vps10p trafficking | 151 |
| Role of ubiquitin in Vps9p function | 154 |
| Bibliography | 160 |
| Vita | 181 |

Publications

Derived from this work:

Bruce F. Horazdovsky, Brian A. Davies, Matthew N.J. Seamen, Steve A. McLaughlin, Suk-Hoon Yoon, and Scott D. Emr. A Sorting Nexin-1 homologue, Vps5p, forms a complex with Vps17p and is required for recycling the vacuolar-protein sorting receptor. *Molecular Biology of the Cell*. 1997. 8:1529-41.

Brian A. Davies, Justin D. Topp, Agnel J. Sfeir, David J. Katzmman, Darren S. Carney, Gregory G. Tall, Andrew S. Friedberg, Li Deng, Zhijian Chen and Bruce F. Horazdovsky. Vps9p CUE domain ubiquitin binding is required for efficient endocytic protein traffic. *Journal of Biological Chemistry*. 2003. 278:19826-33.

Gali Prag, Saurav Misra, Eudora A. Jones, Rodolfo Ghirlando, Brian A. Davies, Bruce F. Horazdovsky, and James H. Hurley. Mechanism of ubiquitin recognition by the CUE domain of Vps9p. *Cell*. 2003. 113:609-20.

Previous publications:

Shai Shaham, Peter Reddien, Brian Davies, H. Robert Horvitz. Mutational analysis of the *C. elegans* cell-death gene *ced-3*. *Genetics*. 1999. 153:1655-71.

Susan E. Hamilton, Anne E. Pitts, Revathi R. Katipally, Xiaoyun Jia, Jared P. Rutter, Brian A. Davies, Jerry W. Shay, Woodring E. Wright, David R. Corey. Identification of determinants for inhibitor binding within the RNA active site of human telomerase using PNA scanning. *Biochemistry*. 1997. 36:11873-80.

List of Abbreviations

| | |
|----------------------|--|
| μg | microgram |
| 2μ | origin of $2\mu\text{m}$ circle, present in high copy plasmids |
| ALP | alkaline phosphatase |
| APE | <i>N</i> -acetyl-DL-phenylalanine β -naphthyl ester |
| API | aminopeptidase I |
| ATP | adenosine triphosphate |
| bp | basepair of DNA |
| BSA | bovine serum albumin |
| CBZ-pheleu | <i>N</i> -CBZ-L-phenylalanyl-L-leucine |
| CEN | centromeric origin of replication for yeast plasmids |
| CH ₃ COOK | potassium acetate |
| CN-Br | cyanogens bromide |
| CPS | carboxypeptidase S |
| CPY | carboxypeptidase Y |
| CPY-INV | carboxypeptidase Y-invertase fusion |
| CUE | coupling of ubiquitin to ER degradation domain |
| CVT | cytoplasm-to-vacuole |
| Da | Dalton (atomic mass) |
| dATP | deoxyadenosinetriphosphate |
| DMSO | dimethyl sulfoxide |
| DNA | deoxyribonucleic acid |
| DSP | dithio <i>bis</i> -succinimidylpropionate |
| DTT | dithiothreitol |
| E1 | ubiquitin activating enzyme |
| E2 | ubiquitin conjugating enzyme |
| E3 | ubiquitin protein ligase |
| EDTA | ethylenediamine-tetraacetic acid |
| EGF | epidermal growth factor |
| EGF-R | epidermal growth factor receptor |
| ER | endoplasmic reticulum |
| ESCRT | endosomal sorting complex required for transport |
| FM4-64 | vital dye for staining yeast vacuole |
| FYVE | specialized Zn ⁺² binding RING-finger, binds PtdIns(3)P |
| G418r | same as NEO |
| GAPs | GTPase activating protein |
| GDP | guanosine diphosphate |
| GEFs | GDP/GTP exchange factor |
| GFP | green fluorescent protein |
| GGA | Golgi localized, γ -ear-containing, ARF-binding |
| Glc | glucose |
| Grd | Golgi retention defective |
| GTP | guanosine triphosphate |

| | |
|-------------------|---|
| HA | Influenza Hemagglutinin |
| HECT | E3 ubiquitin ligase domain |
| His6 | hexahistidine tag |
| HRP | horseradish peroxidase |
| IPTG | isopropyl-b-D-thiogalactopyranoside |
| kb | kilobase of DNA |
| K_d | association constant |
| kDa | kilo Dalton (atomic mass) |
| LB | Luria Broth |
| LiOAc•TE | lithium acetate buffered TE |
| MBP | maltose binding protein |
| mCi | milliCurie |
| mCPY | mature carboxypeptidase Y |
| MgOAc | magnesium acetate |
| ml | millileter |
| mM | millimolar |
| MPR | mannose-6-phosphate receptor |
| NEM | <i>N</i> -ethylmaleimide |
| NEO | neomycin/kanamycin/G418 resistance |
| NMR | nuclear magnetic resonance |
| OD ₆₀₀ | optical density at 600nm |
| P100 | pellet from 1 hr, 100,000 x g centrifugation |
| P100 | pellet from 100,000 x g spin |
| P13 | pellet from 10 min, 13,000 x g centrifugation |
| p1CPY | ER/Golgi modified carboxypeptidase Y precursor |
| p2CPY | late-Golgi modified carboxypeptidase Y precursor |
| PCR | polymerase chain reaction |
| PDB | protein databank |
| Pep | peptidase defective |
| PMSF | phenylmethanesulfonyl fluoride |
| PrA | proteinases A |
| PtdIns(3)P | phosphatidylinositol-3-phosphate |
| PX | phox, or <u>NADPH</u> oxidase p40/47 similar domain |
| r.m.s.d. | root mean square deviation |
| RA | ras association domain |
| Rin | ras inhibitor |
| RING | E3 ubiquitin ligase domain |
| Rsp5p | HECT E3 ubiquitin ligase |
| S100 | supernatant from 1 hr, 100,000 x g centrifugation |
| S13 | supernatant from 10 min, 13,000 x g centrifugation |
| S5 | supernatant from 5 min, 500 x g centrifugation |
| SDS | sodium dodecyl sulfate |
| SDS-PAGE | sodium dodecyl sulfate-polyacrylamide gel electrophoresis |
| SeMet | selenium methionine |
| SH2 | Src homology domain 2 |
| SM | yeast synthetic media |

| | |
|-----------|--|
| SNARE | soluble NEM-sensitive factor attachment protein receptor |
| SNX | sorting nexin |
| Ste2p | α factor receptor |
| Ste3p | a factor receptor |
| TBS | Tris-buffered saline |
| TCA | trichloroacetic acid |
| Ub | ubiquitin/ubiquityl |
| UBA | ubiquitin associated domain |
| UBC | ubiquitin conjugating enzyme (E2) |
| Ubiquityl | protein-conjugated ubiquitin |
| UEV | ubiquitin E2 variant domain |
| UIM | ubiquitin interacting motif |
| Vam | vacuolar morphology |
| VPS | vacuolar protein sorting |
| Vpsl | vacuolar protein localization |
| Vpt | vacuolar protein transport |
| YNB | yeast nitrogen base |
| YPD | yeast extract, peptone, dextrose |
| YPF | yeast extract, peptone, fructose |
| Ypt | yeast protein; rab protein |

List of Figures, Tables

Figures

| | |
|---|-----|
| 1. Anterograde transport to the endosome | 19 |
| 2. Retrograde transport to the Golgi | 23 |
| 3. Vps5p is a member of the sorting nexin-1 subfamily | 42 |
| 4. Morphological analysis of wild-type, $\Delta vps5$ and $\Delta vps17$ cells | 45 |
| 5. Intracellular sorting of vacuolar hydrolases | 46 |
| 6. Subcellular fractionation of Vps10p | 48 |
| 7. Subcellular fractionation of the <i>VPS5</i> gene product | 51 |
| 8. Localization of Vps5p and Vps17p by Accudenz density gradient analysis | 53 |
| 9. Cross-linking Vps5p and Vps17p | 54 |
| 10. Vps5p native immunoprecipitation | 56 |
| 11. Vps5p and Vps17p function in retrograde traffic | 59 |
| 12. Density gradient flotation analysis of Vps5p, Vps10p and Vps17p | 73 |
| 13. Vps5p fractionation in $\Delta vps26$, $\Delta vps29$ and $\Delta vps35$ | 74 |
| 14. Crosslinking the Vps5p, Vps17p, Vps26p, Vps29p and Vps35p complex | 76 |
| 15. Characterization of Vps5 Δ PXp | 78 |
| 16. Analysis of Vps5 Δ PXp complex formation and fractionation | 80 |
| 17. Vps5p fractionation in $\Delta vps34$ and $vps34^{ts}$ under restrictive conditions | 81 |
| 18. Model of Vps5p, Vps17p, Vps26p, Vps29p and Vps35p coordinated function | 86 |
| 19. Analysis of the CUE domain | 101 |
| 20. Vps9p binds ubiquitin | 103 |
| 21. Vps9p CUE domain is not required for CPY sorting | 105 |
| 22. Vps9p CUE domain functions in endocytic traffic | 106 |
| 23. Vps9p ubiquitylation in vivo | 108 |
| 24. Vps9p ubiquitylation is dependent on Rsp5p | 110 |
| 25. Two mechanisms for ubiquitin regulation | 114 |
| 26. CUE domain is related to UBA domain | 127 |
| 27. Structure of the CUE Dimer:ubiquitin complex | 130 |
| 28. Dimerization of Vps9p in vitro and in vivo | 133 |
| 29. Functional analysis of the CUE dimer in vitro | 135 |
| 30. Functional analysis of the CUE dimer in vivo | 137 |
| 31. Vps9p ubiquitylation is increased in Class D <i>vps</i> mutants | 140 |
| 32. Lysine-arginine scanning of residues 328 to 451 | 143 |

Tables

| | |
|--------------------------------------|-----|
| 1. Mutation analysis of CUE function | 136 |
|--------------------------------------|-----|

Appendices

| | |
|---|-----|
| 1. Strains used in these studies | 157 |
| 2. Crystallographic data, phasing and refinement statistics | 158 |

Chapter 1. Introduction to the Vacuolar Protein Sorting Pathway

One of the defining characteristics of eukaryotic cells is the presence of organelles. These membrane bound compartments allow the generation of discrete microenvironments where distinct and sometimes competing chemical reactions occur. The maintenance of these organelles is essential for cellular homeostasis. Elaborate transport systems serve to populate the compartments with the unique repertoire of proteins required to generate the particular environment. In some cases, these transport systems involve direct import of proteins into the target organelle. In other systems, proteins are first segregated into a membrane-bound structure, and specific inter-compartment trafficking events deliver the cargo to its final destination. The primary example of this second mode is the translocation of proteins into the endoplasmic reticulum and subsequent trafficking through the secretory pathway. The secretory pathway is responsible both for the delivery of material to the plasma membrane and the population of intracellular compartments including the lysosome.

Lysosomal Protein Transport

The lysosome is an acidic compartment involved in macromolecular degradation; as such, the compartment is enriched in hydrolases involved in both protein and lipid turnover (reviewed in (Kornfeld and Mellman 1989)). Defects in lysosome function result in congenital diseases progressive in nature and characterized by skeletal, neurological and muscular defects. These diseases can result from mutations in particular lysosomal hydrolases, such as defects in β -hexosaminidase in Tay-Sachs disease

(reviewed in (Gravel, M.K. et al. 2001)), or abnormal trafficking of lysosomal substrates, as implicated in Niemann-Pick type C disease and mucopolipidosis type IV (reviewed in (Bach 2001; Patterson, Vanier et al. 2001)). A defect in the biosynthetic transport of soluble hydrolases also leads to the lysosomal storage diseases pseudo-Hurler polydystrophy (mucopolipidosis type III) and the more severe I-cell disease (mucopolipidosis type II); in both cases, generation of the mannose-6-phosphate lysosomal sorting signal is affected (reviewed in (Kornfeld and Sly 2001)).

Sorting of soluble hydrolases to the lysosome is mediated by a mannose-6-phosphate-dependent diversion from the late secretory pathway (reviewed in (Kornfeld and Mellman 1989)). The enzymes are initially translocated into the ER and undergo glycosylation with high-mannose oligosaccharides. During transport through the Golgi complex, these glycosylations are trimmed and modified. Lysosomal proteins are specifically recognized (via tertiary structure determinants) and modified by the UDP-*N*-acetylglucosamine:lysosomal enzyme *N*-acetylglucosaminyl-1-phosphotransferase (phosphotransferase activity is defective in I-cell disease); subsequent removal of the *N*-acetylglucosamine residue by *N*-acetylglucosamine 1-phosphodiester-*N*-acetylglucosaminidase leaves the protein-conjugated mannose phosphorylated. In the trans-Golgi compartment, this mannose-6-phosphate moiety is recognized by a type I transmembrane protein of either 270 kDa (cation independent-mannose-6-phosphate receptor) or 46 kDa (cation dependent-MPR) (reviewed in (Kornfeld 1992; Ghosh, Dahms et al. 2003)). The MPR is then packaged into clathrin-coated vesicles through interactions between the cytoplasmic tail and the Golgi-localized, γ -ear-containing, ARF-binding (GGA) proteins (Zhu, Doray et al. 2001; Doray, Bruns et al. 2002; Doray, Ghosh

et al. 2002), and these vesicles are transported to the endosome. Upon fusion with the endosome, the lysosomal cargo dissociates from the receptor and is transported on to its final destination through an endosomal maturation process. The MPR is recycled back to the trans-Golgi network to repeat this sorting event or is transported to the plasma membrane to scavenge proteins for endocytosis (reviewed in (Ghosh, Dahms et al. 2003)). Although the basic paradigm for this transport pathway was established in mammalian systems, elucidation of the cytosolic components responsible for mediating this process have been identified primarily in the yeast *Saccharomyces cerevisiae*.

Vacuolar Protein Transport

The yeast vacuole is an acidic compartment involved in macromolecular degradation as well as osmoregulation, amino acid storage, and pH and ion homeostasis; thus, the vacuole is considered the functional equivalent of the mammalian lysosome (reviewed in (Klionsky, Herman et al. 1990)). The vacuole contains a wide array of hydrolases, and genetics and biochemistry have proved useful in dissecting the pathways transporting proteins to this compartment. The predominant pathway for transport of soluble vacuolar hydrolases, including carboxypeptidase Y (CPY) and proteinases A (PrA), is similar to the lysosomal transport process described above and will be discussed in detail. However, alternative systems have been identified including the cytoplasm-to-vacuole targeting (CVT) pathway by which aminopeptidase I (API) is transported (reviewed in (Kim and Klionsky 2000)); briefly, API precursors form oligomers in the cytosol that sequester membrane to form an autophagic-like CVT vesicle, which then

fuses with the vacuole. Pathways mediating the transport of transmembrane zymogens have also been elucidated and will be discussed.

The initial screens for mutants defective in vacuolar proteolytic activity were conducted by Elizabeth Jones, utilizing the CPY substrate *N*-acetyl-DL-phenylalanine β -naphthyl ester (APE) (Jones 1977). Wild-type yeast were mutagenized, and an overlay assay with APE and Fast Garnet ABC was used to identify colonies with reduced CPY or peptidase (*pep*) activity. Tom Stevens developed a genetic selection based on a similar principle (Rothman and Stevens 1986). CPY can cleave the N-blocked dipeptide N-CBZ-L-phenylalanyl-L-leucine (CBZ-pheleu), liberating leucine; however activation of CPY is dependent upon PrA unless CPY is secreted. Therefore, leucine auxotrophs lacking PrA (*leu2 pep4*) can grow on CBZ-pheleu media only if CPY is missorted. The vacuolar protein localization (*vpl*) mutants were selected by plating mutagenized *leu2 pep4* cells on CBZ-pheleu media. At about the same time, Scott Emr utilized a CPY-invertase fusion to isolate the vacuolar protein targeting (*vpt*) mutants (Bankaitis, Johnson et al. 1986). Invertase is normally secreted into the periplasm to permit sucrose catabolism; however, fusion with CPY mislocalizes invertase to the vacuole and blocks sucrose utilization. Yeast harboring this CPY-Invertase fusion were plated on sucrose media in the presense of antimycin A (to block respiration) to select for yeast missorting the CPY trafficking reporter. From the combination of these 3 genetic approaches and additional screens, thousands of *pep*, *vpl* and *vpt* mutants defective in CPY trafficking were isolated and have been assigned to more than 50 vacuolar protein sorting (*vps*) complementation groups (Jones 1977; Jones 1984; Bankaitis, Johnson et al. 1986; Rothman and Stevens 1986; Robinson, Klionsky et al. 1988; Rothman, Howald et al.

1989; Raymond, Howald-Stevenson et al. 1992). With the completion of the yeast genome and the development of the yeast knockout collection, high throughput screens for mutants defective in CPY sorting have suggested 93 additional genes involved in this process (Bonangelino, Chavez et al. 2002). The large number of genetic loci identified by these methods indicates the complexity of the vacuolar protein sorting pathway.

To gain insight into the functional relationships between these *vps* genes, two additional phenotypes were examined: 1.) vacuolar morphology, and 2.) sorting of other vacuolar enzymes (Banta, Robinson et al. 1988; Raymond, Howald-Stevenson et al. 1992). The analysis of vacuolar morphology has proved extremely valuable for grouping the *vps* loci. In wild-type cells, the vacuole is apparent as 1-3 circular structures when examined by staining with fluorescent dyes or vacuolar-ATPase immunofluorescence. The Class A mutants exhibit wild-type vacuolar morphology and include *vps10*, *vps13*, *vps29*, *vps30*, *vps35*, *vps38*. The Class B mutants exhibit a fragmented vacuole phenotype; interestingly, the phenotypes of *vps5* and *vps17* appear slightly distinct from *vps39*, *vps41* and *vps43*. The Class C mutants (*vps11*, *vps16*, *vps18*, *vps33*) lack a coherent vacuolar structure; by contrast, the Class D mutants (*vps3*, *vps6*, *vps8*, *vps9*, *vps15*, *vps19*, *vps21*, *vps34*, *vps45*) exhibit an enlarged vacuole. In class E mutants (*vps2*, *vps4*, *vps20*, *vps22*, *vps23*, *vps24*, *vps25*, *vps27*, *vps28*, *vps31*, *vps31*, *vps36*, *vps37*, *vps44*), the vacuole appears normal; however, a perivacuolar compartment is also apparent. The Class F mutants (*vps1*, *vps26*) appear to be an intermediate between wild-type and the Class B phenotype. Many of these morphological classes correlate with differential protease sorting phenotypes and the determined site of function, as described below.

CPY Sorting

Carboxypeptidase Y transits the early secretory pathway through the Golgi complex (Stevens, Esmon et al. 1982). In a late Golgi compartment, CPY interacts with a type I transmembrane protein, Vps10p (Class A; Figure 1) (Vida, Hoyer et al. 1993; Marcusson, Horazdovsky et al. 1994). This interaction is analogous to the interaction between mannose-6-phosphate modified lysosomal proteins and the MPR; however, the CPY sorting determinant is a peptide sequence rather than a glycosylation (Johnson, Bankaitis et al. 1987; Valls, Hunter et al. 1987; Valls, Winther et al. 1990). There are 2 redundant GGA proteins (Gga1p, Gga2p) in yeast and both are capable of functioning

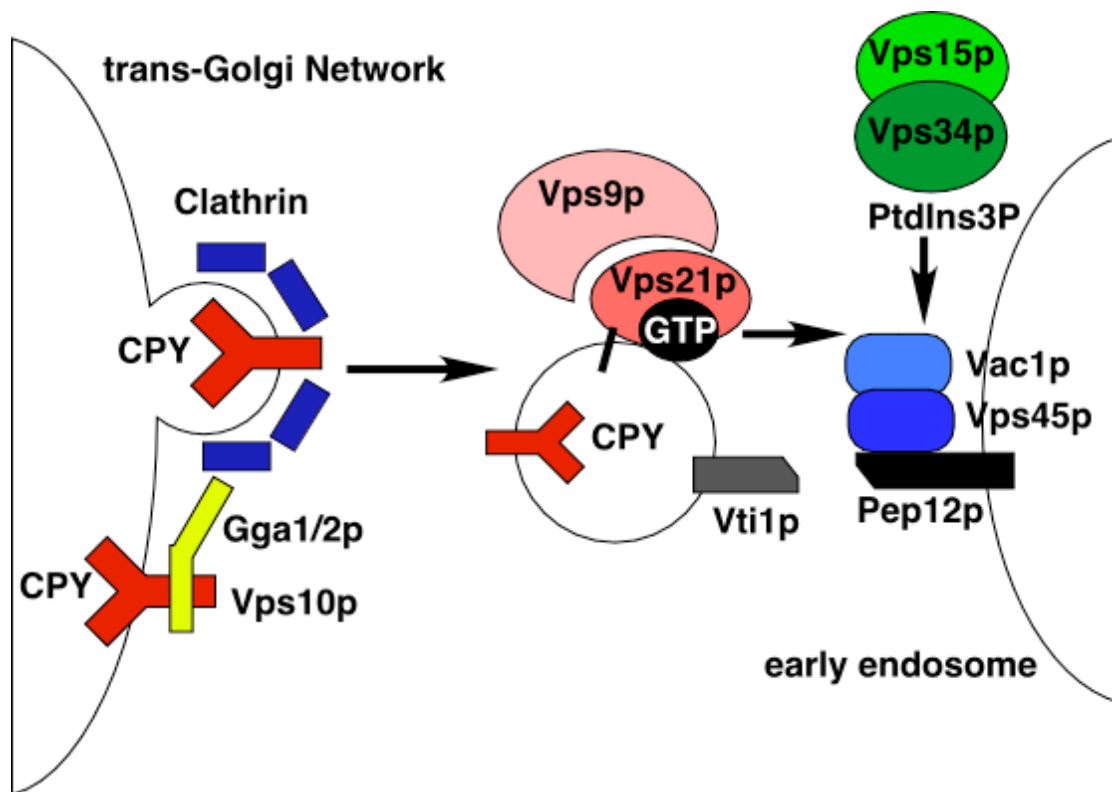


Figure 1. Anterograde transport to the endosome. CPY is recognized by Vps10p and sorted into clathrin-coated vesicles. Fusion with the early endosome is mediated by the Class D proteins. Vps9p activates the rab Vps21p. Vac1p coordinates signals from both Vps21p and PtdIns3P to modulate SNARE complex formation.

with the Vps10p cytoplasmic tail (Hirst, Lui et al. 2000). GGA proteins interact with both clathrin and GTP-bound arf proteins to package Vps10p into clathrin-coated vesicles (Seeger and Payne 1992; Deloche, Yeung et al. 2001; Deloche and Schekman 2002). Two observations suggest that the dynamin family protein Vps1p (Class F) may facilitate this budding process: 1.) dynamin proteins have been implicated in vesicle budding and membrane fission events (van der Bliek and Meyerowitz 1991; Vater, Raymond et al. 1992), and 2.) Vps10p is diverted into the secretory pathway and transported to the plasma membrane in *vps1* mutants (Nothwehr, Conibear et al. 1995).

In wild-type yeast, the trans-Golgi network-derived clathrin-coated vesicle is targeted, docked and fused with the early endosomal compartment through the combined activities of the Class D gene products (Figure 1). The central components in this process are the rab protein Vps21p and the SNARE¹ proteins Pep12p/Vps6p and Vti1p. Vps21p can bind either GDP or GTP, and the state of bound nucleotide determines activation (Horazdovsky, Busch et al. 1994). Vps9p is the guanine nucleotide exchange factor that generates the active GTP-bound Vps21p (Burd, Mustol et al. 1996; Hama, Tall et al. 1999). [Regulation of Vps9p will be examined in Chapters 4 and 5.] GTP•Vps21p interacts with Vac1p/Vps19p in a nucleotide dependent manner, and this interaction is expected to modulate the Vac1p binding partner Vps45p (Peterson, Burd et al. 1999; Tall, Hama et al. 1999). Vps45p is a member of the Sec1p family, which have been implicated as regulators of SNARE complex formation (Cowles, Emr et al. 1994; Piper, Whitters et al. 1994); in this system, Vps45p binds the syntaxin homolog Pep12p (Burd, Peterson et al. 1997). Thus, Vps9p activates Vps21p, which modulates the SNARE regulators Vac1p

¹ soluble N-ethylmaleimide-sensitive factor (NSF) attachment protein receptors

and Vps45p to facilitate formation of the Pep12p, Vti1p-containing SNARE complex. Formation of the SNARE complex is believed to drive the membranes into sufficient proximity to allow membrane fusion (reviewed in (Chen and Scheller 2001)). This SNARE complex formation is also regulated by phosphatidylinositol-3-phosphate [PtdIns(3)P]. Vps15p (serine/threonine kinase) and Vps34p (PtdIns 3-kinase) form a complex that generates PtdIns(3)P, and Vac1p binds PtdIns(3)P via the FYVE domain (Peterson, Burd et al. 1999; Tall, Hama et al. 1999). Thus, Vac1p appears to integrate signals from both Vps15p•Vps34p via PtdIns(3)P and Vps9p via Vps21p to modulate SNARE complex formation. Vps8p possesses a RING finger Zn⁺² binding motif (Chen and Stevens 1996; Horazdovsky, Cowles et al. 1996) and exhibits E3 ubiquitin ligase activity (Andrew Friedberg, Bruce Horazdovsky, unpublished results); in addition, Vps8p positively regulates Vps21p function, but the mechanism of Vps8p action is unclear (Andrew Friedberg, Pamela Marshall, Bruce Horazdovsky, unpublished results). Vps3p may form a scaffold based on its size (117 kDa) (Raymond, O'Hara et al. 1990). Together, these nine Class D gene products along with Vti1p² deliver Vps10p and CPY into the endosome (von Mollard, Nothwehr et al. 1997).

In the endosome, the reduced pH, possibly generated by the Na/H exchange protein Nhx1p/Vps44p (Class E) (Nass and Rao 1998; Bowers, Levi et al. 2000), is thought to facilitate dissociation of the Vps10p•CPY complex. CPY then continues on to the vacuole through an endosomal maturation process involving the Class E *VPS* gene products (formation of multivesicular bodies, discussed below). The late endosome then fuses with the vacuole via the action of the Class C (Vps11p, Vps16p, Vps18p, Vps33p)

² Vti1p is also involved in transport through the Golgi complex and is essential for viability, explaining the absence of *vti1* in the *vps* screens.

and a subset of Class B gene products (Vps39p, Vps41p, Vps43p, Ypt7p). The rab protein is Ypt7 (Wichmann, Hengst et al. 1992) and is activated by a guanine nucleotide exchange factor complex of Vps39p and Vps41p (Wurmser, Sato et al. 2000). Vps33p is a Sec1p family member and forms a protein complex with Vps11p, Vps16p, and Vps18p (the Class C complex) (Rieder and Emr 1997). This Class C complex also binds to Vps39p•Vps41p, forming the homotypic fusion and vacuolar protein sorting (HOPS) complex (Seals, Eitzen et al. 2000; Wurmser, Sato et al. 2000). This HOPS complex interacts with GTP•Ypt7p and with vacuolar SNARE proteins including Vam3p and Vam7p; these interactions facilitate endosome-vacuole fusion (as well as vacuole-vacuole fusion) and deliver CPY to its destination (reviewed in (Wickner and Haas 2000)).

Vps10p Recycling

While CPY is transported on to the vacuole, Vps10p (Class A) is transported back from the early endosome to the trans-Golgi complex to repeat this sorting process (Figure 2). This is analogous to the retrieval of mammalian MPRs. Vps10p recycling is dependent on the cytoplasmic tail of Vps10p (Cereghino, Marcusson et al. 1995; Cooper and Stevens 1996) and on the Class A gene products (Vps13p, Vps29p, Vps30p, Vps35p, Vps38p), the Class B proteins Vps5p and Vps17p (Kohrer and Emr 1993; Horazdovsky, Davies et al. 1997; Nothwehr and Hinds 1997), and the Class F protein Vps26p. Analysis of this process is presented in Chapters 2 and 3. Vps29p and Vps35p form a complex which binds to Vps10p via Vps35p (Seaman, Marcusson et al. 1997; Seaman, McCaffery et al. 1998; Nothwehr, Bruinsma et al. 1999; Nothwehr, Ha et al. 2000). Vps29p•Vps35p interacts with Vps26p as well as with the sorting nexins Vps5p and

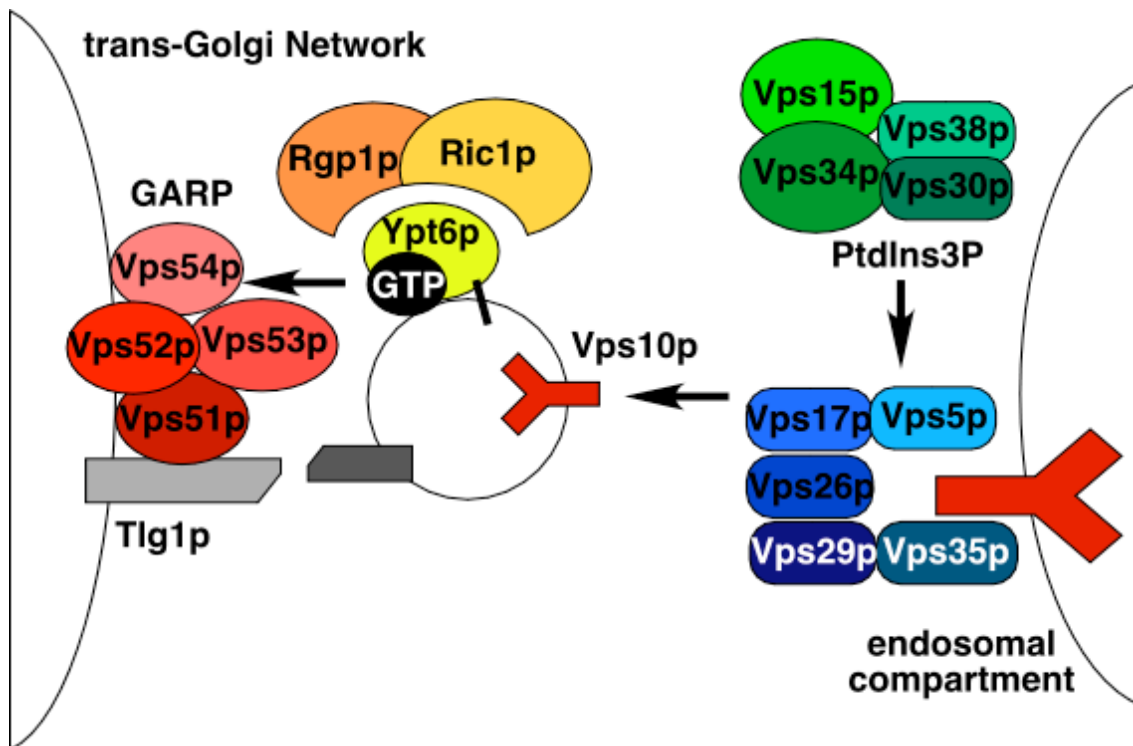


Figure 2. Retrograde transport to the Golgi. Vps10p recycling is mediated by a Class B and Class A VPS gene products. Vps5p and Vps17p are sorting nexins that integrate a PtdIns(3)P signal. Vps29p and Vps35p associate with the receptor tail. These 2 complexes are joined by Vps26p to mediate receptor recycling, although how these protein facilitate trafficking is unknown. Fusion with the trans-Golgi is mediated by interaction between the rab Ypt6p and the GARP complex. Ypt6p is activated by Ric1p and Rgp1p.

Vps17p to form a pentameric complex (Chapter 3, (Seaman, McCaffery et al. 1998)).

Vps30p and Vps38p form a distinct complex that interacts with the Vps15p•Vps34p PtdIns 3-kinase complex (Kihara, Noda et al. 2001; Burda, Padilla et al. 2002). Vps5p and Vps17p bind PtdIns(3)P via the PX domain, and this interaction is important for recycling (Chapter 3, (Burda, Padilla et al. 2002; Seaman and Williams 2002)). Thus, Vps30p•Vps38p appear to regulate Vps10p recycling via PtdIns(3)P and Vps5p•Vps17p. Vps13p/Soi1p is a large protein (357 kDa) that may act as a scaffold (Brickner and Fuller 1997). These 8 proteins seem to function together to mediate Vps10p recycling through vesicle budding; however, whether they do so as a coat protein or by another mechanism is unclear.

The retrograde vesicle then fuses back with the trans-Golgi network via interactions between Ypt6p, Vps51p, Vps52p, Vps53p, Vps54p, and Tlg1p. Ypt6 is the rab protein in this process (Bensen, Yeung et al. 2001; Luo and Gallwitz 2003) and is activated by the Ric1p•Rgp1p complex (Siniossoglou, Peak-Chew et al. 2000). Vps51p, Vps52p, Vps53p and Vps54p form the Golgi-associated retrograde protein (GARP) complex, which exhibits similarities to the late secretory pathway exocyst complex. GARP interacts both with the SNARE Tlg1p via Vps51p and with Ypt6p, suggesting that the complex forms a tethering function (Siniossoglou and Pelham 2001; Conibear, Cleck et al. 2003; Reggiori, Wang et al. 2003). Together, these components along with other unidentified proteins facilitate Vps10p recycling to the trans-Golgi compartment, and the CPY sorting process can be repeated.

Formation of the Multi-vesicular Body

Carboxypeptidase S (CPS) is another soluble vacuolar protease; however, CPS is transported to the vacuole as transmembrane precursor. This distinction requires an additional sorting process mediated by the Class E gene products for CPS to mature in the vacuole (reviewed in (Katzmann, Odorizzi et al. 2002)). CPS is initially transported through the secretory pathway as a type II transmembrane protein and is delivered to the early endosome by the Class D Vps proteins described above. During the endosomal maturation process, CPS is sorted into endosomal membrane invaginations that form the intra-organelle vesicles of the multivesicular body (Odorizzi, Babst et al. 1998). Defects in this sorting process retain CPS in the endosomal limiting membrane, initially, and in the vacuolar limiting membrane, eventually.

The sorting of CPS occurs by a ubiquitin dependent process. Ubiquitin is a small 76 amino acid protein conserved from yeast to man that is covalently attached through its carboxy-terminus to lysines of protein substrates (reviewed in (Weissman 2001)). This ubiquitylation is mediated by the concerted action of three activities: the ubiquitin activating enzyme (E1), the ubiquitin conjugating enzyme (E2) and the ubiquitin protein ligase (E3). The E1 (Uba1p) covalently binds ubiquitin and transfers the molecule to the E2 proteins (10-15 E2's in yeast); the E3 enzymes then bind to target molecules and either direct the transfer of ubiquitin from the E2 to the substrate, as in the RING motif E3 proteins, or serve as a covalent intermediary in the process, as in the HECT domain E3 proteins (reviewed in (Joazeiro and Weissman 2000; Rotin, Staub et al. 2000)). Lysine48 of a ubiquityl (protein conjugated ubiquitin) moiety can serve as the target in this reaction, leading to the formation of polyubiquitin chains; these polyubiquitin chains direct the substrate for degradation by the 26S proteasome. However, CPS modification is limited to mono-ubiquitylation. The monoubiquityl moiety serves a protein-protein interaction determinant. Several small domains have been identified as mediating recognition of ubiquitin, including the ubiquitin E2 variant (UEV; also referred to as UBC-like), the ubiquitin interaction motif (UIM) (Hofmann and Falquet 2001), the ubiquitin-associated domain (UBA) (Hofmann and Bucher 1996) and the coupling of ubiquitin-conjugation to ER degradation domain (CUE) (Ponting 2000) (reviewed in (Buchberger 2002)). Analysis of the CUE domain-ubiquitin interaction and its role in Vps9p function will be discussed in Chapters 4 and 5.

Mono-ubiquitylation of lysine8 of the CPS cytoplasmic domain serves to direct the protein into the multivesicular body (Katzmann, Babst et al. 2001). The initial

recognition event is dependent on the UIMs of Vps27p and Hse1p; an interaction between the Vps27p FYVE domain and PtdIns(3)P is also important for this process (Bilodeau, Urbanowski et al. 2002; Shih, Katzmann et al. 2002). Vps23p, Vps28p and Vps37p form the endosomal sorting complex required for transport-I (ESCRT I) (Katzmann, Babst et al. 2001). Vps27p interacts with ESCRT-I and recruits the complex to the site of action (David Katzmann, personal communication); this complex also interacts with ubiquitin via the Vps23p UEV domain (Katzmann, Babst et al. 2001). The ubiquitin1-CPS•ESCRT-I complex likely serves to recruit the Vps22p, Vps25p and Vps36p complex (ESCRT-II) (Babst, Katzmann et al. 2002). Membrane association of the ESCRT-III complexes, formed by Vps20p•Snf7p/Vps32p and Vps2p•Vps24p subcomplexes, is dependent on ESCRT-II (Babst, Katzmann et al. 2002). Thus, a four step process involving Vps27p and ESCRT-I, II and III serves to localize the Class E gene products to the maturing endosome for CPS sorting into multivesicular bodies; however, the mechanism by which these interactions generate the membrane invagination is unclear. Dissassembly of the complex appears to be required and is facilitated by the AAA-ATPase Vps4p (Babst, Sato et al. 1997; Babst, Wendland et al. 1998; Katzmann, Babst et al. 2001; Babst, Katzmann et al. 2002; Babst, Katzmann et al. 2002). Although the Class E mutants missort CPY, a role for ubiquitin in CPY and Vps10p trafficking has not been demonstrated.

Endocytosis

The trafficking of the yeast cell surface transmembrane receptors and small molecule transporters is regulated by ubiquitin at multiple steps in the endocytic process (reviewed in (Hicke 2001; Katzmann, Odorizzi et al. 2002)). In the case of the α -factor receptor Ste3p, this ubiquitylation and subsequent degradation in the vacuole is a constitutive process (Davis, Horecka et al. 1993; Roth and Davis 1996). By contrast, the α -factor receptor Ste2p, the uracil permease Fur4p, and the general amino acid permease Gap1p are subject to regulated endocytosis and degradation. In response to the presence of α -factor or changes in the nutritional environment, these plasma membrane proteins are ubiquitylated on one or multiple lysine residues, and this modification serves to target the protein for vacuolar degradation. Rsp5p has been implicated as the E3 protein responsible for the modification (reviewed in (Rotin, Staub et al. 2000)).

Components of the endocytic and vacuolar protein sorting machinery recognize the ubiquityl-moiety to mediate the sorting process. At the plasma membrane, UIM domains in the epsins Ent1p and Ent2p as well as the UBA domain in Ede1p act redundantly to mediate the internalization process through linking the plasma membrane proteins to AP2 and clathrin (reviewed in (Wendland 2002)). Subsequent fusion of these endocytic vesicles with the early endosome is facilitated by the interaction between ubiquitin and the CUE domain of Vps9p, as will be discussed in Chapters 4 and 5 (Davies, Topp et al. 2003; Donaldson, Yin et al. 2003). The endocytosed receptors and channel proteins then enter the multivesicular body in a process involving the Vps27p UIM and Vps23p UEV domains, as discussed for CPS. Thus, multiple components mediating the pathway to the vacuole are involved in this ubiquitin-dependent trafficking process.

Research Aims

The vacuolar protein sorting pathway is a complex process and mediates both the population of the compartment with the requisite hydrolases and the delivery of endocytosed material to the compartment for degradation. I have been interested in understanding two aspects of this process: 1.) the recycling of Vps10p from the endosome back to the trans-Golgi, and 2.) the regulation of endosome fusion involving Vps9p and ubiquitin.

The recycling of the vacuolar protein sorting receptor Vps10p from the endosome to the trans-Golgi compartment is dependent on the cytoplasmic tail of the receptor (Cereghino, Marcusson et al. 1995; Cooper and Stevens 1996). This observation suggested the existence of cytosolic components that mediate the retrograde transport pathway. To test this hypothesis and identify the components required in this process, I have undertaken characterization of Vps5p and the associated complex (Chapters 2 and 3).

The fusion of vesicles with the endosome is mediated through Vps21p activation by the guanine nucleotide exchange factor Vps9p; however, the catalytic domain of Vps9p accounts for only a third of the protein (Greg Tall, Darren Carney, Bruce Horazdovsky, manuscript in preparation). This observation suggested that other portions of the molecule serve to localize and regulate Vps9p activity. To test this hypothesis, I have examined the interaction between the Vps9p CUE domain and ubiquitin and its role in Vps9p function (Chapters 4 and 5).

Chapter 2. The yeast Sorting Nexin-1 homolog, Vps5p, forms a complex with Vps17p and is required for recycling the vacuolar protein-sorting receptor, Vps10p.

Summary.

Sorting of soluble proteases to the yeast vacuole is mediated by a system analogous to the mammalian lysosomal biosynthetic pathway. In both systems, inactive precursors are translocated into the endoplasmic reticulum, transported through the early stages of the secretory pathway, and diverted towards the vacuole/lysosome through interaction with a sorting receptor in a late Golgi compartment. Using genetic selections for yeast mutants defective in vacuolar trafficking, more than 40 loci have been implicated in mediating this vacuolar protein sorting (VPS) pathway. To identify the role of Vps5p in this process, the gene defective in *vps5* mutants was cloned by functional complementation. *VPS5* encodes a 76 kDa protein homologous to human sorting nexin 1 (hSNX1). Cells deficient for Vps5p exhibited anomalous vacuolar morphology and missorted a subset of soluble vacuolar proteases. These phenotypes were shared by another yeast sorting nexin, Vps17p. Vps5p and Vps17p co-localized to a VPS pathway compartment distinct from the endosome or Golgi, and the two sorting nexins were demonstrated to form a protein complex. Vps5p also associated with the vacuolar protein sorting receptor, Vps10p, and cells deficient for Vps5p mislocalized Vps10p to the vacuole. These results indicated that the yeast sorting nexins Vps5p and Vps17p function together to regulate Vps10p trafficking, analogous to hSNX1 regulation of epidermal growth factor receptor trafficking to the lysosome.

Introduction.

Intracellular organelles serve a vital function in generating discrete subcellular environments where distinct and sometime competing biochemical reactions occur. The generation and perpetuation of these environments is essential for eukaryotic cells to maintain cellular homeostasis. Specific transport pathways are used to populate organelles with the unique repertoire of enzymes and proteins required to generate the particular environments. One of the best characterized targeting systems is the lysosomal protein transport pathway (reviewed in (Kornfeld and Mellman 1989)). Lysosomes are acidic compartments involved in macromolecular turnover as well as the degradation of material brought into the cell by endocytosis. To accomplish these functions, the lysosome is populated with a large number of hydrolytic enzymes that would otherwise be toxic to the cell. The predominant system for transport of these hydrolases to the lysosome involves a late diversion in the secretory pathway. Soluble lysosomal enzymes, such as Cathepsin D, are synthesized as inactive zymogens and cotranslationally translocated into the endoplasmic reticulum (ER) to enter the secretory pathway. Prior to exit from the ER, the zymogens are modified by the addition of N-linked oligosaccharides. The proteins are then transported through the Golgi complex, wherein the core glycosylations are modified by the addition of mannose-6-phosphate. This mannose-6-phosphate serves as the lysosomal targeting epitope and is recognized by one of two mannose-6-phosphate receptors (MPR-I and II) in the trans-Golgi network (reviewed in (Kornfeld 1992; Ghosh, Dahms et al. 2003)). This interaction with the receptor allows the lysosomal cargo to be diverted from the secretory pathway and transported along with the receptor to an endosomal compartment via clathrin-coated

vesicles. The receptor and cargo then dissociate in the endosome, and the zymogen is transported on to the lysosome for proteolytic activation. The MPR is recycled back either to the TGN to repeat this sorting process or to the cell surface to scavenge for aberrantly transported lysosomal cargos. While this basic paradigm for lysosomal sorting has been well established, little was known about the cellular machinery regulating trafficking of the receptors.

Studies in *Saccharomyces cerevisiae* have provided insights into this process through examination of trafficking to the yeast vacuole. The vacuole is an acidic compartment involved in macromolecular degradation, osmoregulation, and pH and ion homeostasis; as such, the vacuole is considered the functional analog of the mammalian lysosome (reviewed in (Klionsky, Herman et al. 1990)). The biosynthetic delivery of soluble proteases to the vacuole is also largely analogous to the lysosomal sorting pathway. Soluble vacuolar proteases are transported as inactive zymogens through the early stages of the secretory pathway (Stevens, Esmon et al. 1982) until they reach a late Golgi compartment and are diverted toward the vacuole (Graham and Emr 1991; Vida, Huyer et al. 1993). In the lysosomal sorting pathway, the mannose-6-phosphate moiety specifies the cargo to be diverted; however, in the yeast system, the vacuolar localization determinant is a peptide sequence in the amino-terminus (Johnson, Bankaitis et al. 1987; Valls, Hunter et al. 1987; Valls, Winther et al. 1990). For carboxypeptidase Y (CPY), this 50 amino acid sorting signal is recognized by a specific receptor, Vps10p, in the trans-Golgi network (Marcusson, Horazdovsky et al. 1994), and the CPY-Vps10p complex is transported to an endosomal/prevacuolar compartment via clathrin-coated vesicles (Deloche, Yeung et al. 2001). The CPY precursor is then released and

transported on to the vacuole for proteolytic activation. The vacuolar protein sorting receptor, Vps10p, is transported back to the trans-Golgi network to repeat the sorting process (Cereghino, Marcusson et al. 1995; Cooper and Stevens 1996).

This initial understanding of the vacuolar protein sorting (VPS) pathway had been made possible by genetic selections for mutants missorting vacuolar cargos (Jones 1984; Bankaitis, Johnson et al. 1986; Rothman and Stevens 1986; Robinson, Klionsky et al. 1988; Rothman, Howald et al. 1989) and the subsequent characterization of the proteins affected in these mutants; however, there are still many *vps* mutants isolated from these genetic selections that are as yet uncharacterized. Complementation analyses assigned the thousands of isolated mutants to more than 40 genetic loci (Robinson, Klionsky et al. 1988; Raymond, Howald-Stevenson et al. 1992). Characterization of vacuolar morphology in these complementation groups divided these mutants into six distinct classes (A-F) (Banta, Robinson et al. 1988; Raymond, Howald-Stevenson et al. 1992). The Class B mutants are particularly interesting as they exhibit a fragmented vacuole phenotype with 10-20 small vacuole-like structures. This class can be further divided into mutants in which the structures are randomly distributed (*vps39*, *vps41*, *vps43*) and mutants (*vps5*, *vps17*) that retain clustering of the structures reminiscent of wild-type yeast (Raymond, Howald-Stevenson et al. 1992).

To gain insight into the function of Vps5p in the VPS pathway, the gene complementing the *vps5* mutant was cloned (Horazdovsky, Davies et al. 1997). *VPS5* encodes a highly charged, 76kDa protein that is peripherally associated with a novel vacuolar pathway compartment. Cells devoid of Vps5p ($\Delta vps5$) contain fragmented vacuolar structures as observed in the originally isolated mutants, missort a subset of

soluble vacuolar proteins, and alter trafficking of the vacuolar protein-sorting receptor, Vps10p. These phenotypes are also apparent in *vps17* mutant cells (Kohrer and Emr 1993). Vps5p and Vps17p are dependent on each other for membrane association, and Vps5p is demonstrated to physically interact with Vps17p and Vps10p. In addition, Vps5p exhibits sequence similarity to human sorting nexin-1 (SNX1), a protein implicated in regulating epidermal growth factor receptor (EGFR) trafficking (Kurten, Cadena et al. 1996). These results suggest that the yeast SNX1 homolog, Vps5p, functions in complex with Vps17p to maintain recycling of the CPY-sorting receptor through interacting with the receptor.

Materials and methods

Media and Reagents

Escherichia coli cells were grown in LB and M9 media supplemented with appropriate antibiotics and amino acid (Miller, Lee et al. 1999). *S. cerevisiae* was propagated in yeast extract-peptone-dextrose (YPD), yeast extract-peptone-fructose (YPF), or synthetic dextrose (SD) supplemented with amino acids as required (Sherman, Fink et al. 1979). The strains used in this study are listed in Appendix 1. Restriction and modifying enzymes were purchased from Boehringer Mannheim, New England Biolabs, and Stratagene. Zymolyase 100-T (Kirin Brewery Co.) was obtained from Seikagaku Kogyo Co. (Tokyo, Japan). DSP [dithiobis(succinimidylpropionate)] was purchased from Pierce. Glusulase was from DuPont Co. 5-Bromo-4-chloro-3-indoyl- β -D-galactoside, phenylmethylsulfonyl fluoride, α_2 -macroglobulin, aprotinin, leupeptin, pepstatin, and isopropyl- β -D-thiogalactopyranoside were acquired from Boehringer

Mannheim. Tran³⁵S-label was supplied by ICN Biochemicals. [α -³⁵S]dATP was provided by Amersham Corp. Production of antisera to vacuolar hydrolases (CPY, ALP, PrA) has been described previously (Klionsky, Banta et al. 1988; Klionsky and Emr 1989). All other reagents were purchased from Sigma.

Plasmid Constructions

Plasmid constructions were performed using previously described recombinant DNA manipulation methods (Sambrook, Fritsch et al. 1989). The glass bead method of Vogelstein and Gillespie was used for DNA fragment isolations (Vogelstein and Gillespie 1979). The *CEN*-based *VPS5* plasmid pBHY5-41 was generated by subcloning the 3.3 kb *SmaI-XhoI* fragment of library plasmid pBHY5-1 (containing *VPS5*) into the *SmaI* and *XhoI* sites of pPHYC18 (Herman and Emr 1990). The 2 micron-based plasmid pBHY5-43 was constructed by ligating the *SmaI-XhoI* fragment of pBHY5-1 into pJSY324 (Herman, Stack et al. 1991). Integrative mapping plasmid pBHY5-39 was made by inserting the *VPS5*-containing *SmaI-XhoI* fragment of pBHY5-1 into pRS304 (Sikorski and Hieter 1989). The *VPS5* deletion/disruption plasmid pBHY5-35 was made by subcloning the 2.3 kb *SmaI-SalI* fragment of pBHY5-1 into pBluescriptKS (Stratagene) and then replacing the 0.7 kb *XbaI-StuI* fragment of the resulting plasmid with the *HIS3* gene. For preparation of a *trpE*-Vps5 fusion protein, pBHY5-1 was digested with *EcoRI* yielding a 914 bp fragment which was purified and ligated into *EcoRI* digested pATH1 fusion vector (Dieckmann and Tzagoloff 1985) (containing *trpE* coding sequences) to generate pBHY5-40.

Nucleic Acid and Genetic Manipulations

Bacterial DNA transformations were accomplished using the method of Hanahan (Hanahan 1983) and yeast transformations employed a LiAc treatment protocol (Ito, Fukuda et al. 1983). All other standard yeast genetic procedures were performed as previously described (Guthrie and Fink 1991). pBHY11 (CPY-invertase::*LEU2*) (Horazdovsky, Busch et al. 1994) was integrated at the *leu2-3,122* locus of SEY5-7 to produce strain BHY156. Integrative mapping studies of cloned *VPS5* were initiated by linearizing pBHY5-39 with *StuI* and transforming BHY11 cells. Trp⁺ transformants (BHY155) were mated with BHY156. Diploid colonies were selected, sporulated, and 56 of the resulting asci were dissected. Trp⁺/Trp⁻ and Vps⁺/Vps⁻ phenotypes segregated 2:2, with all haploid segregants displaying Vps⁻ phenotype also being Trp⁻. Construction of *vps5* chromosomal deletion mutant was initiated by digesting pBHY5-35 with *SmaI* and *SalI*, to excise the $\Delta vps5::HIS3$ fragment. This fragment was used to transform SEY6210. His⁺ transformants were screened for secretion of p2CPY by colony blot (Roberts, Raymond et al. 1991). Genomic DNA was prepared from a His⁺ Vps⁻ isolate and the disruption of the *VPS5* locus was confirmed by PCR as previously described (Herman and Emr 1990).

Isolation of the *VPS5* Gene

A plasmid-based yeast genomic DNA library (*LEU2*, *CEN*; a gift from Philip Hieter) was used to transform SEY5-7 cells harboring a plasmid encoding a CPY-invertase fusion protein (Horazdovsky, Busch et al. 1994). Transformed cells were replica-plated to YPF media, incubated at 30°C overnight, then subjected to an assay

designed to detect extracellular invertase activity (Horazdovsky, Busch et al. 1994). Plasmids were isolated from Vps⁺ cells and used to transform SEY5-7 to confirm complementing activity. Isolated plasmids were digested and fragments containing genomic sequence were subcloned and tested for their ability to complement the SEY5-7 mutant phenotype for the purpose of identifying the minimum complementing DNA fragment. A 2.3 kb *SmaI/SalI* and a 3.4 kb *SacI/SacI* fragment from pBHY5-1 were cloned into the *E. coli* plasmid pBluescriptKS(-) to generate pBHY5-30 and pBHY5-31 respectively. Exonuclease III-mung bean nuclease deletions were constructed using these plasmids (pBHY5-30 and pBHY5-31) according to the pBluescript manual supplied by Stratagene, except nuclease digestion products were size fractionated and isolated from an 1% agarose preparative gel. Nested deletion constructs were identified and denatured plasmid DNA was purified over a 2 ml Sephacryl S-400 spun column using the procedure described in the Pharmacia Miniprep Kit Plus manual. The resultant denatured double stranded templates were hybridized to the T7 or T3 primers and subjected to dideoxy-chain termination sequence analysis using the Sequenase sequencing protocol (United States Biochemical Corp.). An open reading frame was uncovered that covered base pairs 453770-455795 of chromosome XV in the *S. cerevisiae* genome database.

Antiserum Preparation

Bacterial JM101 cells were transformed with *trpE-VPS5* gene fusion plasmid pBHY5-40. Induced production and purification of fusion protein followed the method of Kleid et al. (Kleid, Yansura et al. 1981), as modified by Herman and Emr (Herman and Emr 1990). Immunization of New Zealand white rabbits with fusion protein was

executed as previously described (Horazdovsky, Busch et al. 1994). CN-Br activated Sepharose (Pharmacia) was coupled to purified trpE-Vps5 fusion protein and used to affinity-purify harvested antiserum according to manufacturer's instructions. Eluted antiserum was screened and titrated by immunoprecipitation of labeled yeast cell extracts.

Cell Labeling and Immunoprecipitation

Yeast cells were grown in SD containing required amino acids to an OD₆₀₀ of 0.8. For experiments involving immunoprecipitation of vacuolar hydrolases, 5 OD₆₀₀ units of cells were harvested by centrifugation and suspended in 1 ml of SD medium containing 1mg/ml bovine serum albumin. Cells were preincubated for 10 minutes at 30°C; labeling was initiated via addition of 100 μ Ci Tran³⁵S-label and allowed to proceed for 10-15 minutes. Chase periods were then started by adding methionine, cysteine, and yeast extract to final concentrations of 5 mM, 1 mM and 0.2%, respectively. For experiments involving separation of pellet and media fractions, cells were converted to spheroplasts prior to cell labeling and chase periods (Vida, Graham et al. 1990; Paravicini, Horazdovsky et al. 1992). Following the labeling and chase cultures were then centrifuged at 13,000 x g for 1 minute to yield an intracellular (I) pellet fraction and an extracellular (E) media fraction. The presence of CPY, PrA, and ALP proteins in each fraction was determined by immunoprecipitation (Klionsky, Banta et al. 1988; Robinson, Klionsky et al. 1988).

Subcellular Fractionation and Gradient Analyses

SEY6210, KKY10 (*vps17Δ1*) or BHY152 (*vps5Δ1*) cells were propagated at 30°C to an OD₆₀₀ of 0.8 in SD supplemented with appropriate amino acids. 30 OD₆₀₀ units of cells were collected by centrifugation (2,000 x g for 5 minutes) and spheroplasts were generated as described previously (Vida, Graham et al. 1990; Paravicini, Horazdovsky et al. 1992). Cultures were incubated at 30°C for 10 minutes prior to addition of 1 mCi Tran³⁵S-label. Labeling proceeded for 15 minutes at 30°C and was followed by a chase period of 45 minutes. Spheroplasts were harvested and lysed by douncing six times using a tissue homogenizer in buffer containing 200mM sorbitol, 50mM Tris (pH 7.5), 1mM EDTA and a protease inhibitor cocktail (2μg/ml antipain, 2μg/ml leupeptin, 2μg/ml chymostatin, 2μg/ml pepstatin, 0.1 TIU/ml aprotinin, 100μg/ml phenylmethylsulfonyl fluoride, and 10 μg/ml α₂-macroglobulin). The resultant cell suspension was subjected to sequential centrifugation at 500 x g (5 min), 13,000 x g (10 min) and 100,000 x g (60 min) as previously described (Horazdovsky and Emr 1993). Proteins in supernatant fractions were precipitated by the addition of trichloroacetic acid to 10% and the pellet fractions were washed with a 10% trichloroacetic acid solution. The pelleted proteins were then suspended in 1 ml of immunoprecipitation buffer [50mM Tris (pH 7.5), 150mM NaCl, 0.5% Tween-20, 0.1mM EDTA, 1mg/ml BSA] and the levels of Vps5p, Vps10p, ALP, glucose-6-phosphate dehydrogenase, and Kex2p in each subcellular fraction were determined by immunoprecipitation as previously described (Klionsky, Banta et al. 1988). The membranes in the P100 cell fraction were separated on a Accudenz (Nycodenz) gradient. Spheroplasts (30 OD equivalents) generated from TVY614 were labeled and chased as above, lysed and fractionated as above, except the

lysis buffer consisted of 20mM Hepes-KOH (pH 7.5), 50mM potassium acetate, 1mM EDTA and 200mM sorbitol. P100 membrane fraction was suspended in 1 ml of lysis buffer and loaded onto a 9% - 37% Accudenz gradient prepared by layering the following Accudenz solutions in a Beckman 14x89mm UltraClear tube; 1ml 37%, 1.5ml 31%, 1.5ml 27%, 1.5ml 23%, 1.5ml 20%, 1.5ml 17%, 1ml 13% and 1ml 9%. Accudenz solutions were prepared in a buffer containing 20mM Hepes-KOH (pH 7.5), 50mM potassium acetate, 1mM EDTA. The gradient was subjected to centrifugation at 170,000 x g for 16 hrs and the gradient was fractionated (1 ml fractions). Vps5p, Vps17p, Vps10p and Kex2p were immunoprecipitated from each fraction and the immunoprecipitates were resolved by SDS-PAGE and visualized by fluorography. Refractive indexes of each column fraction was used to calculate the gradient density profile.

Microscopy

Wild-type cells (SEY6210), *vps5ΔI* cells (BHY152) and *vps17ΔI* cells (KKY10) were grown in rich media (YPD) to mid-log phase. The cells were harvested and resuspended at 20 OD₆₀₀ U/ml in YPD media. FM 4-64 (Vida and Emr 1995) was added to 1.6 μ M and the cells were incubated with shaking for 20 min at 30°C. Samples were then diluted 1:20 in YPD, and the incubation was continued for 1 hr at 30°. The cells were harvested and resuspended in YPD media, and placed on standard slides.

Visualization of labeled cells was performed on an Olympus IX70 inverted microscope equipped with a Rhodamine filter. Images were collected with a Photometrix digital camera, and deconvolved using DeltaVision software (Applied Precision Inc., Issaquah, WA).

Cross-linking labeled cell extracts

Cells were grown in SD media to an OD₆₀₀ of 1.0 and harvested by centrifugation. Spheroplasts were generated as described and incubated for 10 minutes at 30°C (Vida, Graham et al. 1990). The spheroplasts were labeled for 10 min at 30°C with 30 μ Ci of Tran³⁵S per OD₆₀₀ unit of spheroplasts. The spheroplasts were then pelleted for 30 seconds and osmotically lysed in 1 ml of a buffer containing 100 mM potassium phosphate (pH 7.5), 5 mM EDTA, 5 μ g/ml antipain, 1 μ g/ml leupeptin, 1 μ g/ml aprotinin, 1 μ g/ml pepstatin, 50 μ g/ml α -2 macroglobulin, and 100 μ g/ml phenylmethanesulfonyl fluoride (Stack, Herman et al. 1993). To initiate the cross-linking reaction, dithiobis(succinimidylpropionate) (DSP) was added to the cell lysates at a final concentration of 200 μ g/ml and the lysates were incubated at room temperature for 30 minutes. The cross-linking agent was then quenched by the addition of hydroxylamine to 20 mM. Proteins in the cross-linking reaction were precipitated with trichloroacetic acid and prepared for sequential immunoprecipitations with Vps5p and Vps17p antisera as detailed above.

Vps5p Native Immunoprecipitation

Following the same procedure described above, ³⁵S-labeled spheroplasts were generated from 20 OD₆₀₀ units of appropriate strains and lysed in 2.2 ml lysis buffer (20mM Hepes, pH 7.5, 200mM Sorbitol, 150mM CH₃COOK, 1mM EDTA, 100 μ g/ml PMSF, Roche EDTA-free Protease Inhibitor mix at recommended concentration) with a Dounce homogenizer. Crude lysates were cleared by centrifugation at 13,000 x g, and

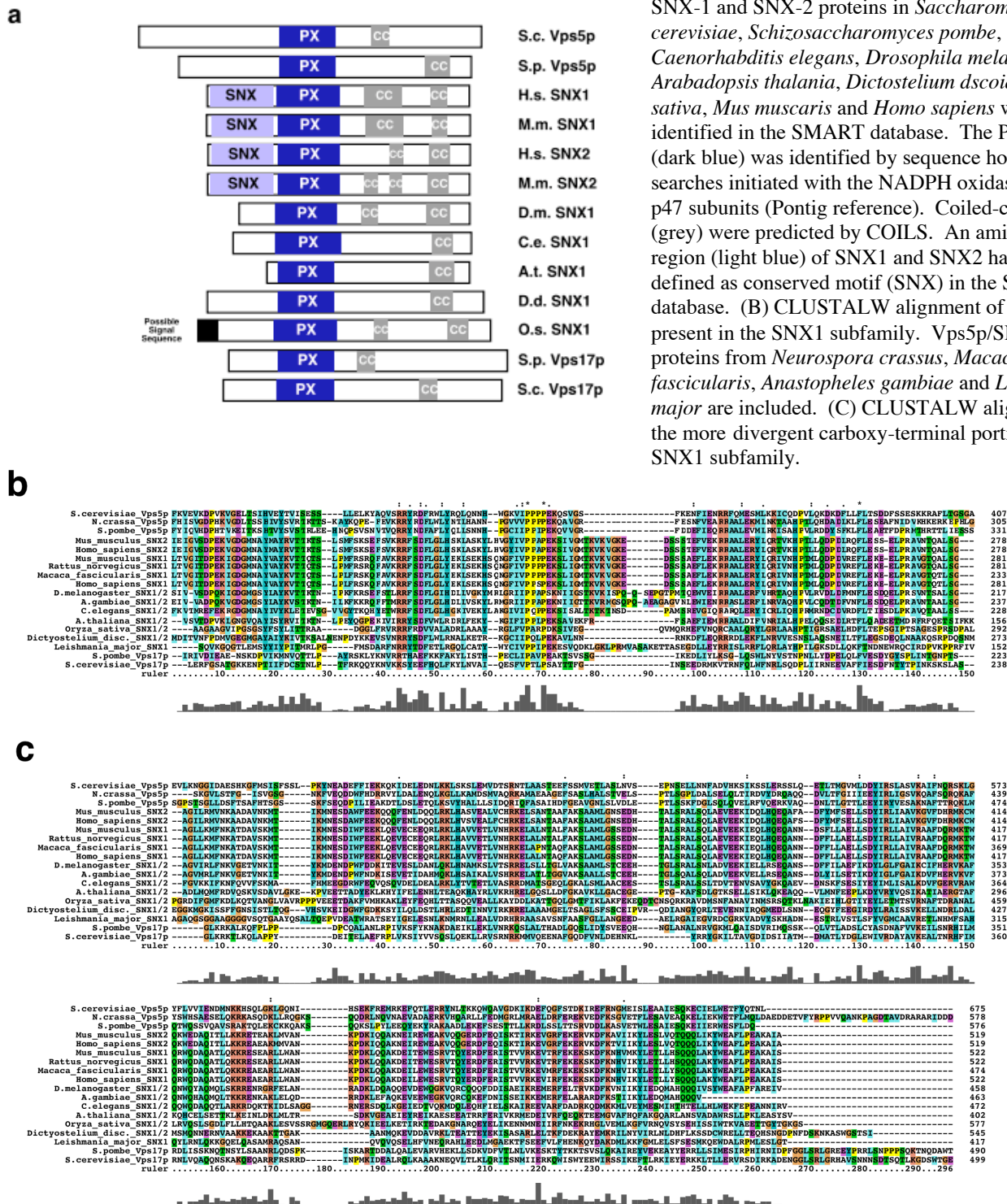
the supernatant was divided into 2 tubes containing Vps5p antiserum and Protein A Sepharose. Following a 1 hour incubation at 4°, the immunoprecipitated material was washed 6 times with either lysis buffer or lysis buffer containing 0.05% Tween-20. Urea Cracking Buffer was added, samples were heated at 65° for 5 minutes, and supernatants were cleared by centrifugation at 13,000 x *g* after the addition of Tween IP buffer (50mM Tris, pH 7.5, 150mM NaCl, 100μM EDTA, 0.5% Tween-20) and bovine serum albumin (BSA ,1mg/ml). From the denatured samples, Vps10p and Vps17p were immunoprecipitated with the addition of appropriate antisera and Protein A Sepharose. Samples were washed with Tween IP buffer, Urea Tween IP buffer (100mM Tris, pH 7.5, 200mM NaCl, 2M Urea, 0.5% Tween-20) and TBS (50mM Tris, pH 7.5, 150mM NaCl). Samples were resolved by SDS-PAGE and the protein visualized by fluorography.

Results.

Vps5p is a member of the sorting nexin family.

Wild-type cells localize CPY to the vacuolar lumen; however, defects in the vacuolar protein sorting pathway result in secretion of CPY. The amino-terminal 50 residues comprise the CPY sorting signal and are sufficient to confer targeting to the vacuole (Johnson, Bankaitis et al. 1987; Valls, Hunter et al. 1987; Valls, Winther et al. 1990). To facilitate identification of *vps* complementation, a reporter containing the CPY sorting signal fused to invertase (CPY-INV) was expressed in a *vps5* strain (SEY5-7) lacking endogenous invertase. As with other *vps* mutants, the SEY5-7 strain secretes the vast majority of the CPY-INV reporter, and this extracellular invertase activity is detected by a colorimetric overlay assay (see Materials and Methods). The SEY5-7

Figure 3. Vps5p is a member of the sorting nexin-1 subfamily. (A) Depiction of the Vps5p, Vps17p, SNX-1 and SNX-2 proteins in *Saccharomyces cerevisiae*, *Schizosaccharomyces pombe*, *Caenorhabditis elegans*, *Drosophila melanogaster*, *Arabidopsis thaliana*, *Dictostelium discoideum*, *Oryza sativa*, *Mus musculus* and *Homo sapiens* with domains identified in the SMART database. The PX domain (dark blue) was identified by sequence homology searches initiated with the NADPH oxidase p40 and p47 subunits (Pontig reference). Coiled-coil regions (grey) were predicted by COILS. An amino-terminal region (light blue) of SNX1 and SNX2 has also been defined as conserved motif (SNX) in the SMART database. (B) CLUSTALW alignment of PX domains present in the SNX1 subfamily. Vps5p/SNX1 proteins from *Neurospora crassa*, *Macaca fascicularis*, *Anastopheles gambiae* and *Leishmania major* are included. (C) CLUSTALW alignment of the more divergent carboxy-terminal portion of the SNX1 subfamily.



strain harboring the CPY-INV reporter was transformed with a centromeric plasmid-based genomic DNA library, and colonies harboring a complementing plasmid were

identified by suppression of the CPY-INV secretion as revealed by the reduced activity in the invertase overlay assay (experiment conducted by Suk-hoon Yoon with Bruce Horazdovsky, 1989). Using this procedure, a 12 kb clone derived from chromosome XV was uncovered that could rescue the SEY5-7 CPY-INV sorting defects. The complementing activity was refined to a 3.3 kb *SmaI-XhoI* fragment containing a single open reading frame, YOR069w (bases 453,770 to 455,795), and integrative mapping studies were used to demonstrate that YOR069w corresponds to the *VPS5* locus.

The *VPS5* locus is predicted to encode a 675 residue protein, 76,437 daltons in mass. No hydrophobic patches capable of forming transmembrane domains are apparent; instead, the protein appears to be highly hydrophilic and charged with a pI of 5.04. When initially identified, Vps5p bore no significant similarity to sequences in the protein databases. The first mammalian protein to exhibit significant similarity was human sorting nexin-1 (SNX1), a protein implicated in regulating EGF receptor trafficking to the lysosome (Kurten, Cadena et al. 1996). Subsequently, SNX1 proteins from nematodes (*Caenorhabditis elegans*), flies (*Drosophila melanogaster*, *Anastopheles gambiae*) and plants (*Arabidopsis thaliana*, *Oryza sativa*) were identified as well as a second mammalian isoform, SNX2 (Figure 3A).

Vps5p residues 281-407 constitute the region of highest sequence similarity to human SNX1 (residues 147-274), and motif identification algorithms initiated with the NADPH oxidase p40 and p47 subunits identified this domain as the phox or PX motif (Figure 3B; PX motif function will be discussed in Chapter 3) (Ponting 1996). This approximately 130 amino acid domain is predicted to be largely helical with a proline loop in the middle. The sequence signatures of the motif are a highly conserved

VKRR(Y/F)SDFxxLxxxL (Figure 3B, motif residues 41-55) preceding the PPPPEK loop (residues 67-72), which is followed by the more varied carboxy-terminal portion of the domain. In addition to the PX domain region, Vps5p exhibits limited sequence homology to the SNX1 and SNX2 proteins over the carboxyl-terminal portion of the molecule (Figure 3C). Residues 548-557 constitute the most striking conservation over the DYIRxLxV(K/R) sequence. The COILS algorithm (Lupas, Van Dyke et al. 1991) identified potential coiled-coil forming regions in the carboxyl-terminal portions of all of these Vps5p, SNX1 and SNX2 proteins from yeast to man (Figure 3A). The combination of the PX domain and the predicted coiled-coil region assigned Vps5p to the general family of sorting nexins, and the extent of sequence conservation indicated that Vps5p is the yeast homolog of human SNX1. The PX domain and a predicted coiled-coil have also been identified in Vps17p (Figure 3A), indicating that Vps17p is also a member of the sorting nexin family although less sequence conservation is apparent (Figure 3B,C).

Vps5p is required for vacuolar morphology maintenance and protein sorting.

To evaluate the role of Vps5p in the vacuolar protein sorting pathway, a *vps5* knockout strain was generated by replacing basepairs 18 to 714 of the open reading frame with the *HIS3* gene cassette. Cells lacking Vps5p are viable but exhibit pronounced defects in vacuolar morphology. The fluorescent lipophilic dye FM4-64 was used to visualize the vacuolar membrane in wild-type cells (Vida and Emr 1995). Following a short labeling period (20 minutes) and an extended chase (1 hour), FM4-64 fluorescence was apparent as 1 to 3 large circular structures (Figure 4, WT) indicative of the wild-type vacuolar limiting membrane. This technique was used to examine vacuolar morphology in cells

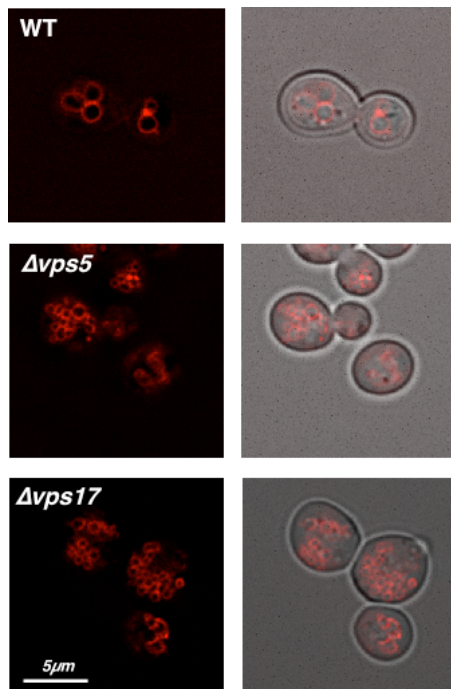


Figure 4. Morphological analysis of wild-type, $\Delta vps5$ and $\Delta vps17$ cells. Wild-type cells (SEY6210), $\Delta vps5$ cells (BHY152) and $\Delta vps17$ cells (KKY10) were incubated for 20 minutes at 30°C in YPD media containing FM4-64. Excess media was then added and incubations were continued for 1 hour. Images were acquired and deconvolved using the DeltaVision system. The left panel is the fluorescence image, and the right panel is fluorescence overlaid on the bright-field image.

completely lacking Vps5p ($\Delta vps5$). In contrast to the wild-type cells, FM4-64 in $\Delta vps5$ cells decorated many smaller circular structures, and the large vacuolar membrane fluorescence was absent. A similar pattern was previously reported for the originally isolated *vps5* mutant, indicating that the initial observations accurately reflected the *vps5* null phenotype (Banta, Robinson et al. 1988; Raymond, Howald-Stevenson et al. 1992). This fragmented vacuolar pattern was also observed in cells lacking Vps17p ($\Delta vps17$). The nature of these FM4-64 positive compartments in the *vps5* and *vps17* mutants is unclear. The structures may represent either the enlargement of prevacuolar compartments that replace the vacuole or the fragmentation of the vacuole itself. The presence of these structures in both *vps5* and *vps17* mutants suggests that these gene products function together to maintain normal vacuolar morphology, either directly or indirectly.

In addition to defects in vacuolar morphology, *vps5* mutants exhibit sorting defects for a subset of vacuolar enzymes. Biosynthetic transport of many vacuolar

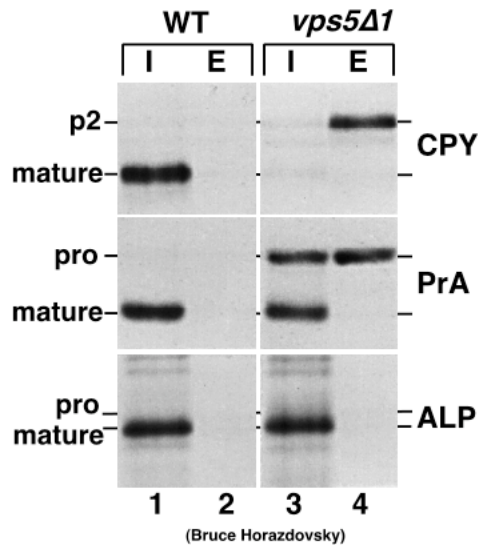


Figure 5. Intracellular sorting of vacuolar hydrolases. Spheroplasts from SEY6120 (WT) and BHY152 (*vps5Δ1*) were labeled for 10 min with Tran³⁵S-label at 30°C, then unlabeled methionine and cysteine were added and the incubation was continued for 30 min. The labeled cultures were split into spheroplast (I, internal) and media (E, external) fractions by centrifugation. The presence of CPY, PrA and ALP in each fraction was determined by immunoprecipitation with appropriate antiserum, resolution by SDS-PAGE and visualization by fluorography. The migration positions of Golgi-modified precursors (p2 or pro) and mature forms are shown.

proteins can be easily monitored due to compartment specific posttranslational modifications, including glycosylation and proteolytic activation. CPY is initially translocated into the endoplasmic reticulum and receives four core glycosylations, yielding the p1CPY zymogen. During transit through the Golgi network, these core glycosylations are extended with addition of mannose residues. This Golgi-modified p2CPY precursor is then sorted into the *VPS* pathway and delivered to the vacuole for activation by cleavage. The p1CPY, p2CPY and mature (mCPY) forms can be resolved by SDS-PAGE, thus enabling inspection of the *VPS* pathway by the conversion of p1CPY to p2CPY to mCPY in a pulse-chase experiment. Spheroplasts were generated from wild-type and $\Delta vps5$ cells and metabolically labeled for 10 minutes by the addition of [³⁵S]-methionine and [³⁵S]-cysteine. Following a 30 minute incubation in excess unlabeled amino acids, the cultures were split into spheroplast (intracellular, I) and media (extracellular, E) fractions. The intracellular and extracellular levels of three vacuolar enzymes, CPY, proteinase A (PrA) and alkaline phosphatase (ALP), were determined by immunoprecipitation with the appropriate polyclonal antisera (Figure 5). In wild-type

yeast (lanes 1 and 2), all three enzymes were found in the internal fraction in the mature form generated by proteolytic activation upon delivery to the vacuole. In the $\Delta vps5$ strain (lanes 3 and 4), the presence of p2CPY in the extracellular fraction indicated that CPY was secreted in the precursor form. This pattern demonstrated that Vps5p is required to maintain CPY trafficking to the vacuole. Analysis of a second soluble vacuolar protease, PrA, yielded a distinct result. A portion of PrA was detected in the extracellular fraction in the precursor form, indicating PrA secretion; however, precursor and mature forms were also apparent in the intracellular fraction. This pattern indicated that PrA sorting to the vacuole is only partially defective in the $\Delta vps5$ cells. ALP is a third vacuolar enzyme which is transported to the vacuole as a type II transmembrane protein via an AP3 pathway that bypasses the endosome (Klionsky and Emr 1989; Cowles, Odorizzi et al. 1997; Cowles, Snyder et al. 1997; Stepp, Huang et al. 1997). In $\Delta vps5$ cells, ALP was found entirely in the intracellular fraction in the mature form. This pattern indicated that Vps5p is not required for ALP transport to the vacuole. These findings revealed a specific requirement for Vps5p in sorting soluble vacuolar proteases and suggested a preferential role in CPY sorting.

Vps10p localization is Vps5p-dependent.

The differential CPY and PrA sorting defects apparent in the $\Delta vps5$ strain was previously observed in the $\Delta vps10$ strain (Marcusson, Horazdovsky et al. 1994). Deletion of *vps10* results in the vast majority of CPY being secreted while only a small portion of PrA fails to mature. *VPS10* encodes a 1579 amino acid single pass transmembrane protein. The amino-terminal 1400 residues protrude into the lumen of the trans-Golgi network and

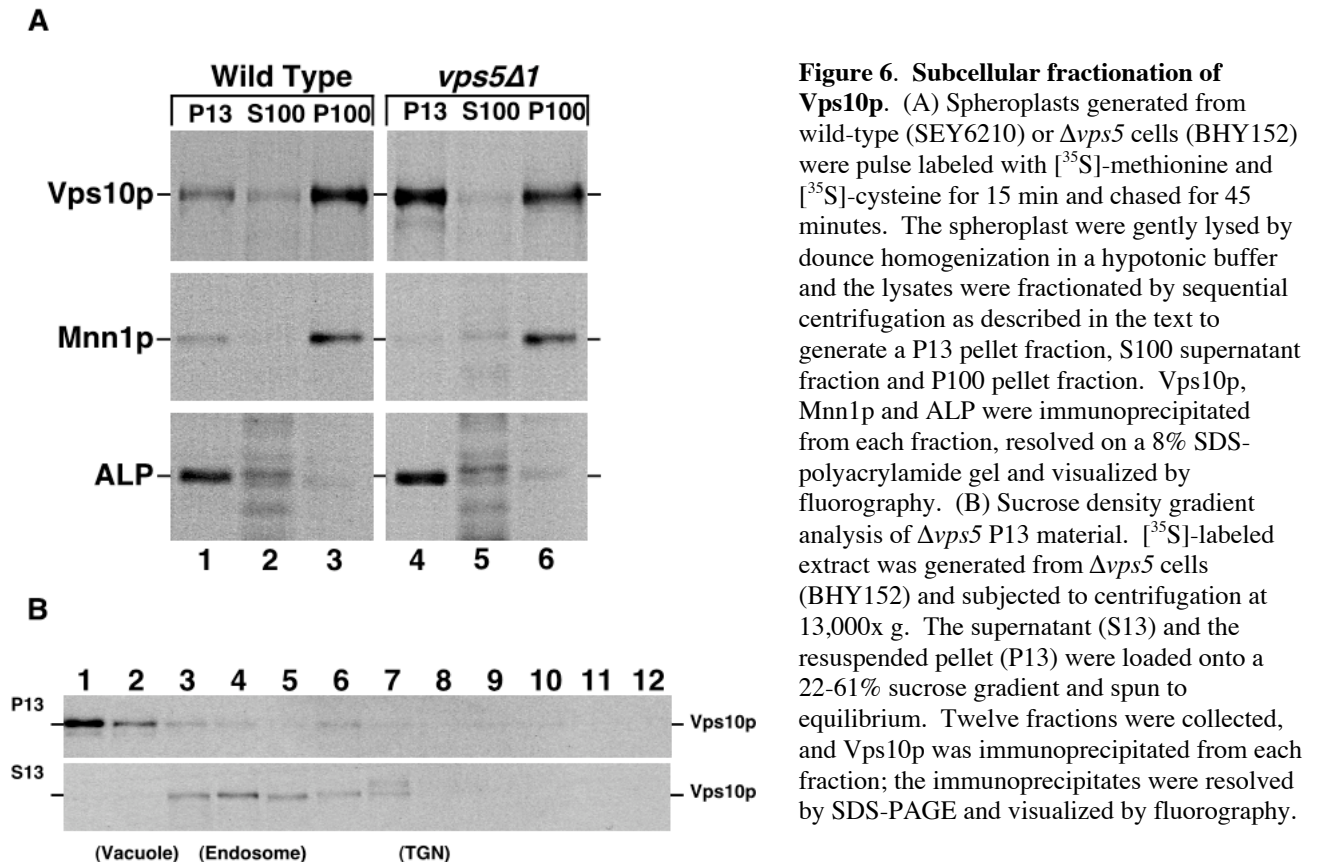


Figure 6. Subcellular fractionation of Vps10p. (A) Spheroplasts generated from wild-type (SEY6210) or $\Delta vps5$ cells (BHY152) were pulse labeled with [35 S]-methionine and [35 S]-cysteine for 15 min and chased for 45 minutes. The spheroplast were gently lysed by dounce homogenization in a hypotonic buffer and the lysates were fractionated by sequential centrifugation as described in the text to generate a P13 pellet fraction, S100 supernatant fraction and P100 pellet fraction. Vps10p, Mnn1p and ALP were immunoprecipitated from each fraction, resolved on a 8% SDS-polyacrylamide gel and visualized by fluorography. (B) Sucrose density gradient analysis of $\Delta vps5$ P13 material. [35 S]-labeled extract was generated from $\Delta vps5$ cells (BHY152) and subjected to centrifugation at 13,000x g. The supernatant (S13) and the resuspended pellet (P13) were loaded onto a 22-61% sucrose gradient and spun to equilibrium. Twelve fractions were collected, and Vps10p was immunoprecipitated from each fraction; the immunoprecipitates were resolved by SDS-PAGE and visualized by fluorography.

directly interact with the CPY sorting signal to mediate diversion of CPY into the *VPS* pathway. As such, Vps10p is considered the vacuolar protein sorting receptor (Jorgensen, Emr et al. 1999). Vps10p transits from the trans-Golgi network to the endosome along with its ligand, p2CPY. Upon fusion with the endosome, p2CPY is released to permit further transport to the vacuole while Vps10p is recycled back to the trans-Golgi network to repeat the sorting process (Cereghino, Marcusson et al. 1995; Cooper and Stevens 1996). The similarity between the CPY and PrA differential sorting phenotypes of the $\Delta vps5$ and $\Delta vps10$ strains suggested a functional link between Vps5p and Vps10p.

Human SNX1, the Vps5p homolog, was previously shown to modulate EGFR localization (Kurten, Cadena et al. 1996), so a role for Vps5p in Vps10p localization was

examined by subcellular fractionation (Figure 6A, see Materials and Methods).

Spheroplasts generated from wild-type and $\Delta vps5$ strains were labeled with [^{35}S]-methionine, cysteine for 15 minutes. Following a 40 minute incubation with excess amino acids, spheroplasts were gently lysed using a dounce homogenizer. The initial lysate was cleared by a 500x g spin and subsequently subjected to differential centrifugation at 13,000x g and 100,000x g. The presence of Vps10p and markers of the Golgi (Mnn1p) and vacuole (ALP) in the 13,000x g pellet (P13), 100,000x g supernatant (S100) and pellet (P100) fractions were detected by immunoprecipitation with appropriate polyclonal antiserum. Utilizing lysates generated from wild-type cells, Vps10p fractionated predominantly in the 100,000x g pellet (lane 3) with some association with the 13,000x g pellet (lane 1) also apparent. This pattern (predominantly P100) is consistent with Vps10p distribution between the Golgi and endosomal compartments as previously described (Marcusson, Horazdovsky et al. 1994; Cereghino, Marcusson et al. 1995). In lysates generated from $\Delta vps5$ cells, a distinct fractionation pattern was observed. Vps10p was enriched in the 13,000x g pellet (lane 4) as compared to wild-type (lane 1). By contrast, the similarity in fractionation patterns of Mnn1p (predominantly P100) and ALP (P13) in extracts derived from wild-type and $\Delta vps5$ strains indicated consistency in the experimental procedure and in the gross composition of the Golgi and vacuole compartments in the two strains. These findings indicated that Vps10p localization is altered upon deletion of Vps5p, and the shift to P13 material suggested that Vps10p might be mislocalized to the vacuole.

To further analyze the altered Vps10p localization in the $\Delta vps5$ strain, sucrose density gradient centrifugation analysis was performed on the P13 material (Figure 6B).

The resuspended 13,000x g pellet material (upper panel) and S13 fraction (lower panel) were loaded onto 22% to 61% sucrose step gradients. The samples were then subjected to high speed centrifugation until equilibrium was achieved (16 hours). The gradients were harvested in twelve fractions, and the presence of Vps10p in each fraction was detected by immunoprecipitation with Vps10p polyclonal antiserum. Vps10p enrichment in the lightest portion of the P13 gradient (fractions 1-3) was apparent. This pattern is consistent with vacuolar localization and is distinct from the Vps10p pattern obtained when extracts are generated from wild-type cells (J. Lin-Cereghino observation; B. Horazdovsky, personal communication). Analysis of the S13 gradient revealed Vps10p fractionating in a pattern consistent with endosomal (fractions 3-5) and Golgi (fractions 6-8) localization, as was previously shown (J. Lin-Cereghino observation; B. Horazdovsky, personal communication). These results indicated that Vps10p is mislocalized to the vacuole in $\Delta vps5$ strains and suggested that Vps5p is involved in recycling Vps10p from the endosome to the trans-Golgi network.

Vps5p associates with novel vacuolar pathway compartment.

To gain insight into the role of Vps5p in Vps10p trafficking, characterization of Vps5p localization was performed. Polyclonal antiserum against Vps5p was generated by injection of a TrpE-Vps5p protein fusion into a New Zealand White rabbit. The crude antiserum was demonstrated to immunoprecipitate a band of approximately 90 kDa using extracts generated from the wild-type strain but not from the $\Delta vps5$ strain; in addition, this band was absent when pre-immune serum was used in the immunoprecipitation (B.

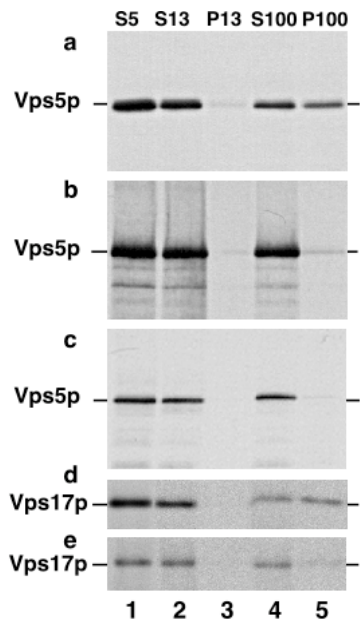


Figure 7. Subcellular fraction of the *VPS5* gene product. Wild-type cells (SEY6210) (A, D), wild-type cells overexpressing Vps5p (B), $\Delta vps17$ cells (KKY10) (C), and $\Delta vps5$ cells (BHY152) (E) were converted to spheroplasts, labeled with Tran³⁵S-label for 15 min, chased for 45 min at 30°C, lysed and subjected to sequential differential centrifugation. Equivalent amounts of the 500 x g supernatant (S5), 13,000 x g supernatant (S13), 13,000 x g pellet (P13), 100,000 x g supernatant (S100) and 100,000 x g pellet (P100) fractions were subjected to quantitative immunoprecipitations with antiserum directed against Vps5p (A-C) or Vps17p (D, E). The immunoprecipitates were resolved by SDS-PAGE and Vps5p and Vps17p were visualized by fluorography.

of the protein. Horazdovsky, personal communication). The difference in apparent and predicted molecular masses (76 kDa) is likely due to the charged nature of Vps5p.

To determine Vps5p subcellular localization, sequential centrifugation of wild-type extracts was performed (Figure 7). Spheroplasts generated from wild-type yeast were labeled with [³⁵S]-methionine, cysteine for 15 minutes and chased for 40 minutes with excess amino acids. Labeled spheroplasts were then gently disrupted with a dounce homogenizer, and unbroken cells were cleared by a 500x g spin. This cleared lysate (S5) was subjected to a 13,000x g spin, and pellet (P13) and supernatant (S13) fractions were collected. An equivalent amount of 13,000x g supernatant was subjected to a 100,000x g centrifugation, generating the P100 and S100 fractions. The presence of Vps5p in each sample was determined by immunoprecipitation with the aforementioned antiserum. Vps5p was found to partially associate with material that pellets in the 100,000x g spin (Panel A, lanes 4 and 5). Present in this fraction are vesicles and large protein complexes as well as portions of the Golgi and endosomal compartments; however, the lack of

significant association with the P13 material argued against this pattern representing Golgi or endosomal localization as well as eliminating the possibility of significant vacuolar association. The presence of Vps5p in the S100 fraction (lane 4) also suggested that Vps5p is peripherally associated with the membranes (lane 5). This conclusion is supported by the absence of predicted transmembrane domains and by the finding that P100 fractionation is sensitive to 1M NaCl (data not shown). Overexpression of Vps5p from a 2 μ plasmid resulted in the vast majority of Vps5p fractionating in the S100 sample (Panel B, lane 4), indicating that the P100 association is saturable.

vps5 and *vps17* mutants share the fragmented vacuolar morphology and the differential CPY and PrA missorting phenotypes (Kohrer and Emr 1993; Horazdovsky, Davies et al. 1997). In addition, the Vps17p fractionation pattern is identical to the Vps5p pattern (Figure 7, Panel D) (Kohrer and Emr 1993). These similarities suggest that Vps5p and Vps17p function at a common site in the vacuolar protein sorting pathway. To determine if Vps17p is required for Vps5p membrane association, extracts generated from the $\Delta vps17$ strain were subjected to sequential centrifugation (Figure 7, Panel C). Significant Vps5p association with P100 material was not evident in the absence of Vps17p (lane 5), demonstrating that Vps17p is required for Vps5p association with the pelletable material. To examine the corresponding dependence, Vps17p fractionation in extracts generated from the $\Delta vps5$ strain was examined (Panel E). In the absence of Vps5p, Vps17p association with P100 material was reduced (lane 5), indicating that Vps5p and Vps17p are dependent on each other for association with the 100,000x g pellet material.

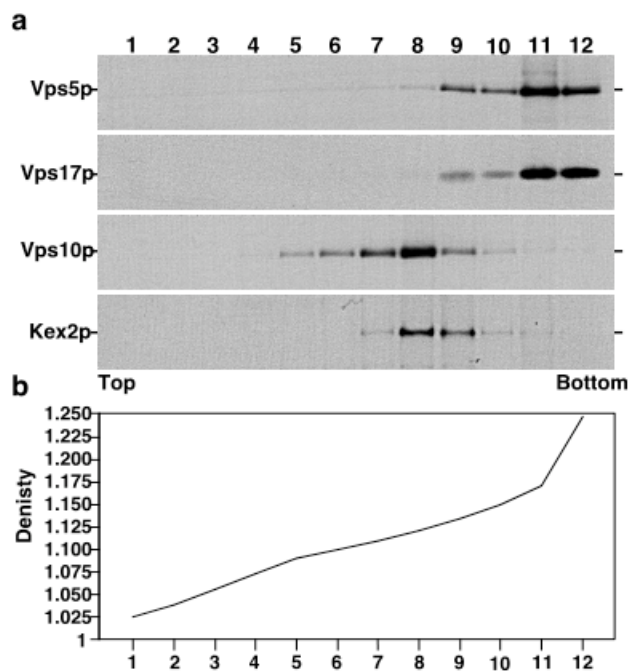


Figure 8. Localization of Vps5p and Vps17p By Accudenz Density Gradient Analysis. Spheroplasts generated from TVY614 cells were labeled with [35 S]-methionine and [35 S]-cysteine for 15 min and then chased for 45 min. After lysis, large membranes were removed by a centrifugation at 13,000 x g for 10 min and the cleared lysate was subjected to centrifugation at 100,000 x g for 60 min. The resultant pellet (P100) was suspended in lysis buffer, loaded onto a 9-37% Accudenz gradient and spun to equilibrium. Twelve fractions were collected, and Vps5p, Vps17p, Kex2p, and Vps10p was immunoprecipitated from each fraction; the immunoprecipitates were resolved by SDS-PAGE and visualized by fluorography. The density of each gradient fraction was derived from its refractive index.

To further refine the subcellular localization, accudenz density gradient analysis was performed (see Materials and Methods). The 100,000x g pellet from wild-type extracts was resuspended and applied to a 9%-37% accudenz density gradient. Samples were subjected to 170,000x g centrifugation for 16 hours to achieve equilibrium positions. Twelve fractions were collected, and the amounts of Vps5p, Vps17p, Vps10p and Kex2p in each sample were determined by immunoprecipitation with the appropriate polyclonal antiserum (Figure 8). Vps5p migrated in the dense portion of the gradient with the majority in fractions 11 and 12 (corresponding to ~1.18 g/ml). This same pattern was apparent for Vps17p, strongly suggesting that Vps5p and Vps17p are present on the same material. Fractionation patterns of Kex2p, a resident Golgi protein, and Vps10p, which cycles between the Golgi and endosome, were examined as markers of endosomal (fractions 5-8) and Golgi membranes (fractions 7-10). The disparity between the Kex2p, Vps10p and Vps5p/Vps17p patterns indicated that Vps5p and Vps17p are

localized to material distinct from the Golgi or endosomal membranes, and the dense nature of the material suggests that Vps5p and Vps17p may be localized to a coated vesicle.

Vps5p and Vps17p physically associate.

Vps5p and Vps17p colocalize to the same P100 material and are dependent on each other for this association. These observations as well as the shared mutant phenotypes raised the possibility that Vps5p and Vps17p might physically interact. To examine this possibility, immunoprecipitation experiments were conducted utilizing the crosslinking agent dithiobis(succinimidylpropionate) (DSP) (Figure 9A). [³⁵S]-labeled extracts generated from wild-type (lanes 1 and 2), $\Delta vps5$ (lane 3) and $\Delta vps17$ (lane 4) strains were

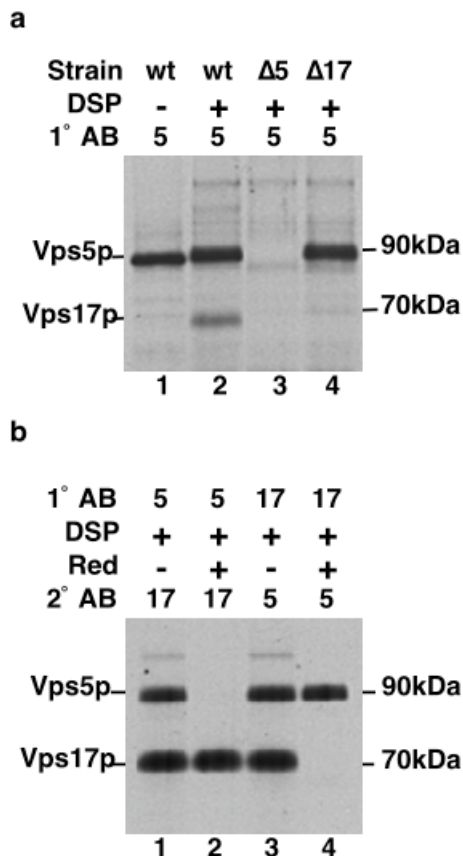


Figure 9. Cross-linking Vps5p and Vps17p. (A) Spheroplasts generated from wild-type cells (wt), *vps5Δ1* and *vps17Δ1* cells ($\Delta 5$ and $\Delta 17$ respectively) were labeled with [³⁵S]-methionine and [³⁵S]-cysteine for 10 min. and then chased for 30 min. Labeled spheroplasts were osmotically lysed and the lysates were untreated (-) or treated (+) with the cross-linking agent dithiobis(succinimidylpropionate) (DSP). The extracts were immunoprecipitated with antiserum directed against Vps5p, the immunoprecipitates were reduced with SDS sample buffer, resolved by SDS-PAGE and the cross-linked products were visualized by fluorography. (B). Spheroplasts were labeled and cross-linked as described above. Cross-linked extracts were subjected to sequential immunoprecipitations under denaturing but none reducing conditions (1° AB) using Vps5p or Vps17p antiserum. The immunoprecipitates were then treated with a reducing or nonreducing buffer (Red +, Red - respectively) and then reimmunoprecipitated with the second antiserum as indicated (2° AB). The final immunoprecipitated material was treated with a reducing sample buffer, resolved by SDS-PAGE and visualized by fluorography.

treated with DSP (lanes 2-4) for 30 minutes to crosslink potential complexes, and then reactions were quenched by hydroxylamine addition. Immunoprecipitations under nonreducing conditions were performed with Vps5p antiserum, and the isolated material was reduced to release the crosslinked components and resolved by SDS-PAGE. A 70 kDa protein was immunoprecipitated from crosslinked wild-type extracts along with Vps5p (lane 2), and the appearance of this band was dependent on both the addition of DSP (compare lanes 1 and 2) and the presence of Vps5p (compare lanes 2 and 3). Vps17p (predicted molecular mass 63,203 Da; migrates as 70kDa) is similar in size to this protein, and the appearance of this band was dependent on Vps17p (lane 4); these observations suggested that the crosslinked species is Vps17p.

To confirm this conclusion, sequential immunoprecipitation with Vps5p and Vps17p antiserum was performed (Figure 9B). Crosslinked [³⁵S]-labeled extracts from wild-type cells were subjected to immunoprecipitation under nonreducing conditions with either Vps5p antiserum (lanes 1 and 2) or Vps17p antiserum (lanes 3 and 4). Following the primary immunoprecipitation, samples were left untreated (lanes 1 and 3) or treated with reducing agent (lanes 2 and 4) to dissolve the DSP crosslink. An immunoprecipitation under nonreducing conditions was then performed with the second antibody, and isolated material was resolved and subjected to SDS-PAGE. In the absence of reducing agent (lanes 1 and 3), Vps5p and Vps17p were copurified by the sequential immunoprecipitation procedure irrespective of the order of antiserum addition. The addition of reducing agent between the primary and secondary immunoprecipitations definitely demonstrates the 70 kDa (lane 2) and 90 kDa (lane 4) proteins to be Vps17p and Vps5p, respectively. These experiments confirm that Vps5p and Vps17p form a

protein complex *in vivo*. The presence of a higher molecular weight band in lanes 1 and 3 will be discussed further in Chapter 3.

Vps10p is physically associated with Vps5p.

Vps5p is required for Vps10p recycling; however, the fractionation patterns for Vps5p and Vps10p appear distinct (Figure 8). To address this disparity and to determine if Vps5p is physically associated with Vps10p, immunoprecipitation experiments with Vps5p antiserum were conducted under non-denaturing conditions (see Materials and Methods; Figure 10). Cleared lysates were generated from ^{35}S -labeled spheroplasts, incubated with Vps5p antiserum and Protein A Sepharose, and washed extensively with lysis buffer. The isolated material was then denatured, and the presence of Vps10p and Vps17p were assessed by immunoprecipitation with appropriate antisera. Vps17p was evident in the Vps5p immunoprecipitate using extracts generated from wild-type cells (lane 3), confirming the physical association previously demonstrated by crosslinking

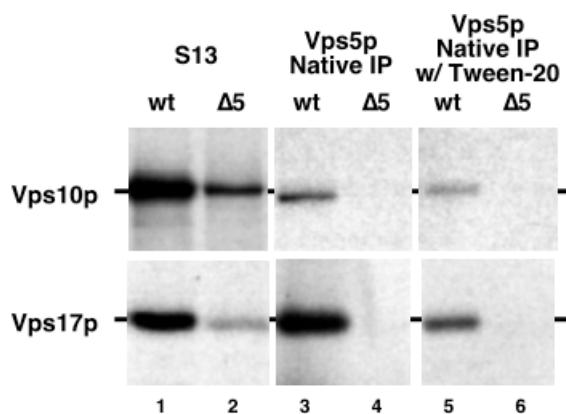


Figure 10. Vps5p native immunoprecipitation. 10 OD₆₀₀ equivalents of 13,000 x g supernatant from [^{35}S]-labeled wild-type (SEY6210) or $\Delta vps5$ (BHY152) spheroplasts were subjected to native immunoprecipitation with Vps5p antiserum. The immunoprecipitate was washed with either lysis buffer (Native IP; lanes 3, 4) or lysis buffer containing 0.05% Tween-20 (Native IP w/ Tween-20; lanes 5, 6). Immunoprecipitated material as well as 1 OD₆₀₀ equivalent of the 13,000 x g supernatant (S13; lanes 1, 2) were then denatured and subjected to immunoprecipitation with Vps10p or Vps17p antisera. Samples were resolved by SDS-PAGE and detected by fluorography.

experiments (Figure 9). In addition, Vps10p was present in the Vps5p immunoprecipitate (Figure 10, lane 3); however, another vacuolar protein sorting transmembrane protein, Pep12p, was not detectable (data not shown). The presence of Vps10p and Vps17p in the immunoprecipitate was dependent on both Vps5p (lane 4) and the Vps5p antiserum, as the proteins were not detected when preimmune serum was used (data not shown). These results indicated an association between Vps5p and Vps10p.

To determine if the apparent interaction between Vps5p and Vps10p represented a physical association or merely colocalization to the same membrane compartment, the coprecipitation experiment was conducted with the detergent Tween-20 included during the non-denaturing immunoprecipitation wash procedure. Vps10p and Vps17p were still detected in the Vps5p immunoprecipitate in the presence of Tween-20 (lane 5), and this association was dependent on both Vps5p (lane 6) and Vps5p antiserum (data not shown). These results determine that Vps5p is physically associated, either directly or indirectly, with Vps10p.

Discussion.

To gain insight into the role of Vps5p in the vacuolar protein sorting pathway, the gene was cloned by complementing the *vps5* sorting defects. Vps5p is a member of the sorting nexin family and is the yeast homolog of human SNX1. Vps5p forms a complex with another sorting nexin, Vps17p, and this interaction is required for the peripheral association with a novel compartment in the *VPS* pathway. Both Vps5p and Vps17p are required to maintain normal vacuolar morphology. Vps5p is also associated with

Vps10p, the vacuolar protein sorting receptor. Deletion of *vps5* results in the aberrant localization of Vps10p to the vacuole and the missorting of soluble vacuolar proteases with CPY exhibiting the most severe defects. These results suggest that the sorting nexins Vps5p and Vps17p form a complex that recycles Vps10p to the Golgi to maintain a functional *VPS* system.

The sorting nexin proteins are characterized by the coincidence of the PX motif with a predicted coiled-coil region (reviewed in (Worby and Dixon 2002)). The PX motif is present in 13 yeast proteins in addition to Vps5p and Vps17p, and eight of these are classified as sorting nexins based on general sequence motifs (YHR105w, YKR078w and YPR079w) or functional evidence. Among these sorting nexins, multicopy suppressor of *VPS1^{dm}* (Mvp1p) has been implicated in the *VPS* pathway both through a genetic interaction with the dynamin-like *VPS1* and the missorting of CPY upon deletion of *mvp1* (Ekena, Vater et al. 1993; Ekena and Stevens 1995). The sorting nexin Golgi retention defective-19 (Grd19p) is not required for Vps10p trafficking or CPY sorting, but Grd19p has been demonstrated to be required for the retrieval of the Golgi protein DPAP-A from the endosome (Voos and Stevens 1998). Grd19p as well as Snx4p/Cvt13p, Snx41p and Snx42p/Cvt20p are also required to recycle the exocytic SNARE Snc1p to the Golgi (Hettema, Lewis et al. 2003), and Snx4p/Cvt13p and Snx42p/Cvt20p have been implicated in the cytoplasm to vacuole (CVT) autophagic process wherein aminopeptidase I (Ape1) is delivered to the vacuole (Nice, Sato et al. 2002). The yeast sorting nexins appear to be regulators of membrane trafficking events, and this is consistent with the initial observation that human SNX1 regulates EGF-R trafficking to the lysosome. The yeast non-sorting nexin PX-containing proteins also

seem to be associated with membrane processes with Bem1p and Bem3p involved in selection of the bud emergence site (Chant, Corrado et al. 1991; Zheng, Hart et al. 1993; Zheng, Cerione et al. 1994; Zheng, Bender et al. 1995), Vam7p functioning as a vacuolar SNARE protein (Wada and Anraku 1992; Sato, Darsow et al. 1998), Mdm1p required for mitochondrion distribution and morphology maintenance (McConnell, Stewart et al. 1990; Fisk and Yaffe 1997), and Spo14p exhibiting phospholipase D activity (Waksman, Eli et al. 1996). This common feature of membrane association for all of the PX motif proteins suggests that the domain may be involved in lipid binding. The specifics of this interaction are not intuitive from the proteins themselves, but further studies identified the PX motif as a phosphatidylinositide binding motif with specificity for particular phosphorylated species, especially phosphorylation of the 3' hydroxyl position. This feature will be addressed further in Chapter 3.

The sorting nexins Vps5p and Vps17p are implicated in retrograde traffic to the trans-Golgi compartment (Figure 11). In what manner might the sorting nexins Vps5p and Vps17p function to regulate Vps10p trafficking? Some insight is gained from the localization pattern observed. The disparity between the Vps5p/Vps17p fractionation

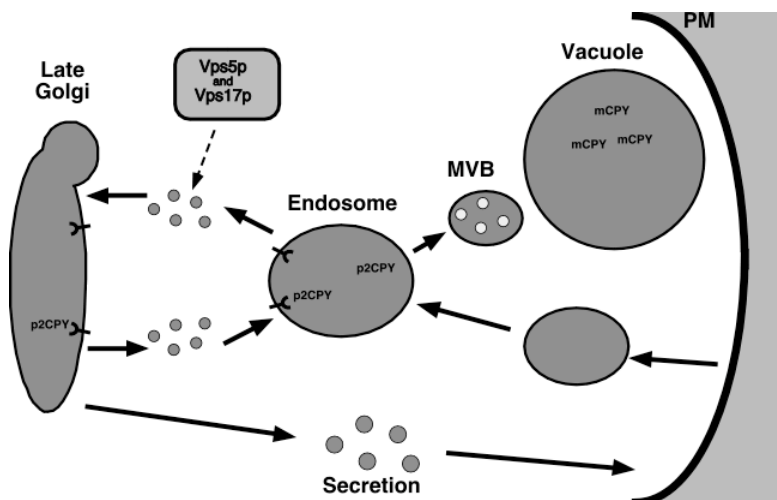


Figure 11. Vps5p and Vps17p function in retrograde traffic. Vps10p is mislocalized to the vacuole in $\Delta vps5$ mutants, implicating the Vps5p-Vps17p complex in Vps10p recycling.

pattern and the patterns of Vps10p and Kex2p fractionation suggest that Vps5p and Vps17p are associated with a novel compartment of the vacuolar protein sorting pathway rather than being present on the Golgi complex or the endosome. As the yeast endosome itself is a poorly characterized membrane system, establishing that the Vps5p/Vps17p compartment is distinct from the endosome is difficult to conclude; this discrepancy may be resolved by emerging models suggesting that multiple endosome/prevacuolar compartments exist. Vps5p and Vps17p fail to localize to the light portion of Vps10p positive compartments which have also been shown to contain the endosomal SNARE Pep12p (Becherer, Rieder et al. 1996); however, markers for the distinct endosomal compartments have not been well characterized, so it is not possible to adequately define Vps5p/Vps17p localization. One intriguing possibility is that Vps5p and Vps17p may reside on a coated vesicle, either functioning as an adaptor complex or a coat complex. This model is supported by the observations that Vps5p and Vps17p are highly charged, similar to subunits of COPII-coated vesicles, and that Vps5p and Vps17p migrate in the sucrose density gradient at a density similar to coated vesicles (Serafini, Stenbeck et al. 1991). The most troubling feature with this model is the extent to which the diversity of the sorting nexin family suggests the presence of large numbers of distinct sorting nexin coated vesicles or adaptor complexes. Alternatively, the sorting nexins could function to segregate receptors into particular membrane subdomains or rafts to regulate the recycling process prior to the actual transport intermediate formation.

Examination of additional *vps* mutants may provide further insight into the role of Vps5p and Vps17p in regulating Vps10p trafficking. Mutants in *vps5*, *vps17* and *vps10* share the common phenotype of selective missorting of soluble vacuolar proteases

(Kohrer and Emr 1993; Marcusson, Horazdovsky et al. 1994; Horazdovsky, Davies et al. 1997; Nothwehr and Hindes 1997). This characteristic is most striking in $\Delta vps10$ cells with >90% CPY secretion and <10% PrA secretion. This differential secretion has also been observed in *vps13/soi1*, *vps26*, *vps29*, *vps30* and *vps35* mutants, suggesting that the 5 proteins encoded by these loci may also participate in regulating Vps10p recycling (Paravicini, Horazdovsky et al. 1992; Bachhawat, Suhan et al. 1994; Brickner and Fuller 1997; Seaman, Marcusson et al. 1997). The function of these proteins with Vps5p and Vps17p will be discussed further in Chapter 3.

Chapter 3. Characterization of Vps5p PX domain function in vacuolar protein sorting receptor recycling..

Summary

Mammalian sorting nexins have been implicated as important regulators of growth factor receptor trafficking. In an analogous manner, the yeast sorting nexins Vps5p and Vps17p mediate the retrograde trafficking of the vacuolar protein sorting receptor, Vps10p, from a prevacuolar endosomal compartment to the Golgi. Vps26p, Vps29p, Vps35p and phosphatidylinositol-3-phosphate [PtdIns(3)P] bind Vps5p and Vps17p and are required for this retrograde transport. Through density gradient analysis we demonstrate that Vps5p and Vps17p associate with a unique membrane compartment and that this association does not require Vps26p, Vps29p, or Vps35p. PtdIns(3)P is also shown to be dispensable for Vps5p membrane association; however, deletion of the PtdIns(3)P-binding PX domain of Vps5p results in a nonfunctional protein complex that exhibits reduced membrane association. These results indicate that the PX domain of Vps5p does not solely mediate the interaction of this protein with cellular membranes via PtdIns(3)P but plays an important regulatory role in the formation and/or function of the receptor-associated complex containing Vps5p, Vps17p, Vps26p, Vps29p and Vps35p.

Introduction

Mammalian sorting nexins have been implicated as important regulators of receptor trafficking (reviewed in (Worby and Dixon 2002)). The first member of the family, Sorting Nexin 1 (SNX1), was identified by its ability to interact with the

epidermal growth factor receptor (EGFR) tail (Kurten, Cadena et al. 1996).

Overexpression of SNX1 resulted in mislocalization of EGFR to the lysosome, indicating that the sorting nexins were mediators of EGFR trafficking. Further analysis of SNX1 and other mammalian members of the family (SNX2, SNX3, SNX6, SNX9/SH3PX1, SNX13/RGS-PX1, and SNX15) have shown that the sorting nexins associate with and influence the trafficking of a large number of receptors, including platelet-derived growth factor receptor, insulin receptor and transforming growth factor β receptor in addition to EGFR (Haft, de la Luz Sierra et al. 1998; Barr, Phillips et al. 2000; Nakamura, Sun-Wada et al. 2001; Parks, Frank et al. 2001; Phillips, Barr et al. 2001; Xu, Hortsman et al. 2001; Zheng, Ma et al. 2001; Lin, Lo et al. 2002). To date over 20 sorting nexins and sorting nexin-like proteins have been identified functionally or through database searches (Schultz, Copley et al. 2000). Despite their prevalence, little is known about the role these proteins play in intracellular protein trafficking.

In *Saccharomyces cerevisiae*, the yeast sorting nexin most similar to SNX1 is Vps5p, a component of the vacuolar protein sorting (VPS) pathway (Horazdovsky, Davies et al. 1997; Nothwehr and Hinds 1997). The VPS pathway is responsible for delivery of many proteases, such as carboxypeptidase Y (CPY) and proteinase A (PrA), to the lysosome-like vacuole of yeast (reviewed in (Jones 1984; Klionsky, Herman et al. 1990; Horazdovsky, DeWald et al. 1995; Bryant and Stevens 1998; Wendland, Emr et al. 1998; Lemmon and Traub 2000)). Through genetic and biochemical analyses, the basic steps in this process have been elucidated, and the pathway is similar to the process by which soluble proteins are sorted to the mammalian lysosome. As previously discussed, the vacuolar protein sorting receptor Vps10p allows p2CPY to be diverted from the

default secretory pathway for transport to the endosome. Upon delivery to the endosome, p2CPY and Vps10p dissociate, and Vps10p is recycled back to the trans-Golgi network to repeat the sorting process (Cereghino, Marcusson et al. 1995; Cooper and Stevens 1996).

Identification of components required for the recycling of Vps10p has been accomplished by a more careful examination of the sorting defects of various *vps* mutants. While deletion of *vps10* results in complete missorting of CPY, the majority of PrA is properly sorted and matured in the absence of Vps10p (Marcusson, Horazdovsky et al. 1994). This differential sorting of CPY and PrA is also apparent in *vps5*, *vps17*, *soi1/vps13*, *vps26/pep8*, *vps29*, *vps30*, *vps35* and *vps38* mutants, suggesting that these 8 Vps components are required for Vps10p trafficking (Paravicini, Horazdovsky et al. 1992; Kohrer and Emr 1993; Bachhawat, Suhan et al. 1994; Brickner and Fuller 1997; Horazdovsky, Davies et al. 1997; Nothwehr and Hindes 1997; Seaman, Marcusson et al. 1997; Seaman, McCaffery et al. 1998; Kihara, Noda et al. 2001). Examination of Vps10p subcellular fractionation in the $\Delta vps5$ mutant demonstrated that Vps10p is mislocalized to the vacuole, indicating that Vps5p is required for Vps10p recycling, as described in Chapter 2 (Horazdovsky, Davies et al. 1997; Nothwehr and Hindes 1997). Independently, alleles of *vps5/grd2*, *vps26/grd6* and *vps35/grd9* were isolated in a screen for mutants defective in Golgi retention (*grd*) of the dipeptidyl aminopeptidase A-alkaline phosphatase fusion (A-ALP) (Nothwehr, Bryant et al. 1996; Nothwehr and Hindes 1997). Together, these studies identified a subset of the Vps components that are required to properly recycle proteins from the endosome to the trans-Golgi network.

From this subset, a pentameric protein complex has been identified. The yeast SNX1 homolog, Vps5p, and Vps17p, another sorting nexin, have been demonstrated to physically associate by crosslinking experiments. Vps5p and Vps17p are both partially associated with dense material in a high speed pellet and are dependent upon each other for this association. Vps26p, Vps29p and Vps35p have also been shown to be present in the high speed pellet and have been demonstrated to associate with Vps5p and Vps17p, as demonstrated later in this chapter (Paravicini, Horazdovsky et al. 1992; Bachhawat, Suhan et al. 1994; Seaman, Marcusson et al. 1997; Seaman, McCaffery et al. 1998). These experiments indicated the existence of a five component complex containing Vps5p, Vps17p, Vps26p, Vps29p and Vps35p. Human homologs have been identified for Vps26p, Vps29p and Vps35p, and evolutionary conservation of the protein complex containing these 3 mammalian subunits and the sorting nexins, SNX1 and SNX2, has been demonstrated (Haft, de la Luz Sierra et al. 2000). However, the mechanism by which the homologous yeast and mammalian protein complexes mediate trafficking of Vps10p and a variety of mammalian receptors, respectively, remains unresolved.

The most prominent feature present among the sorting nexins is the PX (or phox) domain, a sequence motif initially identified conserved between the NADPH oxidase p40 and p47 subunits (Ponting 1996). The PX domain is also present in the lipid modifying enzymes phospholipase D (PLD) and class II Cpk type phosphatidylinositol 3-kinase, the t-SNARE Vam7p, the bud emergence proteins Bem1p and Bem3p (Cdc42p GTPase Activating Protein), and the intermediate filament-like protein involved in nuclear and mitochondrial inheritance Mdm1p (reviewed in (Sato, Overduin et al. 2001; Xu, Seet et al. 2001; Ellson, Andrews et al. 2002)). The PX domain has been demonstrated to be

both a SH3 domain interaction site via a polyprolyl type II helix (Hiroaki, Ago et al. 2001) as well as a lipid binding motif with phosphatidylinositides phosphorylated at the 3'-OH position [PtdIns(3)P and PtdIns(3,4)P] the preferred ligands ((Bravo, Karathanassis et al. 2001; Cheever, Sato et al. 2001; Ellson, Gobert-Gosse et al. 2001; Kanai, Liu et al. 2001; Yu and Lemmon 2001); reviewed in (Misra, Miller et al. 2001; Prehoda and Lim 2001)). While the precise role for the PX domain in sorting nexin function has not been established, mutational analysis of SNX3 suggests that the PX domain is involved in protein localization (Xu, Hortsman et al. 2001).

To gain insight into the function of the PX domain in sorting nexin activity and the function of sorting nexins in receptor trafficking, we have continued the *in vivo* analysis of Vps5p and the Vps5p protein complex. Subcellular fractionation studies and density gradient analyses (Chapter 2) have demonstrated that Vps5p is associated with a unique membrane component. Further analysis reveals that this interaction is not dependent on the associated complex components Vps26p, Vps29p or Vps35p. We also demonstrate that the PX domain is required for Vps5p function but is not essential in formation of the Vps5p, Vps17p, Vps26p, Vps29p, and Vps35p complex. Evidence is also provided indicating that the PX domain plays a role in Vps5p membrane localization, as observed for SNX3. However, PtdIns(3)P is not required for Vps5p membrane localization. These results indicate that the PX domain is important for Vps5p function and localization, but that PtdIns(3)P binding to the PX domain of Vps5p may primarily serve a regulatory role in Vps5p function.

Materials and Methods

Reagents

Bacterial strains were grown in Luria-Bertani (LB) medium containing the antibiotics ampicillin (100 μ g/ml) and kanamycin (50 μ g/ml) when necessary (Miller 1972). Yeast strains were grown in medium containing 2% peptone, 1% yeast extract and 2% glucose (YPD) or in synthetic media supplemented with appropriate amino acids as required (Sherman, Fink et al. 1979). Thermostable DNA polymerases, restriction endonucleases and DNA modifying enzymes were purchased from Invitrogen (Carlsbad, CA), Roche Molecular Biochemicals (Indianapolis, IN) or New England Biolabs (Beverly, MA). [³⁵S]Promix and Protein A Sepharose were purchased from Amersham Biosciences (Piscataway, NJ). Zymolyase 100T was purchased from Seikagaku (Tokyo, Japan). Accudenz A.G. was purchased from Accurate Chemical & Scientific (Westbury, NY). Dithiobis[succinimidyl propionate] (DSP) was purchased from Pierce (Rockford, IL). Other chemicals and reagents were purchased from Sigma-Aldrich (St. Louis, MO) and Fisher Scientific (Pittsburgh, PA). Antisera for Vps5p (Horazdovsky, Davies et al. 1997), Vps17p (Kohrer and Emr 1993), and Vps10p (Marcusson, Horazdovsky et al. 1994) were obtained from Scott Emr (UCSD). Bacterial and yeast strains used in this study are listed in Appendix 1.

Plasmid and Strain Constructions

To generate the *vps5* allele lacking the PX domain (deletion of residues 313 to 385), the 5' - and 3' -*VPS5* portions were amplified by polymerase chain reaction (PCR) using oligos Vps5-11 (5'-CCAATGTGCGGCCGCTAGTGTGCTCATAATACC-3')

with Vps5-12 (5'-TTTGTAGCTCGAGTAATGATGATTCAGT-3'), and Vps5-13 (5'-AAAGATCTCGAGCTCTTTTGTAGTGTGACTTTAGTTCAGAG-3') with Vps5-14 (5'-TGTGGTACCAACAAAAGATTTCCAATC-3'), respectively. The resulting fragments were digested with *Not I*, *Xho I* and *Xho I*, *Kpn I*, respectively, and subcloned into the *Not I*, *Kpn I* sites of pRS414 (Christianson, Sikorski et al. 1992) to generate pRS414 Vps5ΔPX. To reconstitute the full length gene, the *VPS5* PX domain was amplified using oligos Vps5-15 (5'-TCATTACTCGAGCTAAAATATGCACAGGTA-3') with Vps5-16 (5'-ATCACTAGTCAAAAAGAGTAGAAAATC-3'), and subcloned into pRS414 Vps5ΔPX via the *Spe I*, *Xho I* sites to generate pRS414 Vps5. Constructs were sequenced to confirm the absence of unexpected mutations. pRS414 Vps5 R319Q was generated by overlapping PCR with the oligos Vps5-22 (5'-ATCTCTGTAAACGCTGGCTTACCTGTGCATA-3') and Vps5-23 (5'-TATGCACAGGTAAGCCAGCGTTACAGAGAT-3').

pRS416 Vps17 KK150,1QQ was generated by the combination of PCR with the oligos Vps17-7 (5'-TAATCTCGAGAGTCCTTGTAGCTTTGTC) with Vps17-11 (5'-AATTCTTCGTATGATTGTTGGACATTCTTGTATTG-3') and Vps17-12 (5'-ATACAAGAATGTCCAACAATCATACGAAGAATTCC-3') with Vps17-10 (5'-TATCGAGCTCAAAAATTCTTGGGTGCG-3'), and using the initial PCR products as template in a second amplification reaction with Vps17-7 and Vps17-10. The wildtype Vps17-7/10 PCR product was also cloned into pRS416 (pRS416 Vps17) and pBluescript (pBS-Vps17). The pBS vps17::NEO construct was generated by ligating the *Spe I*, *Sma I* fragment from pBS-NEO (Hama, Tall et al. 1999) with *Spe I*, *EcoR V* digested pBS

Vps17. The *Xho I*, *Sac I* fragment was transformed into BHY152 to generate BDY517 ($\Delta vps5::HIS3$, $\Delta vps17::NEO$).

To generate the *vps26* deletion yeast strain (BDY261), Vps26-1 (5'-CGTGTGCTCGAGTGTAGTTAACTG-3') and Vps26-2 (5'-CGAGCTCCCGGGCCGGGTCCTGTA-3') were used to amplify the *VPS26* region. The resulting fragment was subcloned into pBS via the *Xho I*, *Sma I* sites. This pBS Vps26 construct was digested with *HinD III*, treated with Klenow, and ligated with the *EcoR V*, *Sma I* fragment from pBS-NEO to generate the *vps26::NEO* disruption construct. The disruption construct was digested with *Xho I*, *Sma I* and transformed into SEY6210 following the LiOAC•TE protocol. Disruption of the *VPS26* locus was confirmed by resistance to G418 (Invitrogen), PCR, scoring of a Vps⁻ phenotype by CPY sorting assay and complementation by a pRS414 Vps26HA plasmid.

Subcellular Fractionation of Vps5p

Subcellular fractionation experiments were performed as previously described (Horazdovsky, Davies et al. 1997). Yeast strains were grown in YNB-glucose with appropriate minimal amino acids at 30°, and 20 OD₆₀₀ units of cultures harvested during the log phase of growth (0.6-0.8 OD₆₀₀/ml). Spheroplasts were generated and labeled for 15 minutes with [³⁵S]-Promix. The labeled proteins were chased for 40 minutes in the presence of excess methionine and cysteine. Labeled spheroplasts were resuspended in 4ml lysis buffer (50mM Tris, pH 8.0, 200mM Sorbitol, 1mM EDTA, 100ng/ml phenylmethylsulfonyl fluoride (PMSF), Roche EDTA-free Protease Inhibitor mix at recommended concentration) and lysed by five strokes of a Dounce homogenizer.

Unbroken cells were removed by centrifugation at 500 x g, and the cleared lysate was fractionated by sequential centrifugation at 13,000 x g for 10 minutes and 100,000 x g for 1 hour. Protein components from each fraction were precipitated with trichloroacetic acid (TCA; final concentration 10%), then resuspended in Urea Cracking Buffer [50mM Tris, pH 7.5, 6M Urea, 1% sodium dodecyl sulfate (SDS)]. Vps5p was isolated as previously described (Horazdovsky, Davies et al. 1997). Immunoprecipitated Vps5p was resolved by SDS-PAGE and visualized by fluorography.

Vps5p and Vps10p Gradient Analysis

Density gradient flotation experiments were derived from density gradient experiments previously described (Horazdovsky, Davies et al. 1997). Following the same procedure described in Subcellular Fractionation of Vps5p, ³⁵S-labeled spheroplasts were generated from 30 OD₆₀₀ units of appropriate strains. Labeled spheroplasts were lysed in 1.1 ml lysis buffer (20mM Hepes, pH 7.5, 200mM Sorbitol, 50mM CH₃COOK, 1mM EDTA, 100μg/ml PMSF, Roche EDTA-free Protease Inhibitor mix at recommended concentration) with a Dounce homogenizer. Crude lysates were subjected to sequential centrifugation at 13,000 and 100,000 x g. The 100,000 x g pellet was resuspended with a syringe in 1ml gradient buffer (20mM Hepes, pH 7.5, 50mM CH₃COOK, 1mM EDTA, Roche EDTA-free Protease Inhibitor mix at recommended concentration) containing 50% Accudenz (weight/volume). The resuspended P100 was overlaid with the following Accudenz solutions: 2ml 48%, 2ml 45%, 2ml 40%, 1ml 35%, 1ml 30%, 1ml 20%, 2ml 0%. Following 16 hour, 169,000 x g centrifugation, 1ml

fractions were collected. TCA was added to 10%, and samples were processed and immunoprecipitated as described above.

Crosslinking Vps5p Complex

Crosslinking experiments were performed as previously described (Horazdovsky, Davies et al. 1997). Following the same procedure described in Subcellular Fractionation of Vps5p, ³⁵S-labeled spheroplasts were generated from 10 OD₆₀₀ units of appropriate strains. Labeled spheroplasts were resuspended in 2ml lysis buffer (10mM KHPO₄, pH 7.5, 100μg/ml PMSF, Roche EDTA-free Protease Inhibitor mix at recommended concentration) to promote osmotic lysis. Samples were subjected to centrifugation at 13,000 x g to generate a cleared supernatant. Either 40μl DMSO or 40μl crosslinking agent (20mg/ml DSP in DMSO) was added to 5 OD₆₀₀ equivalents of cleared lysate. Reactions were incubated at room temperature for 30 minutes and terminated by adding 40μl 1M hydroxylamine. Samples were precipitated by the addition of TCA to 10%, processed as described above, and used in sequential immunoprecipitations with Vps5p and Vps17p or Vps5p and Vps35p antisera. Crosslinked components were resolved under reducing conditions by SDS-PAGE, and proteins were visualized by fluorography.

CPY Immunoprecipitation

CPY immunoprecipitation experiments were performed as previously described (Horazdovsky, Busch et al. 1994). Yeast strains grown in YNB-glucose buffered with 25mM KHPO₄, pH 5.4, and labeled at 30° for 10 minutes before the addition of excess methionine and cysteine. Following the 30 minute chase, samples were precipitated with

TCA (final concentration 10%) and resuspended in Boiling Buffer (50mM Tris, pH 7.5, 1mM EDTA, 1% SDS). Glassbeads were added, samples were vortexed, and CPY was isolated as previously described. Immunoprecipitated material was resolved by SDS-PAGE and visualized by fluorography.

Results

Vps5p and Vps17p associate with a distinct membrane fraction.

Previous work described in Chapter 2 indicated that Vps5p is partially associated with material that pellets during centrifugation at 100,000 x *g* (Horazdovsky, Davies et al. 1997). Moreover, density gradient analysis of the 100,000 x *g* pellet indicated that Vps5p is associated with dense material distinct from either the Golgi complex or a Pep12p-containing endosome. To examine the nature of this dense material, additional density gradient analyses have been performed (see Materials and Methods). The profile of the density gradients (Figure 12B) used in this study have been optimized to allow better examination of the dense material. ³⁵S-labeled spheroplasts generated from a wild-type strain (TVY614) were lysed, and the lysate was subjected to sequential centrifugations at 13,000 and 100,000 x *g*. ³⁵S-labeled pellet material from the 100,000 x *g* spin was resuspended in 50% Accudenz, overlaid with an Accudenz gradient from 48% to 20%, and subjected to equilibrium centrifugation. Twelve gradient fractions were harvested, and the fractionation profiles of Vps5p, Vps17p and Vps10p were determined by immunoprecipitation (Figure 12A). The migration of Vps10p was consistent with previously observed fractionation density for Golgi membranes (Horazdovsky, Davies et al. 1997), demonstrating that centrifugation equilibrium had been achieved and that

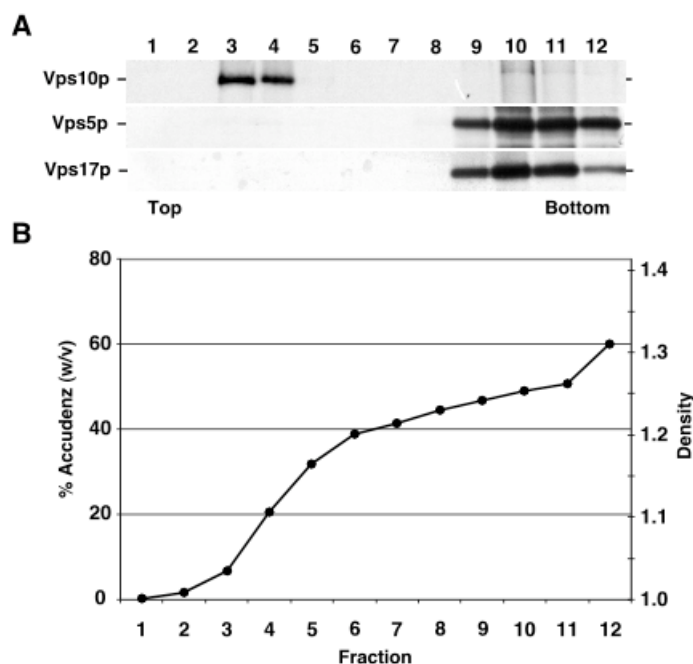


Figure 12. Density gradient flotation analysis of Vps5p, Vps10p and Vps17p.

(A) 30 OD₆₀₀ equivalents of 13,000 x g supernatant material from ³⁵S-labeled TVY614 spheroplasts were used to generate a 100,000 x g pellet. The pellet was resuspended in 50% Accudenz (w/v), overlaid with a 48-20% gradient, and subjected to centrifugation at 169,000 x g for 16hr. 1ml fractions were harvested and subjected to immunoprecipitation with Vps5p, Vps17p and Vps10p antisera. Samples were resolved by SDS-PAGE using 10% acrylamide gels and detected by fluorography. (B) Gradient profile of flotation experiment as determined by refractometry and expressed as either percent Accudenz (primary axis) or specific gravity (secondary axis).

membrane dispersal had occurred. Vps5p and Vps17p were found in fractions 9 through 12, with fraction 12 being the source of loaded material. The ability of both Vps5p and Vps17p to migrate into fractions 9 through 11 indicated an association with buoyant material, consistent with binding to membranes. It is interesting to note that some Vps5p and Vps17p was still associated with fraction 12. This pattern may represent partial association with large protein complexes, possibly the cytoskeleton, or may be material that had dissociated from membranes.

Vps5p membrane association is not dependent on Vps26p, Vps29p or Vps35p.

Vps5p and Vps17p have been implicated in mediating Vps10p recycling along with Vps26p, Vps29p and Vps35p (Horazdovsky, Davies et al. 1997; Nothwehr and Hindes 1997; Seaman, Marcusson et al. 1997; Seaman, McCaffery et al. 1998; Nothwehr, Bruinsma et al. 1999); however, the mechanism by which these 5 proteins mediate this

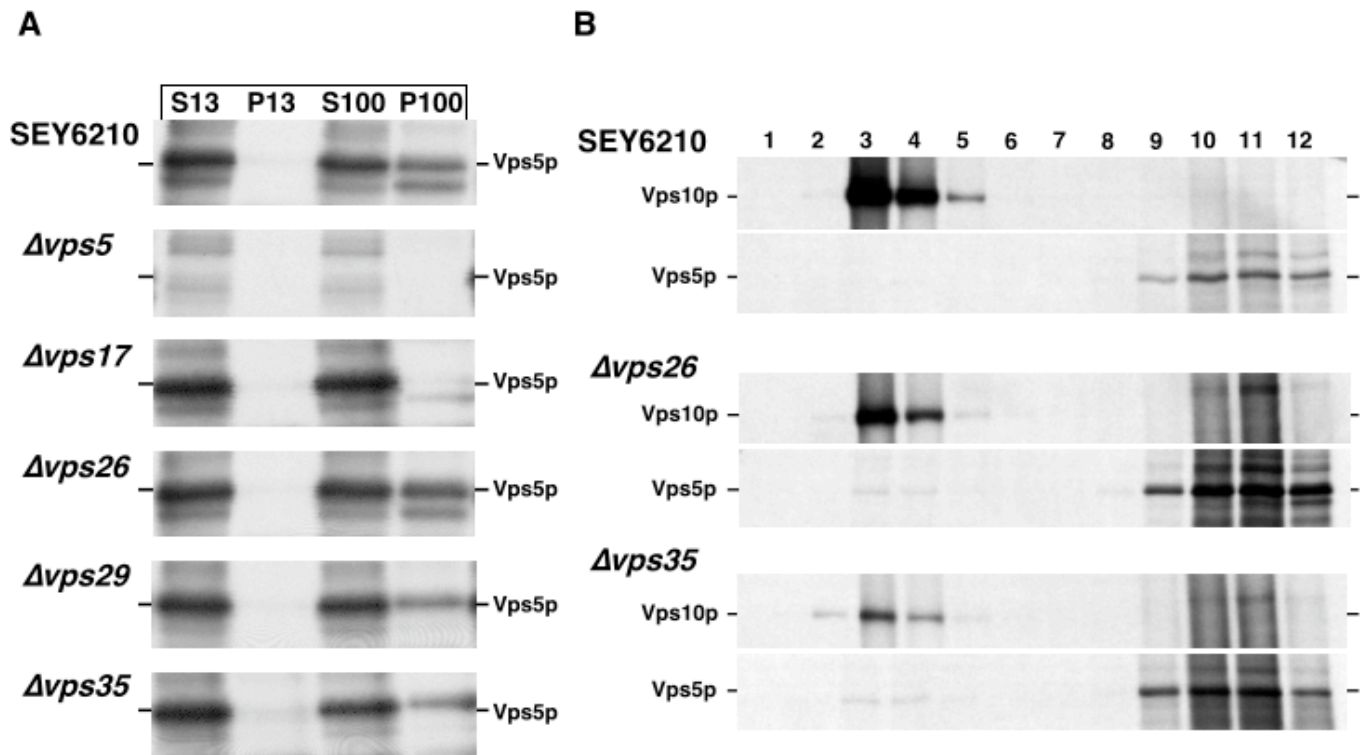


Figure 13. Vps5p fractionation in $\Delta vps26$, $\Delta vps29$ and $\Delta vps35$. (A) 20 OD₆₀₀ equivalents of ³⁵S-labeled spheroplasts were generated from the following strains: SEY6210 (parental), BHY152 ($\Delta vps5$), KKY10 ($\Delta vps17$), BDY261 ($\Delta vps26$), PSY129 ($\Delta vps29$), and EMY18 ($\Delta vps35$). The spheroplasts were lysed and subjected to sequential centrifugation at 500 x g, 13,000 x g, and 100,000 x g to generate 5 OD₆₀₀ equivalents of supernatant (S13, S100) and pellet (P13, P100) fractions. Samples were denatured and subjected to immunoprecipitation with Vps5p antiserum. (B) Density gradient flotation analyses of Vps5p and Vps10p in the P100 from SEY6210, BDY126 ($\Delta vps26$) and EMY18 ($\Delta vps35$).

process is unclear. Vps5p and Vps17p have been demonstrated to be codependent on each other for association with 100,000 x g membrane pellet, as demonstrated in Chapter 2. To examine the requirement for Vps26p, Vps29p and Vps35p in this association, Vps5p subcellular fractionation experiments (Figure 13A) were performed in strains deleted for *vps26* (BDY261), *vps29* (PSY129) or *vps35* (EMY18). In the wildtype strain (SEY6210), Vps5p exhibited a partial association with the 100,000 x g membrane pellet (P100). As previously reported (Horazdovsky, Davies et al. 1997), this association was dependent on the presence of Vps17p as P100 fractionation was lost in the $\Delta vps17$ strain (KKY10). However, in strains lacking either Vps26p, Vps29p or Vps35p, the membrane

association of Vps5p was still observed. Similar results were observed when Vps17p fractionation was examined (data not shown). These findings suggested that the membrane association of Vps5p and Vps17p is independent of the presence of Vps26p, Vps29p or Vps35p.

To confirm that the observed association with P100 material in the absence of Vps26p and Vps35p represented the membrane association indicated in Figure 12, 100,000 x g pelleted material from the $\Delta vps26$ and $\Delta vps35$ strains were subjected to flotation density gradient analysis (Figure 13B). Consistent with the fractionation pattern observed in the wild-type strain, Vps5p was observed in fractions 9 through 12 for both the $\Delta vps26$ and $\Delta vps35$ strains. These results indicated that the association with the P100 material observed in the subcellular fractionation experiments with the strains lacking Vps26p and Vps35p was the same as in the wild-type strain. Therefore, the membrane association of Vps5p and Vps17p is not dependent on other members of the complex.

Vps5p and Vps17p associate with Vps26p independent of Vps29p and Vps35p.

To further address the formation and function of this complex, additional protein crosslinking experiments have been performed (see Materials and Methods). Cleared lysates were generated from ^{35}S -labeled spheroplasts and incubated with the reducible crosslinking agent dithiobis[succinimidyl propionate] (DSP). After quenching the reaction, crosslinked lysates were subjected to sequential immunoprecipitations with Vps5p and Vps17p antisera. Crosslinked complexes were reduced, components were resolved by SDS-PAGE and subunits were detected by autoradiography. In the wild-type strain (SEY6210), Vps5p, Vps17p, Vps26p, Vps29p and Vps35p were evident upon

sequential immunoprecipitation with Vps5p and Vps17p antisera (Figure 14A, lane 1) (the band above Vps29p is Vps26p, compressed by the IgG front). The presence of all five proteins was dependent on the addition of crosslinking agent (lane 2) as well as on the presence of Vps5p (lane 3) and Vps17p (data not shown). In strains deleted for either *vps29* or *vps35* (lanes 5 and 7, respectively), both Vps29p and Vps35p were absent; however, Vps26p appeared to still be present with Vps5p and Vps17p in both the $\Delta vps29$ and $\Delta vps35$ strains.

To further address the apparent codependence of Vps29p and Vps35p for the interaction with Vps5p and Vps17p, a crosslinking experiment utilizing a sequential immunoprecipitation with Vps5p and Vps35p antisera was performed (Figure 14B). In a crosslinker-dependent (lane 2) and both Vps5p- and Vps35p-dependent manner (lanes 3 and 7), Vps5p and Vps35p could be isolated by the procedure (lane 1). In the strain lacking Vps29p, the interaction between Vps5p and

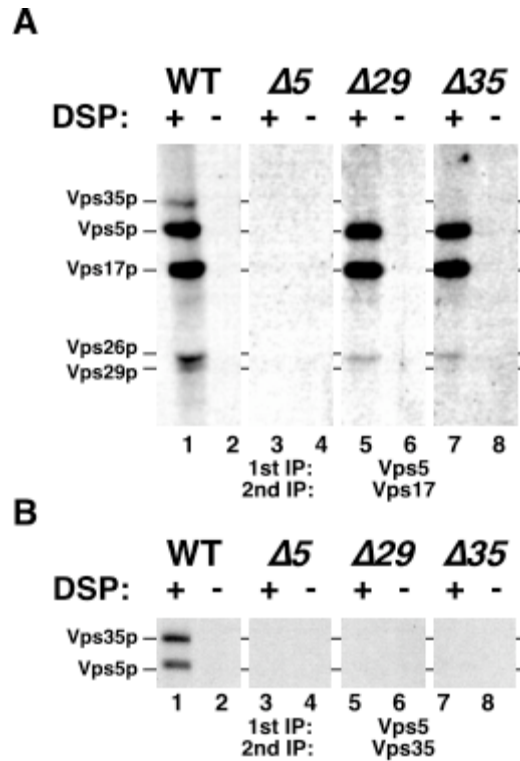


Figure 14. Crosslinking the Vps5p, Vps17p, Vps26p, Vps29p and Vps35p complex. (A) 5 OD₆₀₀ equivalents of 13,000 x g supernatants from ³⁵S-labeled SEY6210 (WT), BHY152 ($\Delta 5$), PSY129 ($\Delta 29$) and EMY18 ($\Delta 35$) were incubated with the reducible crosslinker DSP(+) or vehicle(-). The reactions were quenched, and samples were subjected to non-reducing sequential immunoprecipitation with Vps5p and Vps17p antisera. Crosslinked complexes were reduced, resolved by SDS-PAGE and detected by fluorography. (B) Crosslinking reactions were performed and subjected to non-reducing sequential immunoprecipitation with Vps5p and Vps35p antisera. Crosslinked complexes were reduced, resolved by SDS-PAGE and detected by fluorography.

Vps35p could not be detected (lane 5), consistent with results observed with sequential Vps5p-Vps17p immunoprecipitation (Figure 14A, lane 5). These results taken together with previously published Vps29p and Vps35p crosslinking studies (Seaman, McCaffery et al. 1998) and native immunoprecipitations (Reddy and Seaman 2001) are consistent with a model in which Vps29p and Vps35p form one subcomplex, Vps5p and Vps17p form a second subcomplex, and Vps26p links or stabilizes the interaction between the 2 subcomplexes (Figure 18).

The PX domain of Vps5p is required for VPS5 function.

The most prominent sequence conservation between Vps5p and its mammalian homolog SNX1 is the PX domain (Ponting 1996). To determine if the PX domain is required for function of Vps5p, an allele (*vps5 Δ PX*) lacking residues 313 to 385 was generated and tested for its ability to complement the Δ *vps5* strain. Upon delivery to the vacuole, carboxypeptidase Y (CPY) is cleaved from a precursor form (p2CPY) to the active form (mCPY). This transport process was evaluated by the CPY sorting assay in wild-type (SEY6210), Δ *vps5* (BHY152) and Δ *vps5* (BHY152) harboring the pRS414 *vps5 Δ PX* or pRS414 *VPS5* plasmids. In wild-type yeast, all of CPY was processed to the mature form (Figure 15A, lane 1) indicating vacuolar localization. This transport was dependent on Vps5p (lane 2), since all the CPY is present in the Golgi-modified p2 precursor form. The *vps5 Δ PX* allele was unable to complement the defects of the Δ *vps5* strain (lane 3); however, reintroduction of Vps5p's PX domain (pRS414 Vps5) restored CPY sorting (lane 4). Immunoprecipitation with Vps5p antiserum confirmed that

expression of Vps5 Δ PXp was comparable to Vps5p expression (Figure 15A, lower panel). These results indicated that the PX domain is required for Vps5p function.

The PX domain is also present in Vps17p. To determine if PX domains in both Vps5p and Vps17p are required for function of the complex, alleles of *vps5* and *vps17* were generated harboring PX domain point mutations analogous to a chronic granulomatous disease-associated mutation in the NADPH oxidase p47 subunit (p47-phox R42Q) (Kanai, Liu et al. 2001).

The p47 PX domain has been

demonstrated to bind phosphatidylinositol-3-phosphate in vitro, and structures of the p47 PX domain as well as the NADPH p40 PX domain in complex with PtdIns(3)P has been determined. These structural studies indicate that the R42 residue does not directly contact the phosphoinositide headgroup; however, in vitro analysis of the p47-phox R42Q protein demonstrated that the mutant protein fails to bind PtdIns(3)P (Kanai, Liu et al. 2001). The corresponding arginine319 in Vps5p and lysines 150 and 151 of Vps17p

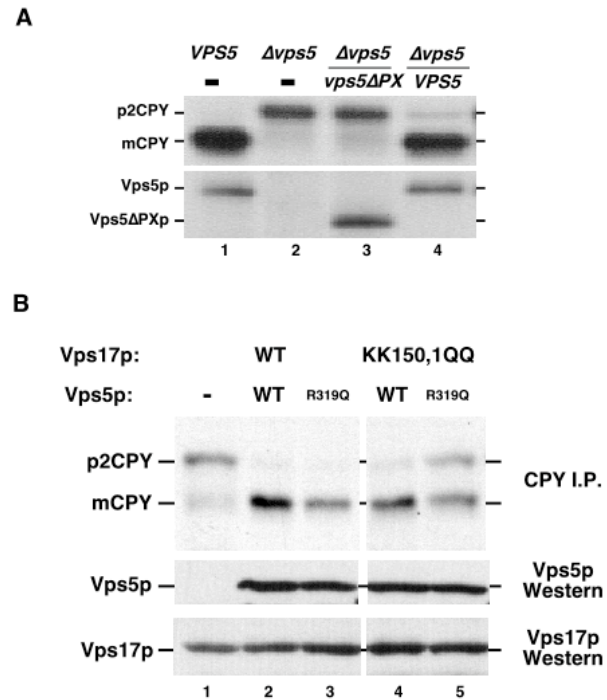


Figure 15. Characterization of Vps5 Δ PXp. (A) 5 OD₆₀₀ equivalents of SEY6210 (*VPS5*), BHY152 (Δ *vps5*) and BHY152 harboring pRS414 Vps5 Δ PX (*vps5* Δ PX) or pRS414 Vps5 (*VPS5*) were labeled with ³⁵S-Met, Cys for 10 minutes, and chased for 30 minutes after the addition of excess cold amino acids. Lysates were subjected to immunoprecipitation with CPY and Vps5p antisera. Samples were resolved by SDS-PAGE and detected by fluorography. The positions of mature vacuolar CPY (mCPY), Golgi-modified precursor CPY (p2CPY), full-length Vps5p and Vps5p lacking the PX domain (Vps5 Δ PXp) are noted. (B) CPY trafficking assessed in the BDY517 (Δ *vps5* Δ *vps17*) harboring *VPS5* and *VPS17* plasmids encoding wildtype of PX domain point mutant alleles. Western analysis with Vps5p and Vps17p antiserum was used to evaluate allele stability.

were mutated to arginine, and the alleles were tested *in vivo* for the ability to complement CPY sorting defects (Figure 15B, upper panel). Expression of either Vps5p R319Q with wildtype Vps17p (lane 3) or Vps17p KK150,1QQ with wild-type Vps5p (lane 4) was sufficient to complement the sorting defects of the BDY517 strain ($\Delta vps5 \Delta vps17$); this result suggested that these mutations in Vps5p and Vps17p only partially affect PtdIns(3)P binding, a finding that will need to be addressed *in vitro*. However, coexpression of Vps5p R319Q with Vps17p KK150,1QQ (lane 5) resulted in a partial CPY missorting phenotype. Equivalent expression of Vps5p alleles and Vps17p alleles in all strains tested was confirmed by western analyses (lower panels). This synthetic phenotype from combining the Vps5p R319Q and Vps17p KK150,1QQ alleles indicated that some level of redundancy exists between the two PX domains and implied that Vps17p PX domain is also involved in function of the complex. Examination of the Vps17 Δ PXp will be needed to confirm this result.

To assess a requirement for the Vps5p PX domain in formation of the Vps5p, Vps17p, Vps26p, Vps29p and Vps35p protein complex, crosslinking experiments were performed in a strain expressing Vps5 Δ PXp. ³⁵S-labeled lysates were incubated with the crosslinking agent DSP, and the complex was isolated by sequential immunoprecipitation with Vps5p and Vps17p antisera. As previously discussed, Vps5p, Vps17p, Vps26p, Vps29p and Vps35p were isolated from wildtype extracts (Figure 16A, lane 1), and this isolation was dependent on Vps5p (lane 3) and DSP (lane 2, 4, 6, 8). Expression of either Vps5 Δ PXp (lane 5) or Vps5p with the PX domain reintroduced (lane 7) was sufficient to reconstitute the complex; however, Vps29p and Vps35p appear to be present in reduced amounts in the Vps5 Δ PXp complex. While the PX domain of Vps5p is not absolutely

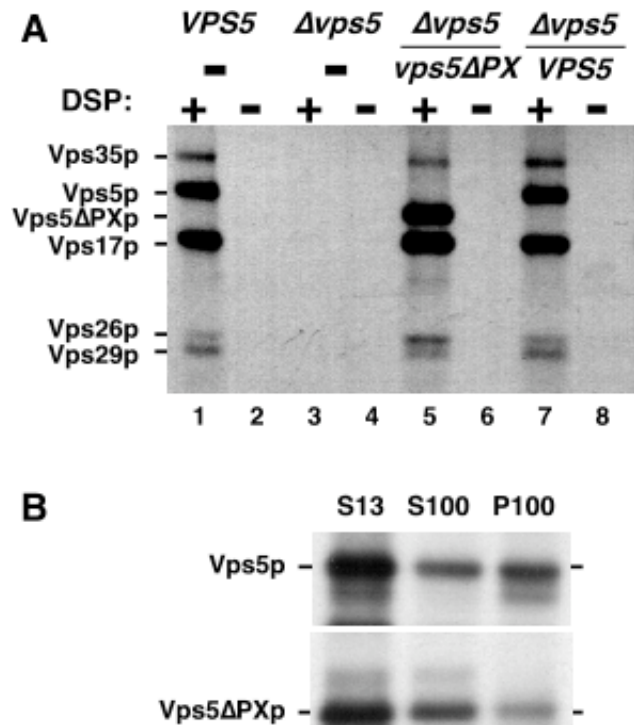


Figure 16. Analysis of Vps5ΔPXp complex formation and fractionation. (A) 5 OD₆₀₀ equivalents of ³⁵S-labeled 13,000 x g supernatants were incubated with the reducible crosslinker DSP(+) or vehicle(-). The reaction was quenched, and samples were subjected to non-reducing sequential immunoprecipitation with Vps5p and Vps17p antisera. Crosslinked complexes were reduced, resolved by SDS-PAGE and detected by fluorography. (B) 5 OD₆₀₀ equivalents of 13,000 x g supernatant (S13) and 100,000 x g supernatant and pellet fractions (S100, P100) from ³⁵S-labeled SEY6210 (upper panel) and BHY152 harboring pRS414 Vps5ΔPX (lower panel) were subjected to immunoprecipitation with Vps5p antiserum. Samples were resolved by SDS-PAGE and detected by fluorography.

required for interaction with the other subunits of the complex, the PX domain may subtly contribute to the associations.

To further characterize the *vps5ΔPX* allele, subcellular fractionation experiments were performed (Figure 16B). Vps5p exhibited a partial association with the 100,000 x g membrane pellet. Vps5ΔPXp also exhibited a reproducible, but diminished, association with the 100,000 x g pellet. Quantitation indicated that Vps5ΔPXp's P100 association was reduced by approximately 50% compared to Vps5p. This result suggested that the PX domain is involved in properly localizing the Vps5p protein complex to the membrane.

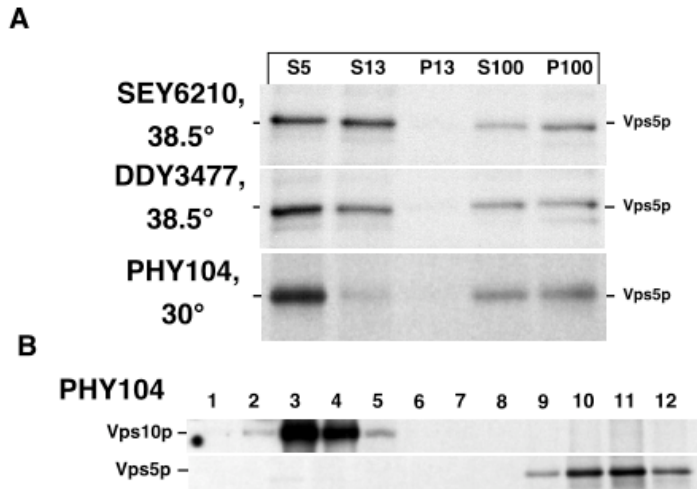


Figure 17. Vps5p fractionation in $\Delta vps34$ and $vps34^{ts}$ under restrictive conditions. (A) 20 OD₆₀₀ equivalents of SEY6210 (*VPS34*) and DDY3477 (*vps34^{ts}*), cultured at 25° prior to labeling, were subjected to a 10 minute ³⁵S-Met, Cys pulse, 40 minute chase at 38°. 20 OD₆₀₀ equivalents of PHY104 ($\Delta vps34$), cultured at 30°, were similarly labeled with ³⁵S-Met, Cys at 30°. Lysates were generated and subjected to sequential centrifugation at 500 x g, 13,000 x g, and 100,000 x g to generate 5 OD₆₀₀ equivalents of supernatant (S5, S13, S100) and pellet (P13, P100) fractions. Samples were denatured and subjected to immunoprecipitation with Vps5p antiserum. (B) Density gradient flotation analysis of Vps5p and Vps10p in the P100 from PHY104 ($\Delta vps34$).

Vps5p membrane association is independent of PtdIns(3)P.

PX domains have been implicated as a phosphatidylinositol binding motifs, with PtdIns(3)P as the predominate ligand (Bravo, Karathanassis et al. 2001; Cheever, Sato et al. 2001; Ellson, Gobert-Gosse et al. 2001; Kanai, Liu et al. 2001; Xu, Hortsman et al. 2001; Yu and Lemmon 2001). To address the possibility that PtdIns(3)P is responsible for properly localizing Vps5p via the PX domain, subcellular fractionation experiments were performed with yeast defective for PtdIns(3)P synthesis. Spheroplasts were generated from the wildtype yeast (SEY6210) and a strain (DDY3477) harboring a temperature-sensitive allele of Vps34p, the yeast PtdIns 3-kinase (Schu, Takegawa et al. 1993; Tall, Hama et al. 1999). The spheroplasts were shifted to non-permissive temperature (38.5°) during the 10 minute labeling and 40 minute chase period, and then fractionated by sequential centrifugation. Shifting strains containing this conditional allele of *vps34* to the nonpermissive temperature of 38.5° results in a rapid loss of PtdIns(3)P (Tall, Hama et al. 1999). Both the wildtype and *vps34^{ts}* strains demonstrate a similar Vps5p fractionation pattern of partial association with the 100,000 x g pellet (Figure 17A). Similar results were obtained when Vps5p subcellular localization was

examined in the $\Delta vps34$ strain (PHY102, Figure 17A), and density gradient analysis of the $\Delta vps34$ P100 material (Figure 17B) indicated that Vps5p fractionated in the same pattern as in SEY6210 (refer to Figure 17B). These results demonstrated that Vps5p localization is unaltered in a $vps34^{ts}$ strain at nonpermissive temperature or in the $\Delta vps34$ strain; therefore, PtdIns(3)P is not required for the membrane association of Vps5p.

Discussion

PX domain containing proteins participate in a large array of cellular activities (reviewed in (Sato, Overduin et al. 2001; Xu, Seet et al. 2001; Ellson, Andrews et al. 2002)). One of the largest groups of PX domain containing proteins is the sorting nexins. Over 20 potential sorting nexin proteins have been identified in both human and yeast sequence databases (Schultz, Copley et al. 2000), many of which have been implicated in the intracellular trafficking of membrane associated receptors (Ekena and Stevens 1995; Kurten, Cadena et al. 1996; Horazdovsky, Davies et al. 1997; Nothwehr and Hindes 1997; Haft, de la Luz Sierra et al. 1998; Voos and Stevens 1998; Otsuki, Kajigaya et al. 1999; Barr, Phillips et al. 2000; Nakamura, Sun-Wada et al. 2001; Parks, Frank et al. 2001; Phillips, Barr et al. 2001; Xu, Hortsman et al. 2001; Zheng, Ma et al. 2001; Lin, Lo et al. 2002). To gain a better insight into sorting nexin function we undertook a detailed analysis of Vps5p and Vps17p. Vps5p and Vps17p are yeast sorting nexins that together with Vps26p, Vps29p, and Vps35p form a complex which mediates the retrograde trafficking of the vacuolar protein sorting receptor, Vps10p, from a prevacuolar endosomal compartment to the Golgi (Horazdovsky, Davies et al. 1997; Nothwehr and Hindes 1997; Seaman, McCaffery et al. 1998). Through detailed density gradient

analysis we demonstrate that Vps5p and Vps17p are associated with a unique membrane compartment and that this association does not require Vps26p, Vps29p, or Vps35p. Further analysis indicated that Vps5p and Vps17p associate with Vps26p independent of Vps29p and Vps35p and that Vps29p and Vps35p are dependent on each other for association with Vps5p and Vps17p. Vps5p's PX domain has been shown to be required for function but is not required for Vps5p's interaction with Vps17p, with Vps26p, or with Vps29p and Vps35p. Though the Vps5p PX domain has been shown to bind PtdIns(3)P (Yu and Lemmon 2001), PtdIns(3)P is not required for Vps5p membrane association. These results indicate that the PX domain of Vps5p does not solely mediate the interaction of this protein with cellular membranes via PtdIns(3)P but plays an important function regulating Vps5p activity in intracellular receptor trafficking.

Vps5p and Vps17p were previously shown to be associated with a very dense material distinct from the Golgi or endosomal compartments (Horazdovsky, Davies et al. 1997). Using density gradient flotation we demonstrate that this distinct dense material contains a membrane component. These results are consistent with those reported by Seaman, et al., whose cryoelectron microscopy analysis indicated that Vps5p is associated with vesicular or tubulovesicular structures (Seaman, McCaffery et al. 1998). The density of this membrane fraction uncovered here is consistent with that of a coated vesicle. Whether Vps5p, Vps17p, Vps26p, Vps29p and Vps35p serve as a vesicle coat remains to be determined.

Analysis of subcellular fractionation in the $\Delta vps26$, $\Delta vps29$ and $\Delta vps35$ strains indicates that Vps5p and Vps17p associate with membrane structures independent of Vps26p, Vps29p and Vps35p. This finding is consistent with the unique phenotypes

associated with *vps5* and *vps17* mutant cells (Banta, Robinson et al. 1988; Raymond, Howald-Stevenson et al. 1992). *Vps5* and *vps17* are classified as Class B *vps* mutants due to a fragmented vacuole (10-20 small vacuole-like structures per cell). In contrast, *vps29* and *vps35* mutants exhibit a normal vacuole structure (3-5 vacuoles per cell; Class A), and *vps26* is classified as a Class F mutant (a combination of the Class A and Class B vacuole morphology phenotypes). Although they are not associated with the vacuolar membrane, Vps5p and Vps17p retain some function in maintaining vacuolar morphology independent of Vps26p, Vps29p and Vps35p; thus, it is not surprising that the Vps5p and Vps17p membrane association is unaltered in the $\Delta vps26$, $\Delta vps29$ and $\Delta vps35$ strains. Similarly, the ability of Vps26p to associate with Vps5p and Vps17p in crosslinking experiments independent of Vps29p and Vps35p is also consistent with the distinct vacuolar phenotypes exhibited by *vps26* mutants and *vps29* or *vps35* mutants. Additionally, it had been previously demonstrated that Vps26p can associate with Vps29p and Vps35p independent of Vps5p and Vps17p (Seaman, McCaffery et al. 1998; Reddy and Seaman 2001). These results are consistent with a model in which Vps5p and Vps17p form one subcomplex, Vps29p and Vps35p form a second subcomplex, and Vps26p links or stabilizes the interaction between the two subcomplexes.

To address if the Vps5p PX domain is required for protein function, an allele lacking the PX domain was generated (Vps5 Δ PXp). This allele is unable to complement the CPY sorting defects of $\Delta vps5$ but retains interaction with the other components of the protein complex; thus, the PX domain is not required to form the protein complex, but the assembled complex is not functional. Subcellular fractionation experiments suggest that the defect associated with deletion of the Vps5p PX domain is a decreased association

with the membrane. The PX domains of Vps5p and Vps17p have been demonstrated to bind PtdIns(3)P (Yu and Lemmon 2001), consistent with the decreased membrane association for Vps5 Δ PXp. However, a similar effect on Vps5p localization was not observed by eliminating PtdIns(3)P with either the Δ *vps34* mutant or the *vps34ts* strain at nonpermissive temperature. In addition, the discovery that Vps30p and Vps38p appear to modulate the Vps15p-Vps34p (PtdIns 3-kinase) complex and *vps30* and *vps38* mutants affect Vps10p localization further implicate a role for PtdIns(3)P in the retrograde trafficking of Vps10p (Seaman, Marcusson et al. 1997; Kihara, Noda et al. 2001); yet, mutations in *vps30* and *vps38* do not alter vacuolar morphology (Class A mutants) (Banta, Robinson et al. 1988; Raymond, Howald-Stevenson et al. 1992), and Vps5p fractionation is unaltered in the Δ *vps30* strain (data not shown). Taken together these results indicate that Vps5p and Vps17p can associate with membranes independent of PtdIns(3)P and that this PtdIns(3)P independent membrane association correlates with maintenance of vacuolar morphology; correspondingly, Vps5 Δ PXp is unable to complement the vacuolar morphology defects of the Δ *vps5* strain (data not shown). Though PtdIns(3)P is required for Vps10p retrograde trafficking, the data presented here indicate that PtdIns(3)P may serve an important regulatory role in this process and is not merely involved in recruitment of Vps5p and Vps17p to the membrane.

The prevailing model for function of the Vps5p, Vps17p, Vps26p, Vps29p and Vps35p complex in Vps10p recycling is as a vesicle coat (termed the retromer; (Seaman, McCaffery et al. 1998; Pfeiffer 2001)), although the ability of these proteins to function as such has yet to be demonstrated. However, other functionalities have been assigned to members of the Vps5p protein complex. Experiments by Nortwehr et al. (Nothwehr,

Bruinsma et al. 1999; Nothwehr, Ha et al. 2000) have shown that *VPS35* can genetically interact with a *VPS10* cytoplasmic-tail point mutation and that Vps35p can physically interact with other transmembrane proteins that undergo retrograde trafficking to the Golgi compartment. These genetic data and the physical association indicate that Vps35p and Vps29p constitute a receptor-associated adaptor-like complex. We have demonstrated by coimmunoprecipitation experiments that Vps5p is also physically associated with Vps10p (Chapter 2). This association is presumably mediated by the interaction with Vps29p and Vps35p; however, direct association between Vps5p and Vps10p may also occur since the mammalian Vps5p homolog SNX1 was initially identified in a 2-hybrid screen with the cytoplasmic domain of the EGF receptor (Kurten, Cadena et al. 1996). Additional experiments are needed to address further the Vps5p-Vps10p association now that this interaction has been demonstrated.

From the results presented here together with those previously reported a model can be constructed

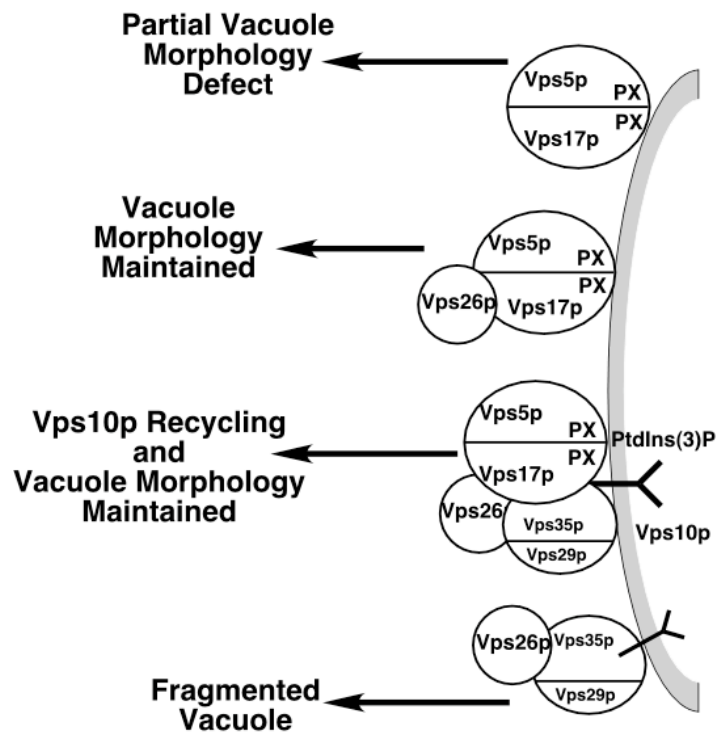


Figure 18. Model of Vps5p, Vps17p, Vps26p, Vps29p and Vps35p coordinated function. Vps5p and Vps17p associate with membranes independent of Vps26p, Vps29p, Vps35p and PtdIns(3)P and are sufficient to maintain most vacuolar morphology. Vps26p can bind Vps5p and Vps17p and potentiates the Vps5p-Vps17p morphology maintenance activity. The adaptor-like subunits Vps29p and Vps35p can also bind Vps26p as well as interact with the cytoplasmic tail of Vps10p. In the presence of PtdIns(3)P, Vps5p, Vps17p, Vps26p, Vps29p and Vps35p interact in a productive manner with Vps10p to facilitate retrograde transport.

describing the functional contribution of Vps5p and its associated proteins to retrograde trafficking and the maintenance of vacuolar morphology (Figure 18). Vps5p and Vps17p associate with a prevacuolar compartment independent of Vps26p, Vps29p and Vps35p. This association is largely sufficient to maintain proper vacuolar morphology, although the mechanism by which this maintenance occurs is unclear. Vps26p binds Vps5p and Vps17p and potentiates this activity to allow complete maintenance of vacuolar morphology. However, to mediate Vps10p recycling, the presumed adaptor proteins Vps29p and Vps35p must bind to Vps5p, Vps17p and Vps26p. PtdIns(3)P, generated through the concerted action of Vps30p and Vps38p with the Vps15p-Vps34p (PtdIns 3-Kinase) complex, is also required for the coordinated function of Vps29p and Vps35p with Vps5p, Vps17p, and Vps26p. PtdIns(3)P interacts with the PX domains of Vps5p and Vps17p and likely serves to regulate the formation and/or function of this complex; however the PX domain has an additional role in mediating Vps5p localization independent of PtdIns(3)P. Further examination of this sorting nexin protein complex in vivo and particularly in vitro will be required to expand this model and determine if this Vps5p, Vps17p, Vps26p, Vps29p and Vps35p complex functions as a coat complex or serves some other function in regulating retrograde protein trafficking events.

Preface to Chapters 4 and 5

In the course of using Vps9p reagents as controls for experiments investigating Vps5p function, a higher molecular weight form of Vps9p was observed. This led to the identification of this band as the monoubiquitylated form of Vps9p and the ensuing studies described in Chapters 4 and 5. In Chapters 2 and 3, the role of the Vps5p-Vps17p protein complex in regulating Vps10p recycling from the endosome was explored. The focus of the following chapters will be upon regulation of traffic into the endosome through ubiquitin interaction with Vps9p.

Chapter 4. Vps9p CUE domain ubiquitin binding is required for efficient endocytic protein traffic.

Summary

Rab5 GTPases are key regulators of protein trafficking through the early stages of the endocytic pathway. The yeast Rab5 ortholog Vps21p is activated by its guanine nucleotide exchange factor Vps9p. Here we show that Vps9p binds ubiquitin and that the CUE domain is necessary and sufficient for this interaction. Vps9p ubiquitin binding is required for efficient endocytosis of Ste3p but not for the delivery of the biosynthetic cargo CPY to the vacuole. In addition, Vps9p is itself monoubiquitylated. Ubiquitylation is dependent on a functional CUE domain and Rsp5p, an E3 ligase that participates in cell surface receptor endocytosis. These findings define a new ubiquitin binding domain and implicate ubiquitin as a modulator of Vps9p function in the endocytic pathway.

Introduction

Rab proteins are critical regulators of the vesicle targeting and fusion events (reviewed in (Pfeffer 1999; Zerial and McBride 2001)). Discrete classes of these small GTPases mediate very specific transport events, showing little if any functional overlap. For example, the Rab5 family members appear to be involved exclusively in targeting events within the early stages of the endocytic pathway (Gorvel, Chavrier et al. 1991; Bucci, Parton et al. 1992). The activation of Rab5 GTPases like all Rab proteins is dependent on the state of bound nucleotide, GDP or GTP. Two classes of proteins that

modulate the Rab nucleotide occupancy are the GTPase activating proteins (GAPs) and the guanine nucleotide exchange factors (GEFs). GAPs stimulate GTP hydrolysis, leaving the Rab in the GDP-bound, inactive state; conversely, GEFs initiate GDP release to permit GTP binding and thereby Rab activation. Multiple GAPs and GEFs for the Rab proteins have been identified, and an interesting distinction has been observed (reviewed in (Segev 2001)). The Rab GAPs share a conserved sequence motif and exhibit substrate promiscuity among the Rab families ((Du, Collins et al. 1998; Albert and Gallwitz 1999), and reviewed in (Scheffzek, Ahmadian et al. 1998)). In contrast, the GEF proteins for different Rab families are dissimilar at the sequence level and show great specificity for their cognate Rab proteins. Consequently, the GEFs appear to be the primary mechanism to control specific Rab activity.

A number of exchange factors for Vps21p/Rab5 family members have been identified in mammalian and yeast systems. In yeast, Vps9p is the exchange factor for the Rab5 ortholog Vps21p (Hama, Tall et al. 1999). *VPS9* was initially identified in genetic screens for mutants defective in vacuolar protein sorting (Burd, Mustol et al. 1996). *In vitro* reconstitution of Vps9p-stimulated GDP-release and GTP-loading onto Vps21p demonstrated that Vps9p is the GEF for Vps21p (Hama, Tall et al. 1999). Concurrently, Rabex5 was identified as a Rab5-binding protein and demonstrated to exhibit *in vitro* GEF activity (Horiuchi, Lippe et al. 1997). In addition to conserved functions in activating Rab5 proteins, yeast Vps9p (451 aa) and human Rabex5 (491 aa) share 27% overall sequence identity (Horiuchi, Lippe et al. 1997). A peptide comprised of residues 157-347 of Vps9p was identified as the domain necessary and sufficient for GEF catalytic activity (Gregory Tall, Darren Carney and Bruce Horazdovsky, manuscript

in preparation). While Vps9p is the only known GEF for Vps21p in yeast, seven human proteins have been identified with the Vps9 domain in addition to human Rabex5 (SMART database) (Schultz, Copley et al. 2000; Letunic, Goodstadt et al. 2002). These human Rab5 GEF proteins contain well defined signaling, protein-protein interaction and structural domains, including Src homology 2 (SH2) and Ras Association (RA) motifs (Schultz, Copley et al. 2000; Letunic, Goodstadt et al. 2002; Saito, Murai et al. 2002), Rho GEF and seven-bladed β propeller domains (Hadano, Hand et al. 2001; Yang, Hentati et al. 2001; Eymard-Pierre, Lesca et al. 2002), a Ras GAP motif (Nagase, Kikuno et al. 2000) and Ankyrin repeats (Wiemann, Weil et al. 2001). The coincidence of these signaling motifs with the Vps9 domain suggests that these proteins serve as key integrators of signal transduction pathways and the receptor endocytosis machinery. This concept has been demonstrated for the Rab5 GEF, Rin1 (Tall, Barbieri et al. 2001).

In contrast to Rin1, the mechanisms regulating Vps9p and Rabex5 are unclear. Here we provide evidence that ubiquitin binding and monoubiquitylation regulate yeast Vps9p. The CUE domain of Vps9p is shown to mediate an interaction with ubiquitin, and we show that this interaction is required to potentiate Vps9p function in endocytic traffic to the vacuole. We demonstrate that Vps9p is monoubiquitylated and that this modification is dependent on CUE-dependent ubiquitin binding and the E3 ubiquitin ligase Rsp5p. Together, these findings identify a novel role for ubiquitin in regulating endocytosis by the Vps21p/Rab5 exchange factor Vps9p.

Materials and Methods

Strains and Reagents

Bacterial strains used in this study were DH5 α (Invitrogen) and HMS174 DE3 (Novagen). The *Saccharomyces cerevisiae* strains used in this study were SEY6210 (*MATa trp1 lys2 leu2 his3 ura3 suc2 Δ 9*) (Robinson, Klionsky et al. 1988), CBY1 (SEY6210; *vps9 Δ 1::HIS3*) (Burd, Mustol et al. 1996), PSY83 (SEY6210; *vps8 Δ 1::HIS3*) (Horazdovsky, Cowles et al. 1996), MYY290 (*MATa his3 leu2 ura3*) (Smith and Yaffe 1991), MYY808 (MYY290; *smm1/rsp5^{ts}*) (Fisk and Yaffe 1999) and L40 (*MATa trp1 leu2 his3 LYS2::lexAop₄-HIS3 URA3::(lexAop₄-lacZ)*) (Fisk and Yaffe 1999). The bacterial strains were grown in Luria-Bertani (LB) medium supplemented with ampicillin (100 μ g ml⁻¹) and kanamycin (50 μ g ml⁻¹) when necessary (Miller 1972). Yeast strains were grown in media containing 2% peptone, 1% yeast extract and 2% glucose (YPD) or synthetic media supplemented with appropriate amino acids as required (Sherman, Fink et al. 1979). Thermostable DNA polymerases, restriction endonucleases and DNA modifying enzymes were purchased from Invitrogen (Carlsbad, CA), Roche Molecular Biochemicals (Indianapolis, IN) or New England Biolabs (Beverly, MA). EasyTag Expre³⁵S³⁵S Protein Labeling Mix was purchased from PerkinElmer Life Sciences (Boston, MA). Protein A Sepharose was purchased from Amersham Biosciences (Piscataway, NJ). Zymolyase 100T was purchased from Seikagaku (Tokyo, Japan). Glass beads (0.5 mm) were purchased from Biospec Products, Inc. (Bartlesville, OK). Ni-NTA agarose and penta-His antibody were purchased from Qiagen Inc. (Valencia, CA). Bioscale Q2 was purchased from Biorad Laboratories, Inc. (Hercules, CA). HA.11 monoclonal antibody (raw ascites fluid) was purchased from Covance Inc. (Princeton,

NJ). Antiserum for Vps9p was obtained from Scott Emr (UCSD). SuperSignal West Femto Maximum Sensitivity Substrate was purchased from Pierce Biotechnology Inc. (Rockford, IL). FM4-64 was purchased from Molecular Probes Inc. (Eugene, OR).

Plasmid construction

VPS9 was amplified with Vent DNA Polymerase and oligos Vps9-20 (5'-TCCTCTCGAGAATAGTACCGCAATAGGAGA-3') with Vps9-21 (5'-CCGCGGCTAGCGGCCGCCTTCTGACAGAGAAAGTAGAGC-3') and Vps9-22 (5'-GGCGGCCGCTAGCCGCGGTGATCTCATGCACATATTTC-3') with Vps9-23 (5'-TATAGAGCTCTGGCAGGCCCGTTTACGTAGGC-3'), and the products were used as template in overlapping polymerase chain reaction (PCR) with Vps9-20 and Vps9-23. The resultant 2.9 kb fragment was subcloned into pRS416 (Christianson, Sikorski et al. 1992) via the *Xho I* and *Sst I* sites present in the oligos to generate pRS416 Vps9. *Vps9ΔCUE* was amplified in two portions, via Vps9-20 with Vps9-24 (5'-GCTAGCGGCCGCGGTTCTCTTCAATTTTCTTAATTAACG-3') and Vps9-22 with Vps9-23. The resultant fragments were then used as a template for overlapping PCR with Vps9-20 and Vps9-23 and subcloned into pRS416 via the *Xho I*, *Sst I* sites to yield pRS416 Vps9ΔCUE. *Vps9 M419A* was amplified in two portions via Vps9-20 with Vps9 M419A Noncoding (5'-TCCATATCTGGAAACGCGTTCTGTAATGTGTTC-3') and Vps9 M419A Coding (5'-GAACACATTACAGAACGCGTTTCCAGATATGGA-3') with Vps9-23. The resultant fragments were digested with *Xho I*, *Mlu I* and *Mlu I*, *Sst I*, respectively, and cloned into the *Xho I*, *Sst I* sites of pRS315 (Christianson, Sikorski et al. 1992) to generate pRS315 Vps9 M419A. *VPS9 M419A* open reading frame was then

amplified with Vps9-3 (5'-AATCGGATCCCATGACTGATGATGAAAAGAGG-3') and Vps9-4 (5'-TGTGCATGGTCGACTTATTCTGACAGAGAAAGTAG-3') and subcloned into the *BamH I*, *Sal I* sites of pMBP parallel 1 (Sheffield, Garrard et al. 1999) to generate pMBP Vps9 M419A. The *BamH I*, *Sal I* fragment from pGT9-1 (Hama, Tall et al. 1999) was subcloned into pMBP parallel 1 (pMBP Vps9) and pET28b (Novagen, pET28 Vps9) as well. The CUE domains from *VPS9* wildtype and M419A were amplified with Vps9-26 (5'-TTGAGGATCCCGAACGAAAGGACACGTTGAACAC-3') and Vps9-4 and subcloned into pMBP parallel 1 (pMBP Vps9 CUE wt and M419A). To generate His₆-Vps9p carboxyl-terminal (Δ C) and amino-terminal (Δ N) truncations, Vps9-3 with Vps9-13 (5'-GGGTTTCAGTAAAGTGTCGACTGGCTGTAACTAATCCGG-3') and Vps9-8 (5'-TCTTTAGGATCCTATGCAGAAACCATTAGACGATGAGCAT-3') with Vps9-4 were used in PCR amplifications with template pGT9-1, and the resultant fragments were cloned into the *BamH I*, *Sal I* sites of pET28b (pET28 Vps9 Δ C and Δ N). The Vps9-8/4 PCR product was also subcloned into the *BamH I*, *Sal I* sites of pVJL11 (Jullien-Flores, Dorseuil et al. 1995) (Vps9 C-terminal bait). pET28 Vps9 and the truncation constructs (pET28 Vps9 Δ C and Δ N) were used as templates in PCR reactions with pET28-1 (5'-CTTTAAGAAGGAGATCTACCATGGGCAGCA-3') and Vps9-15 (FL, Δ N; 5'-TGTGCATGAGATCTTTATTCTGACAGAGAAAGTAG-3') or Vps9-17 (Δ C; 5'-GGGTTTCAGTAAAGTAGATCTTGGCTGTAACTAATCCGG-3'); the resultant fragments were digested with *Bgl II* and cloned into the *Bgl II* site of pPGK415 to generate pHis9-1 (1-451), pHis9-2 (1-347) and pHis9-3 (158-451). pPGK415 was generated by subcloning the *Hind III* fragment from pEMBLye30/2 (Banroques,

Delahodde et al. 1986) into the *Hind III* site of pRS415. Oligos HA 5' (5'-GGATCCAATGTACCCATACGATGTTCTGAC-3') and Ubiquitin 3' (5'-GAATTCTCAACCACCTCTTAGCCTTAAGAC-3') were used with pEF-HA-Ub (Li Deng and Zhijian Chen, UTSW) to amplify HA-ubiquitin, and the product was cloned into the *BamH I* and *EcoR I* sites of pGPD416 (Mumberg, Muller et al. 1995) and pET28b. Ste3-1 (5'-TGATCTCGAGGCGAATCGCACATTGCGCAAC-3') and Ste3-2 (5'-GTGTTAGCGGCCGCCAGGGCCTGCAGTATTTTC-3') were used to amplify the *STE3* promoter and open reading frame from genomic DNA; the product was digested with *Xho I*, *Not I* and subcloned into the *Xho I*, *Not I* sites of the pRS414 vector (Christianson, Sikorski et al. 1992) containing the HA₃ coding and *VPS26* terminator sequences from the *Not I* to *Ksp I* sites (pRS414 Ste3HA). *UBC5* was amplified from genomic DNA with Ubc5 5' (5'-GGATTCAATGTCTTCCTCCAAGCGTATTG-3') and Ubc5 3' (5'-CAGCTGTCAAACAGCATATTTTTTTAG-3'); the PCR product was cloned into the *Sma I* site of pBluescript (Stratagene), and the *BamH I*, *Sal I* fragment was then subcloned into the *BamH I*, *Sal I* sites of pMBP parallel 1 (pMBP Ubc5). Rsp5-1 (5'-AAAGAGATCTAATGCCTTCATCCATATCCGTC-3') and Rsp5-2 (5'-TGCGCTCGAGTCATTCTTGACCAAACCCTATGG-3') were used with genomic DNA to amplify the *RSP5* open reading frame; the PCR product was digested with *Bgl II*, *Xho I* and subcloned into the pMBP parallel 1 *BamH I*, *Sal I* sites (pMBP Rsp5).

Protein expression and purification

pMBP Vps9, pMBP Vps9 M419A, pMBP Vps9 CUE, pMBP Vps9 CUE M419A, pMBP Ubc5, pMBP Rsp5, pQE31 Vps9, pET28 Vps21 and pET28 HA-Ubiquitin were

transformed into HMS174 DE3. For expression of His₆HA-Ub and His₆Vps21, *E. coli* were cultured at 37°, induced with 500 μ M isopropyl- β -D-thiogalactoside (IPTG), and harvested after 4 hours of protein production at 37°. For the remaining protein-fusions, cultures were shifted from 37° to room temperature prior to induction with 500 μ M IPTG and harvested after 10-15 hours protein production at room temperature. MBP-protein fusions were affinity purified with amylose resin following the manufacturer's instructions (New England Biolabs, Beverly, MA). His₆-tagged proteins were affinity purified with Ni-NTA agarose following the manufacturer's instructions (Qiagen Inc, Valencia, CA); and His₆Vps9p was further purified with the Bioscale Q2 column following the manufacturer's recommended conditions (Biorad Laboratories Inc., Hercules, CA). Protein fusions were concentrated, buffer switched to 50 mM Tris (7.5), 150 mM NaCl, and stored at -80° for later use.

Ubiquitin binding assay

Putative Ubiquitin binding protein (MBP-Vps9p, MBP-Vps9p M419A; 4 μ g ml⁻¹) was incubated with either His₆HA-Ubiquitin (13 μ g ml⁻¹) or Bovine Serum Albumin (5 μ g ml⁻¹) in 1 ml Binding Buffer (50 mM Tris (pH 7.5), 300 mM KOAc with protease inhibitors (N-tosyl-L-phenylalanine-chloromethyl ketone (TPCK), N α -p-tosyl-L-lysine-chloromethyl ketone (TLCK), phenylmethyl sulfonyl fluoride (PMSF), leupeptin, trypsin inhibitor)) with Ni-NTA agarose (40 μ l). Binding reactions were incubated > 1 hour at 4° in a Rotator. The Ni-NTA agarose was then washed 6 times with 1 ml Binding Buffer. 50 μ l Elution Buffer (Binding Buffer with 200 mM Imidazole) was added, and the samples were incubated 10 minutes on ice. The supernatant was transferred, 5x Laemmli

Sample Buffer (0.312 M Tris (pH 6.8), 10% sodium dodecyl sulfate (SDS), 25% β -mercaptoethanol, 0.05% bromophenol blue) was added and the sample was incubated at 37° for 10 minutes. The eluate material was resolved by SDS-PAGE, and western analyses were performed with Vps9p (1:2,000) or Rabex5 (1:1,000) antisera or HA.11 monoclonal antibody (1:10,000), appropriate HRP-conjugated antibody (1:2,000), and SuperSignal West Femto Maximum Sensitivity Substrate (1:4 in 50 mM Tris (pH 7.5), 150 mM NaCl). Analysis of Vps9 CUE domain ubiquitin binding was conducted similarly except that His₆Vps21p (equimolar to His₆HA-Ub) was used as the negative control, Binding Buffer was 50 mM NaPO₄ (pH 7.5), 300 mM KOAc, and western analysis utilized MBP antiserum (1:5,000; New England Biolabs, Beverly, MA).

Whole-cell western analysis

Yeast strains were grown in YPD or YNB-glucose with appropriate amino acids, and 1 OD₆₀₀ equivalent was harvested during log-phase growth (0.5-0.8 OD₆₀₀ ml⁻¹). Samples were resuspended in 100 μ l 5x Laemmli Sample Buffer and approximately 150 μ l of glass beads (0.5 mm) were added. Samples were vortexed in mass for 10 minutes and heated at 95° for 4 minutes. 0.1 OD₆₀₀ equivalent was resolved by SDS-PAGE, and western analysis was performed with Vps9p antiserum (1:2,000), HRP-conjugated anti-rabbit antibody (1:2,000), and SuperSignal West Femto Maximum Sensitivity Substrate (1:4 in 50 mM Tris (pH 7.5), 150 mM NaCl).

CPY immunoprecipitation Assay

CPY immunoprecipitation experiments were performed as previously described (Horazdovsky, Busch et al. 1994). Yeast strains were grown in YNB-glucose, and labeled at 30° for 10 minutes with EasyTag Expre³⁵S³⁵S Protein Labeling Mix (30 μ Ci OD₆₀₀⁻¹) before the addition of excess methionine and cysteine. Following the 30 minute chase, samples were precipitated with trichloroacetic acid (TCA, final concentration 10%) and resuspended in Boiling Buffer (50 mM Tris, pH 7.5, 1 mM EDTA, 1% SDS). Glassbeads were added, samples were vortexed, and CPY was isolated as previously described. Immunoprecipitated material was resolved by SDS-PAGE and visualized by fluorography.

Ste3p degradation assay

Yeast strains harboring the pRS414 Ste3HA plasmid were grown in YNB-glucose, 0.2 % Yeast Extract with appropriate amino acids past log growth phase. Cultures were diluted to 0.2 OD₆₀₀ ml⁻¹ and cultured for 4 hours. 3 OD₆₀₀ equivalents were harvested and resuspended at 1 OD₆₀₀ ml⁻¹ in YNB-glucose, and cyclohexamide (1 mg ml⁻¹ in ethanol) was added to 1.3 μ g ml⁻¹. 0.5 OD₆₀₀ equivalents were removed at 0, 20, 40 and 60 minutes after cyclohexamide addition and NaN₃ and NaF added to 10 mM. Samples were resuspended in 100 μ l 2x Urea Sample Buffer (6 M Urea, 125 mM Tris (pH 6.8), 6% SDS, 10% β -mercaptoethanol, 0.01% bromophenol blue) and approximately 150 μ l of glass beads (0.5 mm) were added. Samples were vortexed in mass for 10 minutes and heated at 65° for 4 minutes. An additional 100 μ l 2x Urea Sample Buffer was added, and samples were subjected to 5 min, 14,000 rpm

centrifugation. 0.05 OD₆₀₀ equivalent was resolved by SDS-PAGE, and western analysis was performed with HA.11 monoclonal antibody (1:5,000), HRP-conjugated anti-mouse antibody (1:2,000), and SuperSignal West Femto Maximum Sensitivity Substrate (1:5 in 50 mM Tris (pH 7.5), 150 mM NaCl). The ABI Computing Densitometer 300 A was used with ImageQuant V1.2 for quantitation. Similar degradation patterns were observed when analyses were performed using Ste3p antiserum (Greg Payne, UCLA) to detect endogenous receptors, indicating that the Ste3HA reporter recapitulates Ste3p trafficking (data not shown).

In vivo ubiquitylation assay

Yeast strains harboring the pGPD416 HA-Ubiquitin plasmid were grown in YNB-glucose with appropriate amino acids. 10 OD₆₀₀ equivalents were harvested in late log growth phase (approximately 1 OD₆₀₀ ml⁻¹) and resuspended in 100 mM Tris (pH 9.4), 10 mM DTT. Following a 10 minute room temperature incubation, samples were resuspended in Spheroplasting Buffer (25 mM Tris (pH 7.5), 1 M Sorbitol, 1x YNB, 4 % Glucose, 1x amino acids, 100 µg ml⁻¹ Zymolyase 100T) and incubated 10 minutes at 30°. Samples were osmotically lysed in 10 mM NaPO₄ (pH 8.0) with Roche EDTA-free protease inhibitor cocktail. The lysate was then cleared by a 10 minute, 16,000 x g spin at 4°. The cleared lysate was then adjusted to approximately 25 mM NaPO₄ (pH 8.0), 300 mM NaCl, 2 % Glycerol, and 50 µl Ni-NTA agarose was added. Samples were incubated > 1 hour at 4°, and washed 4 times with Wash Buffer (50 mM NaPO₄ (pH 8.0), 300 mM NaCl, 5 % Glycerol). 100 µl Elution Buffer (Wash Buffer with 200 mM Imidazole) was added, and the samples were incubated 10 minutes on ice. The

supernatant was transferred, 5x Laemmli Sample Buffer was added and the sample was incubated at 37° for 10 minutes. The eluate material was resolved by SDS-PAGE, and western analyses were performed with penta-His (1:2,000) or HA.11 antibody (1:10,000), HRP-conjugated anti-mouse antibody (1:2,000), and SuperSignal West Femto Maximum Sensitivity Substrate (1:1 in 50 mM Tris (pH 7.5), 150 mM NaCl).

In vitro ubiquitylation assay

The in vitro ubiquitylation assay was modified from Huibregtse et al. (Huibregtse, Yang et al. 1997). MYY290 (*RSP5*) and MYY808 (*rsp5^{ts}*) cultures were grown in YPD at 25° to approximately 5 OD₆₀₀ ml⁻¹. Pelleted yeast were resuspended in 25 mM Tris (pH 7.5), 150 mM NaCl with protease inhibitors (TPCK, TLCK, PMSF, leupeptin, trypsin inhibitor). The samples were frozen at -80°, thawed and lysed by vortexing with glassbeads. The lysate was then cleared by a 5 minute, 16,000 x g spin. The 20 µl ubiquitylation reaction was set up on ice with 25 mM Tris (pH 8.0), 125 mM NaCl, 2 mM MgCl₂, 2.5 mM ATP, MYY290 or MYY808 cleared lysate (0.8 mg ml⁻¹), His₆Vps9p (0.34 mg ml⁻¹), His₆hE1 (3.25 µg ml⁻¹, generously provided by J. Chen laboratory, UTSW), MBP-Ubc5p (0.8 mg ml⁻¹), with or without MBP-Rsp5p (27 µg ml⁻¹) added. Reactions were incubated at 25° for 1 hour, and terminated with the addition of 5x Laemmli Sample Buffer and incubation at 95° for 4 min. A third of the reaction was then resolved by SDS-PAGE, and western analysis was performed with Vps9p antiserum (1:2,000) or HA.11 monoclonal antibody (1:2,000), appropriate HRP-conjugated secondary antibodies (1:2,000) and SuperSignal West Femto Maximum Sensitivity Substrate (1:4 in 50 mM Tris (pH 7.5), 150 mM NaCl).

Results

Vps9p CUE domain binds Ubiquitin.

To identify potential regulators of Vps9p function, a yeast two-hybrid screen was conducted using the carboxy-terminal portion of Vps9p (amino acids 157-451; screen conducted by Greg Tall). From this screen, ubiquitin was repeatedly isolated as a potent Vps9p interaction partner. The specificity of this interaction in the yeast two-hybrid system was verified using a variety of unrelated protein expression constructs (data not shown). This region of Vps9p contains a sequence motif called CUE (Figure 19A). This domain (amino acids 408-450) (Figure 19B) was originally identified by reiterative

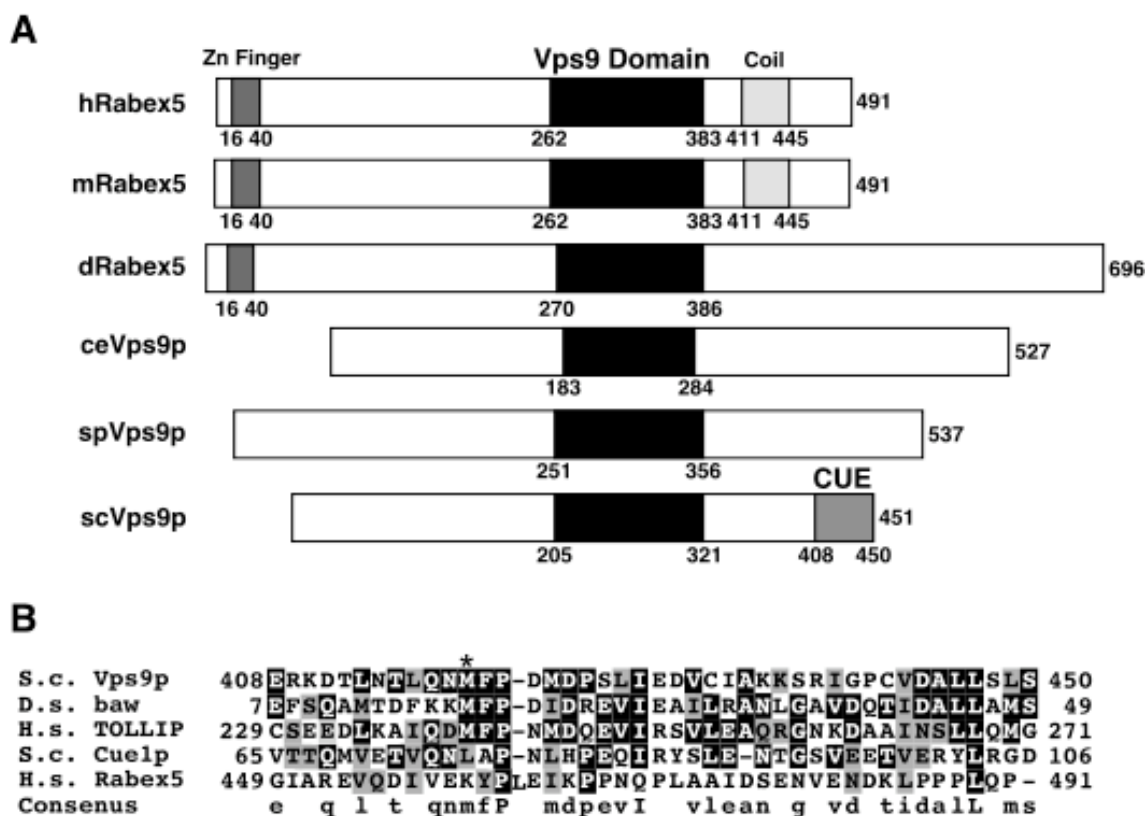


Figure 19. Analysis of the CUE domain. (A) Depiction of the Vps9p and Rabex5 proteins in *Saccharomyces cerevisiae*, *Schizosaccharomyces pombe*, *Caenorhabditis elegans*, *Drosophila melanogaster*, mouse and human with domains identified in the SMART database. The Vps9 domain (Black) is associated with catalytic exchange on Vps21p/Rab5 family proteins. The CUE domain is indicated in grey. (B) CLUSTALW alignment of a subset of CUE domains from yeast, flies and mammals. The carboxy-terminus of human Rabex5 (residues 449-491) alignment is also shown. Position of the methionine mutated to alanine (M419A) is denoted by an asterisk.

sequence homology searches initiated with the yeast protein Cue1p (Ponting 2000) and can also be found in the SMART and PFAM databases (Schultz, Copley et al. 2000; Bateman, Birney et al. 2002; Letunic, Goodstadt et al. 2002). The CUE domain is found in organisms from yeast to humans (Ponting 2000) (Figure 19B), but its functional role was not defined. Of the Vps21p/Rab5 GEF proteins, the canonical CUE domain has been identified in only *Saccharomyces cerevisiae* Vps9p (Figure 19A); however, human Rabex5 may also harbor a highly divergent CUE domain (Donaldson, Yin et al. 2003) (Figure 19B).

To confirm the Vps9p•ubiquitin interaction and to examine the role of the CUE domain in this interaction, an *in vitro* ubiquitin binding assay was utilized. A gene fusion between the maltose binding protein (MBP) and *VPS9* coding sequences was constructed, and the recombinant protein (MBP-Vps9p) was expressed in *E. coli* and affinity purified (Figure 20A). A His₆- and HA-tagged version of a human ubiquitin coding sequence was also constructed (His₆-HA-Ub), expressed in *E. coli* and affinity purified. MBP-Vps9p was then incubated with His₆-HA-Ub (or BSA as a control), and His₆-HA-Ub together with the potential His₆-HA-Ub•MBP-Vps9p complexes were isolated using Ni-NTA agarose. Following extensive washing, His₆-HA-Ub was eluted from the Ni-NTA agarose with imidazole and the presence of Vps9p in the eluate was determined by western analysis. As shown in Figure 20B, MBP-Vps9p copurified with His₆-HA-Ub (lane 5). When BSA was substituted for His₆-HA-Ub, only a very small amount of MBP-Vps9p was detected representing the level of nonspecific association with the Ni-NTA resin (Figure 20B, lane 4). These results confirm the Vps9p•ubiquitin interaction uncovered in the yeast two-hybrid screen.

To explore the possibility that the CUE domain mediates the interaction between Vps9p and ubiquitin, an allele was generated in which the first residue of the highly conserved signature sequence MFP (Ponting 2000) (methionine at position 419) was mutated to alanine (M419A) (Figure 19B). The methionine was chosen for mutagenesis to minimize potential structural perturbations of this domain. MBP-Vps9p M419A was expressed in *E. coli* and affinity purified. Soluble protein yields from the M419A allele were equivalent to that of wildtype, suggesting that global protein folding and stability were largely unaffected (Figure 20A) (see below). When the mutant protein was tested

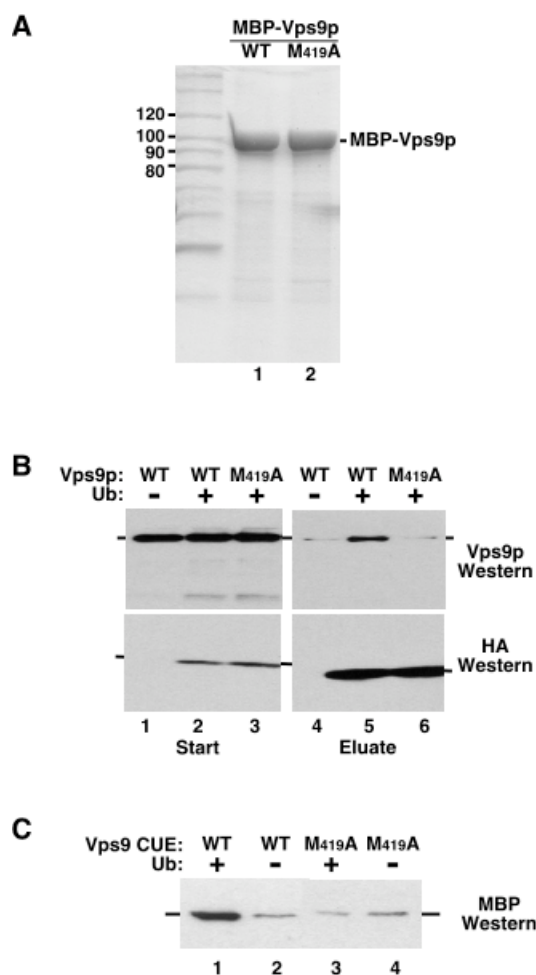


Figure 20. Vps9p binds ubiquitin. (A) MBP-Vps9p (lane 1) and MBP-Vps9p M419A (lane 2) were expressed in *E. coli* and affinity purified with amylose resin as described in Experimental Procedures. Approximately 1 μ g of the purified proteins were resolved by SDS-PAGE and stained with Coomassie Brilliant Blue. The sizes of relevant proteins markers are indicated. (B) Vps9p proteins were combined with His₆HA-Ubiquitin (lanes 2, 3, 5, 6) or BSA (lanes 1, 4) and affinity purified with Ni-NTA agarose as described in Experimental Procedures. Western analysis of the eluate and starting material was performed with Vps9 antiserum (upper panels) or HA.11 monoclonal antibody (lower panels). (C) The CUE domains (residues 408-451) from Vps9p wildtype and M419A were expressed in *E. coli* as MBP fusion proteins. Purified proteins were combined with His₆HA-Ubiquitin (lanes 1, 3) or His₆Vps21p (lanes 2, 4) and affinity purified with Ni-NTA agarose as described in Experimental Procedures. Western analysis of the eluate was performed with MBP antiserum.

for its ability to bind ubiquitin, the M419A mutation precluded the ability of this protein to bind ubiquitin *in vitro* (Figure 20B, lane 6). This finding indicates that the CUE domain is necessary for the Vps9p•ubiquitin association and suggests that the CUE domain itself is a ubiquitin binding motif.

To confirm that the Vps9p CUE domain mediates the ubiquitin interaction, the isolated domain was examined for ubiquitin binding. Residues 408-451 were expressed in *E. coli* as a MBP fusion (MBP-Vps9p CUE). Purified protein was incubated with His₆-HA-Ub (or His₆Vps21p as a control), and His₆-HA-Ub together with the potential His₆-HA-Ub•MBP-Vps9p CUE complexes was isolated using Ni-NTA agarose. As shown in Figure 20C, MBP-Vps9p CUE was highly enriched in eluates upon inclusion of His₆-HA-Ub (lane 1) as compared to His₆-Vps21p (lane 2) indicating a specific association with ubiquitin. Mutation of methionine 419 to alanine (MBP-Vps9p CUE M419A) eliminated the ubiquitin-dependent enrichment (lane 3), consistent with results observed with the full-length protein. Starting material analysis confirmed that equal amounts of Vps9p CUE domain were used in each experiment (data not shown). These results demonstrate that the Vps9p CUE domain is both necessary and sufficient for ubiquitin binding.

CUE domain involvement in the endocytic pathway.

Since an intact CUE domain is required for Vps9p ubiquitin binding *in vitro*, the role this domain plays in the *in vivo* function of Vps9p was examined. Wild-type *VPS9* (WT), the M419A mutant allele, and a truncated allele that eliminated the CUE domain (Δ CUE, 1-407) were expressed in a yeast strain that lacked the chromosomal copy of

VPS9 ($\Delta 9$). Western analysis of whole cell lysates from yeast expressing these forms of Vps9p indicated that all proteins were expressed at or near wild-type levels (Figure 21A). It was previously demonstrated that Vps9p is required for vacuolar delivery of soluble proteases such as carboxypeptidase Y (CPY) (Burd, Mustol et al. 1996). In the absence of Vps9p, cells secrete CPY in its Golgi-modified p2 precursor form. To examine the role of the CUE domain in this biosynthetic pathway, maturation of CPY was assessed in strains expressing wild-type Vps9p,

Δ CUE, or M419A (Figure 21B, lanes 1, 3, and 4). CPY immunoprecipitated from ^{35}S pulse-labeled wild-type or CUE mutant strains was found in its mature form indicative of vacuolar delivery (Figure 21B). Similar analysis of carboxypeptidase S (CPS) processing indicated that CPS maturation is also unaffected in the CUE mutant strains (data not shown). In addition, a time course analysis of CPY processing in strains expressing wild-

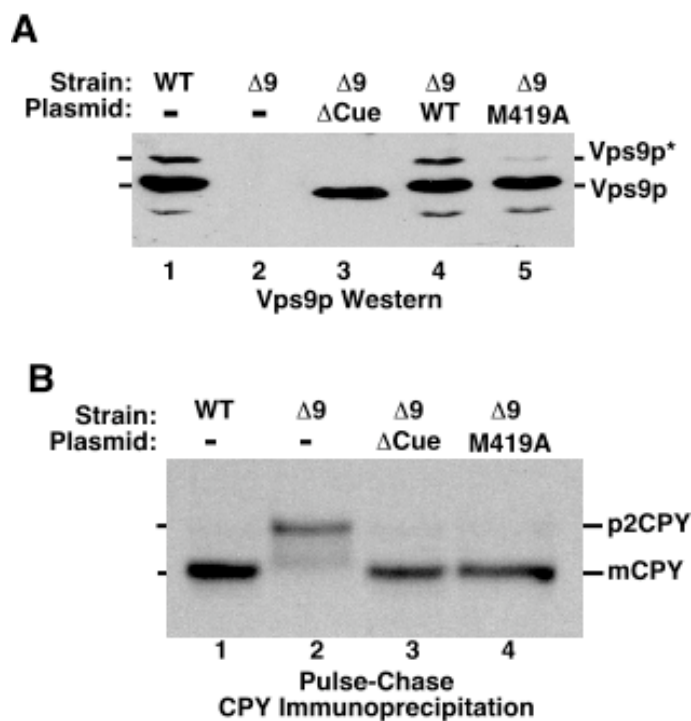


Figure 21. Vps9p CUE domain is not required for CPY sorting. (A) Lysates were generated from wild-type (lane 1), $\Delta vps9$ (lane 2) and $\Delta vps9$ yeast strains expressing Vps9p Δ Cue (lane 3), wild-type (lane 4) or M419A (lane 5) encoded on a plasmid. Western analysis with Vps9p antiserum detected the predominant unmodified form of Vps9p as well as a covalently modified form (Vps9p*). (B) Yeast strains expressing Vps9p wildtype (lane 1), Δ Cue (lane 3), or M419A (lane 4) proteins were labeled with EasyTag Expre ^{35}S ^{35}S Protein Labeling Mix for 10 minutes and chased with excess methionine and cysteine for 30 minutes. Proteins were precipitated with trichloroacetic acid, and CPY was immunoprecipitated from the resolubilized fraction as described in Experimental Procedures. Samples were resolved by SDS-PAGE and detected by fluorography. The positions of mature vacuolar CPY (mCPY) and Golgi-modified precursor CPY (p2CPY) are indicated.

type Vps9p or the M419A allele was performed, and the patterns of CPY maturation are indistinguishable (data not shown). These results demonstrate that the Vps9p CUE domain, and thus ubiquitin-binding, is not required for biosynthetic transport of CPY or CPS to the vacuole.

Ubiquitylation is a critical signal for the endocytosis and vacuolar degradation of plasma membrane proteins (reviewed in (Hicke 1999)), and Vps21p has been demonstrated to participate in endocytosis (Gerrard, Bryant et al. 2000). To address a potential role for Vps9p and the Vps9p CUE domain in the endocytic process, trafficking of the α -factor receptor, Ste3p, was analyzed. In the absence of pheromone, Ste3p is constitutively ubiquitylated, internalized and transported to the vacuole where it is degraded (Davis, Horecka et al. 1993; Roth and Davis 1996). The extent and rate of Ste3p degradation is therefore a good indicator of traffic through the yeast endocytic pathway. To

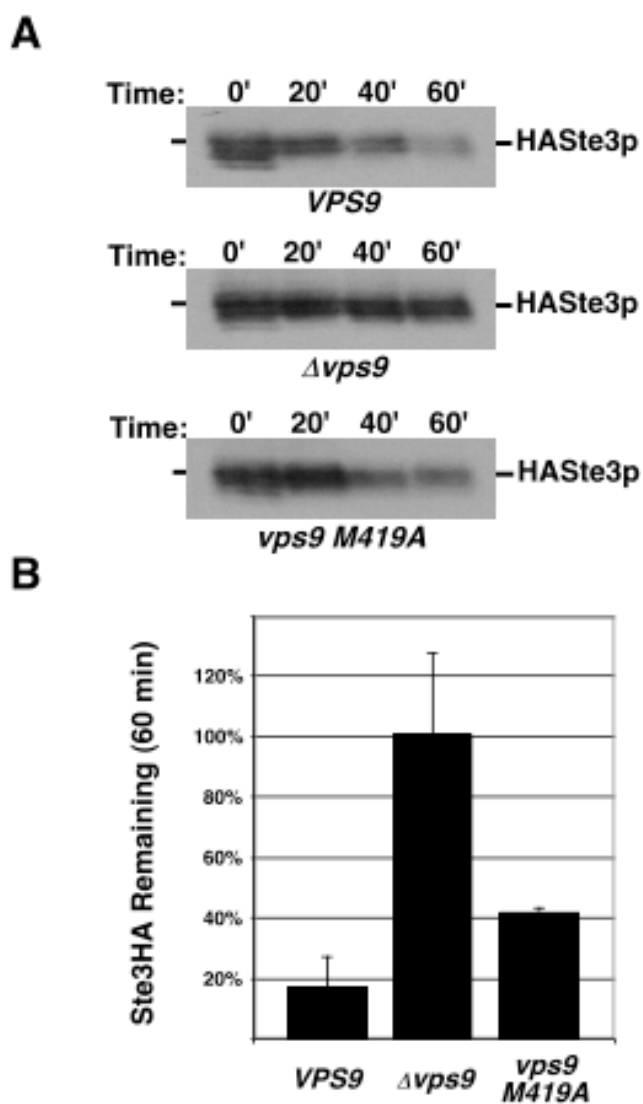


Figure 22. Vps9p CUE domain functions in endocytic trafficking. (A) 0, 20, 40 and 60 minutes after the addition of cyclohexamide, lysates were generated from wildtype (panel 1), Δ *vps9* (panel 2) and Δ *vps9* yeast strains expressing Vps9p M419A (panel 3) encoded on a plasmid as described in Experimental Procedures. Western analysis with HA.11 monoclonal antibody was performed to detect Ste3HAp. (B) Densitometry was performed to quantitative the Ste3HAp degradation at 60 minutes as normalized to the amount at 0 minutes.

quantitatively examine this trafficking process, degradation of Ste3p was examined. Extracts from wild-type and *vps9* mutant strains expressing an HA-tagged Ste3p (Ste3HAp) were generated 0, 20, 40 and 60 minutes after the addition of cyclohexamide (to block further production of Ste3HAp), and the amount of Ste3HAp remaining at each time point was determined by western analysis (Figure 22A,B). In the wild-type strain (*VPS9*), the majority of Ste3HAp had been degraded at 60 minutes, with only 17% remaining. By contrast, complete elimination of Vps9p ($\Delta vps9$) resulted in Ste3HAp stabilization; however, this effect can be attributed to defects in vacuole proteolytic capacity in addition to trafficking defects in the endocytic pathway. Mutation of the CUE domain (*vps9 M419A*) resulted in decreased Ste3p turnover, with 42% Ste3HAp remaining at 60 minutes. A similar defect was observed with the CUE domain deletion allele (data not shown). Since the vacuole is proteolytically active in the *vps9* CUE mutant strains (Figure 21B), these findings indicate that the Vps9p CUE domain is required for efficient delivery of Ste3p to the vacuole for degradation.

Identification of Ubiquityl-Vps9p.

Western analysis of the various Vps9p alleles (Figure 21A), revealed the presence of an immunoreactive band approximately 8 kDa larger than full length Vps9p (denoted by asterisk, Vps9p*). The presence of this band was dependent on Vps9p expression (lane 2), and was also apparent in western analysis of HA-tagged Vps9p (data not shown). These results, in conjunction with serial dilutions (data not shown), indicate that approximately 10% of Vps9p is covalently modified. This modification is dependent on ubiquitin binding as deletion or mutation of the CUE domain eliminated (lane 3) or

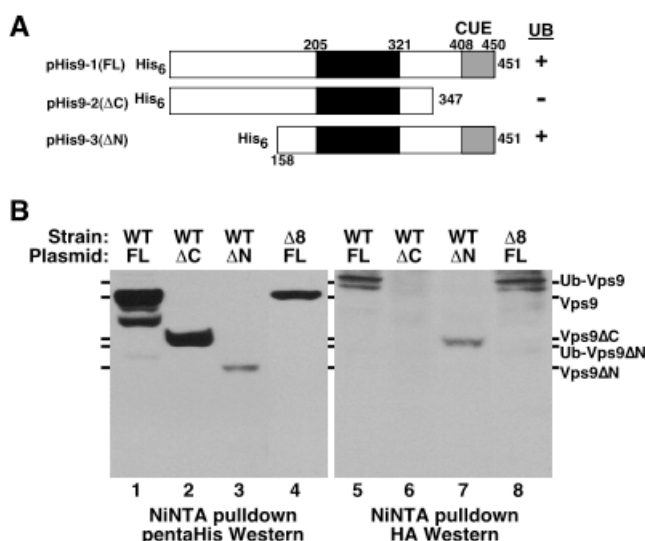


Figure 23. Vps9p ubiquitylation in vivo. (A) Depiction of the His₆-tagged Vps9p proteins expressed in yeast. (B) Lysates were generated from wildtype yeast strains expressing HA-Ubiquitin and His₆Vps9p full-length (lanes 1,5), ΔC (1-347; lanes 2, 6) or ΔN (158-451; lanes 3, 7) and from $\Delta vps8$ yeast strain expressing HA-Ubiquitin and His₆Vps9p (lanes 4, 8). Ni-affinity purification was performed as described in Experimental Procedures, and eluates were analyzed by western analyses with penta-His (lanes 1-4) and HA.11 (lanes 5-8) monoclonal antibodies.

diminished (lane 5) the amount of Vps9p*. These findings suggested that Vps9p might be a target for monoubiquitylation.

To demonstrate that Vps9p* is the monoubiquitylated form of Vps9p, His₆-tagged Vps9p was coexpressed with HA-tagged Ubiquitin in yeast. Vps9p was affinity purified from the lysates with Ni-NTA agarose and the presence of ubiquitylated Vps9p was detected by western analysis using the HA.11 monoclonal antibody (Figure 23). When full length His₆Vps9p was expressed and purified, an HA cross-reactive band approximately 8 kDa larger than His₆Vps9p copurified with His₆Vps9p (lanes 1 and 5); this band is also apparent in penta-His westerns with longer exposure (data not shown). This result indicates that Vps9p* is ubiquityl-Vps9p. A slightly faster migrating HA tagged band was also detected and is believed to result from partial proteolysis of ubiquityl-Vps9p. Expression of a mutant form of Vps9p that lacked residues 347-451 (Vps9p ΔC), including the CUE domain, was robust (Figure 23, lane 2), but no corresponding HA-reactive band was detected (lane 6). These results indicate that Vps9p

lacking residues 347-451, including the CUE domain, is not ubiquitylated, as observed in the Vps9p Δ CUE whole cell western analysis shown in Figure 3A. However, ubiquitylation of Vps9p was unaffected by removal of the amino terminus (Vps9p Δ N, 158-451; lanes 3 and 7). These observations demonstrate that Vps9p is subject to monoubiquitylation and that this modification is dependent on the CUE domain.

Vps9p ubiquitylation is Rsp5p dependent.

Ubiquitylation of proteins involves a multiprotein complex comprised of E1, E2 and E3 components (reviewed in (Weissman 2001)). The E3 of this system is involved in substrate recognition and therefore imparts specificity. Several E3 ubiquitin ligases were examined to uncover their possible roles in Vps9p ubiquitylation. Vps8p was the first candidate investigated. Vps8p is a 134 kDa protein required for CPY sorting to the vacuole (Chen and Stevens 1996; Horazdovsky, Cowles et al. 1996). Like many E3 ubiquitin ligases, Vps8p contains a carboxy-terminal H2 RING finger and has been demonstrated to function as an E3 ubiquitin-protein ligase in vitro (Andrew Friedberg, Pamela Marshall and Bruce Horazdovsky, manuscript in preparation). Since both Vps9p and Vps8p are thought to act at similar sites in the endocytic/vacuolar protein sorting pathway, Vps8p was examined as the putative Vps9p E3 ligase. However, wild-type levels of ubiquitylated Vps9p were still found in extracts generated from cells that lacked Vps8p (Δ vps8) (Figure 23B, lanes 4 and 8). This result indicates that Vps8p is not the E3 ligase that modifies Vps9p.

Rsp5p is a yeast HECT domain E3 ubiquitin-protein ligase of the Nedd4 family (reviewed in (Rotin, Staub et al. 2000)). Rsp5p participates in the endocytosis of plasma

membrane proteins both through ubiquitylation of the substrate proteins themselves as well as components of the endocytic machinery (Dunn and Hicke 2001; Wang, McCaffery et al. 2001; Kaminska, Gajewska et al. 2002). To determine if Rsp5p is the E3 ubiquitin-protein ligase that modifies Vps9p, we examined ubiquitylation of Vps9p in a yeast strain that carried a temperature conditional allele of *RSP5* (*rsp5^{ts}*). Western analysis of cell extracts generated from the *rsp5^{ts}*, wild-type and $\Delta vps9$ strains at permissive temperature (25°) revealed the presence of ubiquityl-Vps9p in both wild-type and the *rsp5^{ts}* strains, though the level of ubiquitylated material was slightly reduced in the *rsp5^{ts}* strain (Figure 24A, lanes 2 and 3). When cells extracts generated from these strains were examined after a 30 min shift to nonpermissive temperature (37°), no ubiquitylated Vps9p was observed in the *rsp5^{ts}* strain (lane 6). The level of ubiquityl-Vps9p in wild-type cells was unaffected by this temperature shift (lane 5). This finding

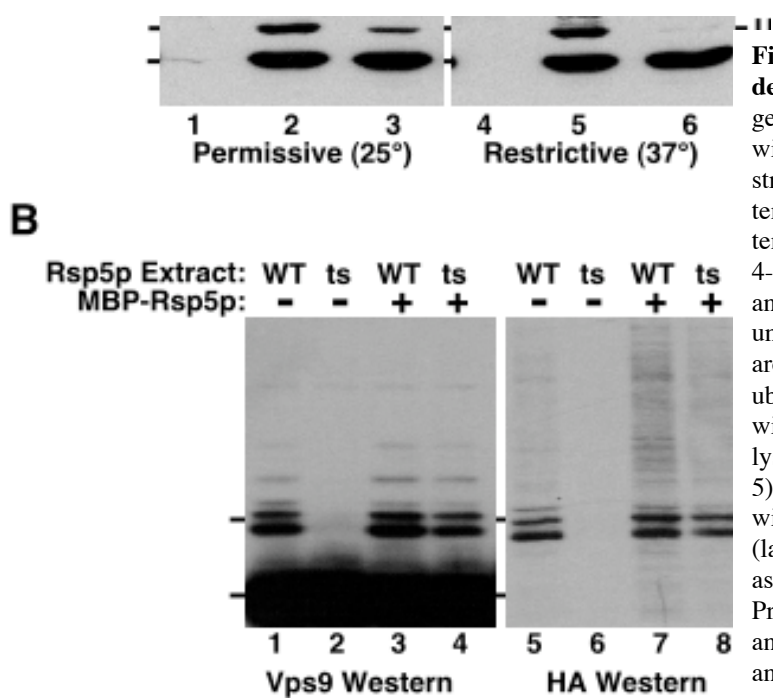


Figure 24. Vps9p ubiquitylation is dependent on Rsp5p. (A) Lysates were generated from $\Delta vps9$ (lanes 1, 4), wildtype (lanes 2, 4) and *rsp5^{ts}* yeast strains (lanes 3, 6) grown at permissive temperature (25°, lanes 1-3) or restrictive temperature (37°) for 30 minutes (lanes 4-6). Western analysis with Vps9p antiserum was performed. Positions of unmodified Vps9p and ubiquityl-Vps9p are indicated. (B) In vitro Vps9p ubiquitylation reactions were performed with His₆Vps9p, His₆HA-Ubiquitin and lysates generated from wildtype (lanes 1, 5) or *rsp5^{ts}* yeast strains (lanes 2, 6) or with MBP-Rsp5p added to the wildtype (lanes 5, 7) or *rsp5^{ts}* lysates (lanes 4, 8), as described in Experimental Procedures. Products were resolved by SDS-PAGE, and western analyses with Vps9p antiserum (lanes 1-4) or HA.11 monoclonal antibody (lanes 5-8) were performed.

demonstrates that Rsp5p is required for Vps9p ubiquitylation *in vivo*.

To further examine the Rsp5p dependence of ubiquityl-Vps9p, an *in vitro* ubiquitylation assay was utilized. Cleared lysates from wild-type and *rsp5^{ts}* strains were generated and incubated with recombinant His₆Vps9p, His₆HA-Ubiquitin and ATP. Following a 1 hr incubation period, western analyses with Vps9p and HA antibodies were performed to detect ubiquityl-Vps9p. Addition of wild-type lysate could support the covalent modification of Vps9p with ubiquitin (Figure 24B, lanes 1 and 5), with monoubiquitylation the predominant form. A small amount polyubiquitylated Vps9p was generated (Figure 24B, lane 1), in these *in vitro* reactions. The faster migrating form of Vps9p seen in both the Vps9p and HA western is likely a ubiquityl-Vps9p degradation product described earlier. In contrast, ubiquitylation of Vps9p was not supported by the *rsp5^{ts}* extract (lanes 2 and 6); however, reintroduction of recombinant Rsp5p, expressed in *E. coli* as an MBP fusion, was able to restore Vps9p ubiquitylation to the *rsp5^{ts}* extract (lanes 4 and 8). Additionally, HA western analysis indicated increased incorporation of HA-ubiquitin in higher molecular weight species with the addition of Rsp5p (Figure 24B, lane 7 and 8); however, Vps9p western analysis demonstrated that the vast majority of these species are not Vps9p (compare lanes 3 and 7). These results indicate that Vps9p ubiquitylation is dependent on Rsp5p both *in vitro* and *in vivo*, and support Rsp5p as the Vps9p E3 ubiquitin-protein ligase.

Discussion

Vps9p and Rabex5 are guanine nucleotide exchange factors for Vps21p/Rab5 protein family members, but how these proteins are regulated has yet to be completely defined. Here, we have demonstrated that Vps9p binds ubiquitin, and that the CUE domain is necessary and sufficient for this interaction. The interaction with ubiquitin is required to potentiate Vps9p function in the endocytic pathway; however, a requirement for the CUE domain in the CPY and CPS biosynthetic pathways is not apparent. Vps9p also is shown to be monoubiquitylated, and this modification is dependent on both the CUE domain and the E3 ubiquitin-protein ligase Rsp5p. These findings implicate ubiquitin as a regulator of Vps9p and identify Vps9p as an intermediary in ubiquitin-regulation of endocytosis.

The CUE domain is found in a large number of proteins that have been implicated in a variety of cellular processes (Ponting 2000), but the role this domain plays in protein function was unclear. We have demonstrated the CUE domain binds monoubiquitin. In addition, recent reports from Donaldson, et al., and Shih, et al., have demonstrated that the CUE domain also binds polyubiquitin as well as monoubiquitin (Donaldson, Yin et al. 2003; Shih, Prag et al. 2003). In what manner might ubiquitin binding or ubiquitylation modulate Vps9p? Two mechanisms can be proposed drawn from the functions of the Ras Association (RA) and SH2 domains in Rin1, a specialized mammalian Rab5 GEF. Binding of GTP•Ras to the RA domain has been shown to stimulate the *in vitro* GEF activity of Rin1, indicating an allosteric regulation that potentiates catalytic activity (Tall, Barbieri et al. 2001). Ubiquitylation or ubiquitin binding may serve a similar role to potentiate or depress the GEF activity of Vps9p by

altering the accessibility to or the conformation of the exchange domain. Alternatively, ubiquitin binding by the CUE domain of Vps9p may serve to localize the exchange factor. The Rin1 SH2 domain has been shown to bind to activated EGF-receptors, thereby concentrating the GEF at sites of stimulated endocytosis (M. Alejandro Barbieri, Chen Kong, Pin-I Chen, Bruce Horazdovsky and Philip Stahl, JBC in press). Vps9p binding to free ubiquitin has been demonstrated here; however, CUE domain binding may be preferential toward protein-conjugated ubiquityl moieties and thereby target Vps9p to ubiquitylated membrane proteins during endocytosis. A similar function has been suggested for the ubiquitin binding motifs found in the yeast proteins Ede1p, Vps27p, Ent1p and Ent2p (Shih, Katzmann et al. 2002). A third possibility is that ubiquitylation or ubiquitin binding regulates Vps9p interaction with other unidentified components of the endocytosis machinery. Potential targets include components of the ubiquitylation machinery itself, by analogy to Cue1p interaction with E2 ubiquitin conjugating enzymes (Biederer, Volkwein et al. 1997), or modulators of the actin cytoskeleton. A fourth possible function for ubiquitylation and ubiquitin binding is an intramolecular interaction whereby the CUE domain binds the ubiquityl moiety on Vps9p. The potential physiological effects of such an interaction are unclear, but this binding could explain the apparent stability of Vps9p monoubiquitylation in lysates. Of these possibilities, we favor the CUE domain serving to localize the exchange factor and Vps9p ubiquitylation serving to modulate its GEF catalytic activity by analogy to Rin1 regulation.

Ubiquitylation of yeast plasma membrane proteins is an essential step in the endocytosis of pheromone receptors (Ste2p, Ste3p) and small molecule transporters,

including the general amino acid permease (Gap1p) and uracil permease (Fur4p) (reviewed in (Hicke 1999; Rotin, Staub et al. 2000). This modification is required for the initial internalization step and is dependent on the E3 ubiquitin-protein ligase Rsp5p. However, ubiquitylation of the endocytic machinery by Rsp5p is also required for transport to the vacuole, as indicated by Dunn and Hicke (Dunn and Hicke 2001). Since Vps9p is required for the efficient endocytosis of Ste3p and Vps9p ubiquitylation is dependent on Rsp5p, Vps9p appears to be one piece of the endocytic machinery positively regulated by Rsp5p ubiquitylation (Figure 25). In addition, ubiquitin binding by the CUE domain positively impacts Vps9p function in the endocytic pathway. We

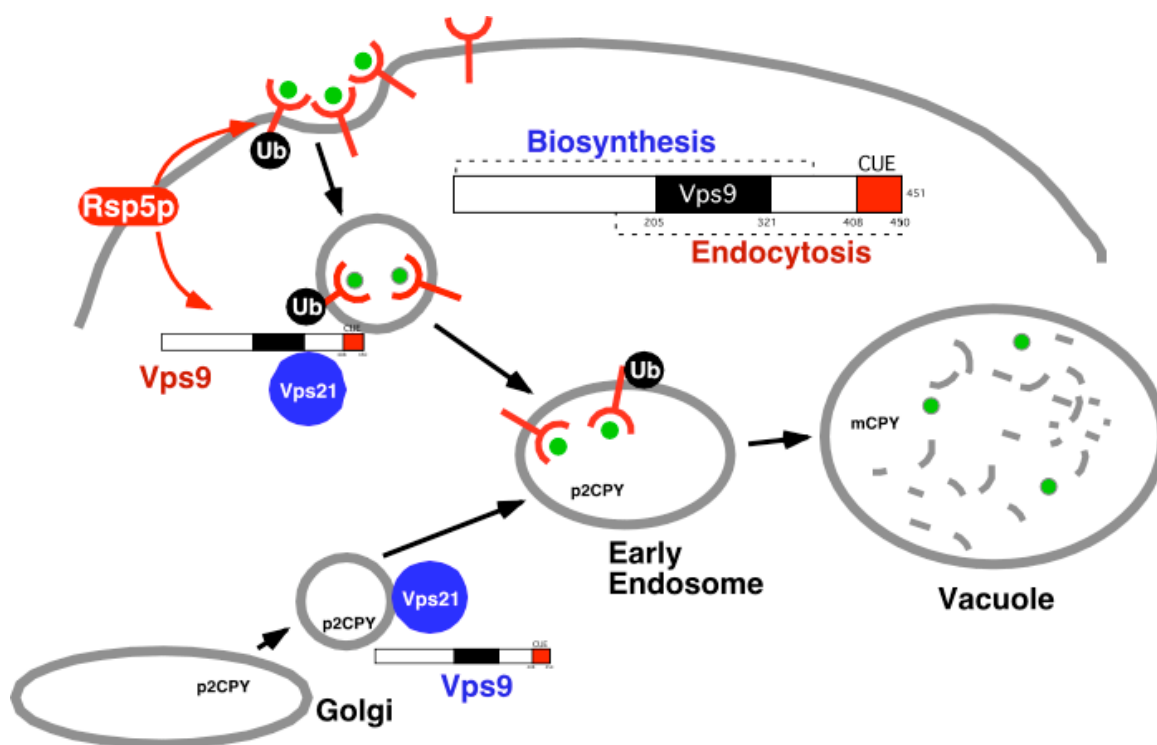


Figure 25. Two mechanisms for ubiquitin regulation. Vps9p binds ubiquitin via the CUE domain and is subject to monoubiquitylation. Both of these events may impact Vps9p function in the endocytic pathway. Ubiquitin might serve to localize Vps9p to the site of action, and ubiquitylation by Rsp5p may stimulate GEF activity.

suggest that the CUE domain may target Vps9p to transport intermediates harboring ubiquitylated receptors and subsequently stimulates their fusion with endosomal structures by the activation of the Rab protein Vps21p. In contrast, the CUE domain and ubiquitylation appear to be dispensable for Vps9p function in the biosynthetic pathway by which CPY and CPS are transported to the yeast vacuole. These findings do not address a role for Vps9p ubiquitin binding in the sorting of other ubiquitin-dependent biosynthetic pathway cargos, including Gap1p; the trafficking of these additional proteins should be examined in the future.

While further experimentation is required to define the precise role of ubiquitin in Vps9p function, similar regulation may occur in mammalian systems. While a canonical CUE domain is not apparent in mammalian Rabex5 proteins, a highly divergent form may be present in the carboxy-terminus (Donaldson, Yin et al. 2003) (Figure 19B). Recombinant human Rabex5 binds ubiquitin weakly in pulldown experiments (data not shown), and we have detected monoubiquitylation of GFP-hRabex5 transiently transfected in CHO cells (Justin Topp, Bruce Horazdovsky, unpublished results). In addition, the Rsp5p orthologous Nedd4 E3 ubiquitin-protein ligase family has been shown to regulate mammalian receptor trafficking (reviewed in (Rotin, Staub et al. 2000)). These preliminary observations suggest that the same ubiquitin-dependent mechanisms regulating Vps9p may modulate mammalian Rabex5 proteins and will be further examined.

Chapter 5. Structure-function analysis of the Vps9p CUE domain.

Summary

Vps9p is the rab5/Vps21p guanine nucleotide exchange factor that facilitates transport to the yeast endosome. The carboxy-terminus of Vps9p contains the sequence signatures of the CUE domain, a short 50 amino acid motif predicted to be largely helical. This domain is necessary and sufficient for ubiquitin binding, and ubiquitin binding is required to potentiate Vps9p function in the endocytic pathway. To gain insight into the mechanism by which the CUE domain binds ubiquitin and the role of this interaction in Vps9p function, a structure-function analysis of the Vps9p CUE domain was undertaken in collaboration with Gali Prag, Saurav Misra, Eudora Jones, Rodolfo Ghirlando and James Hurley (National Institute of Diabetes and Digestive and Kidney Diseases, NIH). Structures of the CUE domain in the absence and presence of ubiquitin were determined to 2.3 Å and 1.7Å, respectively. Sequence analysis suggested that the CUE domain is distantly related to the ubiquitin associated (UBA) domain, and structural similarities between the Rad23 UBA domain solution structure and the modeled apo Vps9p CUE domain monomer group these two domains into a superfamily of three helical ubiquitin binding domains. Determination of the ubiquitin-CUE domain complex yielded the unexpected finding that the Vps9p CUE domain forms a dimer to bind ubiquitin with high affinity. This mechanism is supported by sedimentation equilibrium centrifugation analysis and evaluation of CUE domain point mutations both in vitro and in vivo. In addition, a link between Class D *vps* mutants and Vps9p ubiquitylation is established, and the CUE domain is implicated as the ubiquitylation site.

Introduction

Ubiquitin is a 76-amino acid protein that is coupled to many substrates as a post-translational modification (reviewed in (Weissman 2001)). This covalent attachment is generated between the carboxyl-terminus of ubiquitin and a lysine residue of the target protein via the concerted action of the ubiquitin activating enzyme (E1), the ubiquitin conjugating enzyme (E2) and a ubiquitin protein ligase (E3). Ubiquitin itself can serve as a target for this ubiquitylation machinery leading to the generation of polyubiquitin chains, and formation of these polyubiquitin chains can serve as a signal for degradation of the modified protein by the 26S proteasome. This proteolytic process has historically been the primary system in which ubiquitin function has been investigated; however, more recent studies have identified a discrete role for ubiquitylation in the regulation of transmembrane protein trafficking (reviewed in (Hicke 2001; Katzmann, Odorizzi et al. 2002, Bonifacino, 2003 #2130).

To maintain cellular homeostasis, cells require mechanisms to attenuate activated signal transduction systems. One such mechanism is the endocytosis and subsequent lysosomal degradation of activated receptors. Ubiquitylation of plasma membrane proteins has been demonstrated to play a key role regulating the lysosomal trafficking of receptors both at the initial internalization event, during the early endocytic pathway and in sorting into multivesicular bodies (Shih, Sloper-Mould et al. 2000; Katzmann, Babst et al. 2001). The recognition of these cargoes is facilitated by direct interaction between ubiquitin and components of the endocytic machinery. The ubiquitin E2 variant domain (UEV), ubiquitin interacting motif (UIM), ubiquitin associated domain (UBA) and the

coupling of ubiquitin conjugation to ER degradation domain (CUE) have been identified as structures capable of binding ubiquitin monomers and/or polymers (reviewed in (Buchberger 2002)). The UEV resembles the ubiquitin binding surface of the ubiquitin conjugating enzymes (E2) (Pornillos, Alam et al. 2002). UIM, UBA and CUE domains are small domains (less than 60 amino acids) predicted to be helical in nature. This has been verified for the UBA domain by NMR solution structures and a crystal structure of the human Rad23 and Tap/NXF1 UBA domains (Dieckmann, Withers-Ward et al. 1998; Withers-Ward, Mueller et al. 2000; Mueller and Feigon 2002); the UBA folds into a three helical bundle, generating a hydrophobic patch implicated in binding ubiquitin and other proteins. The crystal structure of the 20 amino acid Vps27p UIM-2 has recently been solved, and the motif forms an amphipathic helix with a hydrophobic strip along one side (Robert Fisher et al., JBC in press). However, the structure of the ubiquitin bound complex has not been determined for these UIM, UBA or CUE domains.

As discussed in Chapter 4, the CUE domain has been demonstrated to mediate Vps9p binding to ubiquitin (Davies, Topp et al. 2003; Donaldson, Yin et al. 2003; Shih, Prag et al. 2003). This association between Vps9p and ubiquitin is required to potentiate Vps9p function in the endocytic pathway and for Vps9p monoubiquitylation. Vps9p functions in the biosynthetic and endocytic pathways to the yeast vacuole by activating the rab5 homolog Vps21p (Burd, Mustol et al. 1996; Hama, Tall et al. 1999). Cells deficient in Vps9p or Vps21p exhibit an enlarged vacuole phenotype (Horazdovsky, Busch et al. 1994; Burd, Mustol et al. 1996). This abnormal morphology is also apparent in *vps8*, *pep12/vps6*, *vps45*, *vac1/vps19*, *vps15*, *vps34* and *vps3* mutants, collectively referred to as the Class D *vps* mutants (Banta, Robinson et al. 1988; Raymond, Howald-

Stevenson et al. 1992). The phenotypic similarities and biochemical characterization of these gene products indicate that these Class D proteins function together to mediate docking and fusion with the endosome; however, the role of Vps9p ubiquitin binding and Vps9p ubiquitylation in facilitating transport to the endosome is unclear.

To gain insights into the ubiquitin regulation of Vps9p, a structure-function analysis was undertaken in collaboration with Gali Prag, Saurav Misra, Eudora Jones, Rodolfo Ghirlando and James Hurley (National Institute of Diabetes and Digestive and Kidney Diseases, NIH). Sequence analysis suggested that the CUE domain is related to the ubiquitin associated (UBA) domain, and structure determination of the Vps9p CUE domain supported this finding with significant similarity between the modeled CUE monomer and the solution structure of the human Rad23 UBA domain. However, in contrast to the ubiquitin-UBA monomer interaction implicated by NMR and mutational studies, crystal structure determination of the ubiquitin-CUE domain complex revealed that the Vps9p CUE domain forms a dimer to bind ubiquitin, with residues from both subunits combining to form an asymmetric binding surface. Analytical centrifugation and yeast 2 hybrid assay analyses were conducted and support the ubiquitin-CUE dimer interaction model. Mutational analysis of the ubiquitin binding surface was undertaken. Vps9p residues forming both surface 1 (M419, F420, V443, D444 and L447) and surface 2 (L427 and D430) were demonstrated to be important for in vitro ubiquitin binding as well as efficient Ste3p-GFP trafficking to the vacuole. Alleles defective for ubiquitin binding exhibited reduced ubiquitylation and altered fractionation patterns. These findings support the model that Vps9p forms a dimer to bind ubiquitin with high affinity and that this interaction is important to localize Vps9p. Ubiquitylation of Vps9p also

appears to be functionally regulated as *vps* mutants defective in transport to the endosome exhibited increased levels of Ub-Vps9p, and the CUE domain is implicated as the site of covalent modification as mutation of lysines 402, 403, 435 and 436 exhibited reduced ubiquitylation. These results suggest that ubiquitylation of the CUE domain is an important regulator of Vps9p.

Material and Methods

Crystallization of the Vps9p-CUE domain

The G440E mutant of the CUE domain of *S. cerevisiae* Vps9p was expressed and purified (Shih, Prag et al. 2003). SeMet G440E Vps9p CUE domain was expressed in *E. coli* strain B834 (DE3) and purified. The Vps9p CUE domain was concentrated to 30 mg/mL, dialyzed into 50 mM NaCl, 20 mM Tris pH 7.7, and 10 mM DTT, and crystallized in 2 μ L hanging drops over 0.5 mL reservoirs of 1.9-2.1 M ammonium sulfate, 100 mM Tris-HCl pH 8.2-8.8. Crystals were cryoprotected in mother liquor supplemented with 25% ethylene glycol and frozen in liquid propane.

Crystallization of the Vps9p-CUE:ubiquitin complex

The Vps9p-CUE K435A/K436A mutant was mixed with bovine ubiquitin (Sigma) at a 1:1 molar ratio. The complex was isolated from unbound material on a Superdex 75/S60 gel filtration column (Pharmacia). Native protein was concentrated to 43 mg/ml and crystallized in the presence of 17% polyethylene glycol 3350 and 200 mM MgCl_2 . SeMetl CUE:ubiquitin crystals were obtained in similar conditions. Crystals of

the complex were cryoprotected in mother liquor supplemented with 18% glycerol and frozen in liquid propane or in the cryostream.

Structure determination

MAD data sets were collected from apo and ubiquitin-bound CUE crystals at beamlines 19ID and 22ID, respectively, at the Advanced Photon Source, Argonne National Laboratory. MAD data were collected at three wavelengths, at 95 K, and in 1° oscillation frames, and reduced using DENZO and Scalepack (Otwinowski and Minor 1997). Se atoms were located and phases were calculated with SOLVE (Terwilliger and Berendzen 1999). Density modification of the initial maps was performed using RESOLVE (Terwilliger 2000). The resulting maps were used to build atomic models in O (Jones, Zou et al. 1991). The models were initially refined using CNS ((Brunger, Adams et al. 1998); Appendix 2). The complex model was subsequently refined at 1.7 Å using Refmac5 of the CCP4 Suite-programs (Bailey et al, 1994).

Site-directed mutagenesis

Site-directed Vps9p CUE domain mutants and lysine-arginine mutants were constructed using the GeneTailor mutagenesis kit (Invitrogen) and confirmed by DNA sequencing.

Isothermal Titration Calorimetry

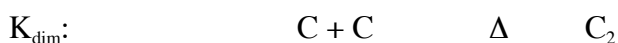
CUE domains and bovine ubiquitin (Sigma) were dialyzed against 100 mM NaCl, 50 mM Na/K phosphate buffer pH 7.5, and 1 mM DTT. Protein concentrations were

adjusted to 200 μM and 4.0 mM for CUE and ubiquitin respectively. Measurements were performed on a MicroCal VP-ITC instrument at 30°C. Ubiquitin was injected into 1.4 mL of buffer containing CUE domain in 21 injections of 10 μL each. Traces were corrected by subtracting blank measurements and analyzed using Origin 5.0 (MicroCal). Binding constants were calculated by fitting the integrated titration data to a one-site binding model (Table 1).

Sedimentation equilibrium

CUE, CUE-L427D, and ubiquitin in 150 mM NaCl, 50 mM Tris·HCl (pH 7.5) and 1 mM Tris (2-carboxylethyl) phosphine hydrochloride (TCEP) or 2- mercaptoethanol were loaded at 0.5 - 0.9 A_{280} . Mixtures containing 1:1 and 2:1 molar ratios of CUE:ubiquitin and CUE L427D:ubiquitin were loaded at 0.85 A_{280} . Experiments were conducted at 20.0°C and 280 nm on a Beckman Optima XL-A analytical ultracentrifuge at rotor speeds of 24,000, 26,000, and 28,000 rpm. Data for ubiquitin were analyzed as a single ideal solute to obtain the buoyant molecular mass, $M_1(1 - \nu_1\rho)$. Values of M_1 were calculated using densities obtained from standard tables and calculated values of ν_1 (Perkins, 1986). Sedimentation equilibrium data for CUE and CUE-L427D were analyzed as reversible monomer-dimer equilibria to obtain a dimerization equilibrium constant, K_{dim} (Jenkins, et al., 1996).

Data for the 1:1 and 2:1 mixtures of CUE:ubiquitin and CUE-L427D:ubiquitin were analyzed in terms of the following equilibria:



| | | | |
|------------|------------|----------|----------|
| K_0 : | $C + U$ | Δ | CU |
| K_{01} : | $C_2 + U$ | Δ | C_2U |
| K_{10} : | $C_2 + U$ | Δ | UC_2 |
| K_2 : | $C_2U + U$ | Δ | C_2U_2 |

where C and U are CUE and ubiquitin. Two models were considered. In the cooperative model, the cooperativity results in the exclusive formation of C_2U with $\Delta G_{01} = 2\Delta G_0$, or $K_{01} = K_1 = (K_0)^2$. In the non-cooperative model the complexes C_2U and UC_2 are symmetrically indistinguishable with $K_{01} = K_{10} = K_0$ and $K_{01} + K_{10} = K_1$. In both models, it is assumed that $K_2 = K_0$. The model equations, values for the constants, and their error limits, are described in supplementary material.

Strains, reagents, and plasmids for in vivo experiments

The *Saccharomyces cerevisiae* strains used were SEY6210 (MAT α *leu2-3,112 ura3-52 his3- Δ 200 trp1- Δ 901 lys2-801 suc2- Δ 9*) (Robinson, Klionsky et al. 1988), BHY165 (SEY6210; *vps21 Δ ::HIS3*) (Horazdovsky, Busch et al. 1994), PSY83 (SEY6210; *vps8 Δ ::HIS3*) (Horazdovsky, Cowles et al. 1996), PHY112 (SEY6210; *vps15 Δ ::HIS3*) (Herman, Stack et al. 1991), PHY102 (SEY6210; *vps34 Δ ::TRP1*), SEY6210; *pep12 Δ ::HIS3* (Becherer, Rieder et al. 1996), SEY6210; *vps45 Δ ::HIS3* (Cowles, Emr et al. 1994), GTY104 (SEY6210; *vac1 Δ ::G418^r*) (Tall, Hama et al. 1999), MBY3 (SEY6210; *vps4 Δ ::HIS3*) (Babst, Wendland et al. 1998), BHY152 (SEY6210; *vps5 Δ ::HIS3*) (Horazdovsky, Davies et al. 1997), TVY614 (SEY6210; *pep4 Δ ::LEU2, prc1 Δ ::HIS3, prb1 Δ ::HISG*) (Gerhardt, Kordas et al. 1998), SF838-10 (Δ *vps3*)

(Raymond, O'Hara et al. 1990), CBY1 (SEY6210; *vps9ΔI::HIS3*) (Burd, Mustol et al. 1996) and BHY93, which was constructed by integrating pRS304 Ste3GFP (linearized with *EcoRV*) into CBY1. Reagents and plasmids used are described in Chapter 4.

FM4-64 labeling and Ste-GFP localization assay

Vacuolar morphology was analyzed by labeling with FM4-64 (Molecular Probes, Eugene, OR) as described (Vida and Emr 1995) except that labeling was at a concentration of 16 μ M at 30°, cells were chased 1 hour, and cyclohexamide was added (3 μ g/ml) during the last 45 min of the chase period. Labeled cells were visualized on an Olympus IX70 inverted microscope with a Rhodamine filter. Ste3-GFP was visualized with a FITC filter. Images were collected with a Photometrix digital camera, and deconvolved using DeltaVision (Applied Precision).

Two-Hybrid Analysis

Yeast strain L40 (Vojtek, Hollenberg et al. 1993) was transformed with bait plasmid alone (pVJL11) (Jullien-Flores, Dorseuil et al. 1995), or with bait plasmids that also encoded the indicated portions of Vps9p. These transformants were cotransformed with the prey plasmid alone (pGAD-GH), or prey plasmids encoding full-length or the indicated portions of Vps9p, or a prey plasmid expressing ubiquitin. Cotransformants were selected on minimal media and interaction was scored using a β -galactosidase filter assay (Vojtek, Hollenberg et al. 1993).

Whole-cell western analysis

Yeast strains were grown in YPD or YNB-glucose with appropriate amino acids, and 2 OD₆₀₀ equivalent was harvested during log-phase growth (0.5-0.8 OD₆₀₀ ml⁻¹). Samples were resuspended in 100 μ l 5x Laemmli Sample Buffer and approximately 150 μ l of glass beads (0.5 mm) were added. Samples were vortexed in mass for 10 minutes and heated at 95° for 4 minutes. 0.2 OD₆₀₀ equivalent was resolved by SDS-PAGE, and western analysis was performed with Vps9p antiserum (1:3,000), HRP-conjugated anti-rabbit antibody (1:3,000), and SuperSignal West Femto Maximum Sensitivity Substrate (1:4 in 50 mM Tris (pH 7.5), 150 mM NaCl).

Subcellular Fractionation

Yeast strains were grown in YNB-glucose with appropriate amino acids, and 5 OD₆₀₀ equivalent was harvested during log-phase growth (0.5-0.8 OD₆₀₀ ml⁻¹). Spheroplasts were generated by enzymatic digestion with Zymolyase 100T as previously described. Samples were resuspended at 10 OD₆₀₀ ml⁻¹ in 20 mM Pipes•KOH (pH 6.8), 100 mM KCl, 50 mM KOAc, 5 mM MgOAc, 100 mM Sorbitol, 10 mM NEM with protease inhibitors and incubated on ice for 10 minutes. Samples were then subjected to 13,000 x g centrifugation for 10 minutes at 4°. 100 μ l of the supernatant was combined with 50 μ l 5x Laemmli Sample Buffer, and the remainder of the supernatant was aspirated. The pellet was resuspended in 150 μ l 5x Laemmli Sample Buffer. Samples were incubated at 95° for 4 minutes. 0.1 OD₆₀₀ equivalent of supernatant and 0.5 OD₆₀₀ equivalent of pellet material was resolved by SDS-PAGE, and western analysis was performed with Vps9p antiserum (1:3,000), HRP-conjugated anti-rabbit antibody

(1:3,000), and SuperSignal West Femto Maximum Sensitivity Substrate (1:4 in 50 mM Tris (pH 7.5), 150 mM NaCl).

Coordinates

The coordinates have been deposited in the PDB under identifiers 1MN3 and 1P3Q.

Results

CUE domain is related to the UBA ubiquitin binding domain.

The CUE domain was initially identified by sequence homology searches initiated with the yeast CUE1p (coupling of ubiquitin to ER degradation (Biederer, Volkwein et al. 1997)) (Ponting 2000), and has been demonstrated to mediate Vps9p binding to ubiquitin, as discussed in Chapter 4. The domain is approximately 50 amino acids in length and is predicted to be largely helical in nature (Figure 26A). The most prominent characteristics are the MFP sequence corresponding to Vps9p residues 419-421 and the Fxx(I/V/L)L corresponding to VDALL (Vps9p 443-447). Similar secondary structure and sequence motifs [MG(F/Y); FxxL(I/L/F)] are present in another ubiquitin binding domain, the ubiquitin associated domain (UBA) (Hofmann and Bucher 1996); however, the overall sequence similarities between the two motifs are minimal.

To gain insight into the similarities between the CUE and UBA domains, the structure of the Vps9p CUE domain (residues 394-451, G440E allele) was determined by multiwavelength anomalous dispersion using the signal from SeMet 419 and 423, and refined to 2.3 Å resolution (Table 2; structure determined by Saurav Misra). The structure (Figure 26B, residues 398-451) consists of three α -helices and two connecting

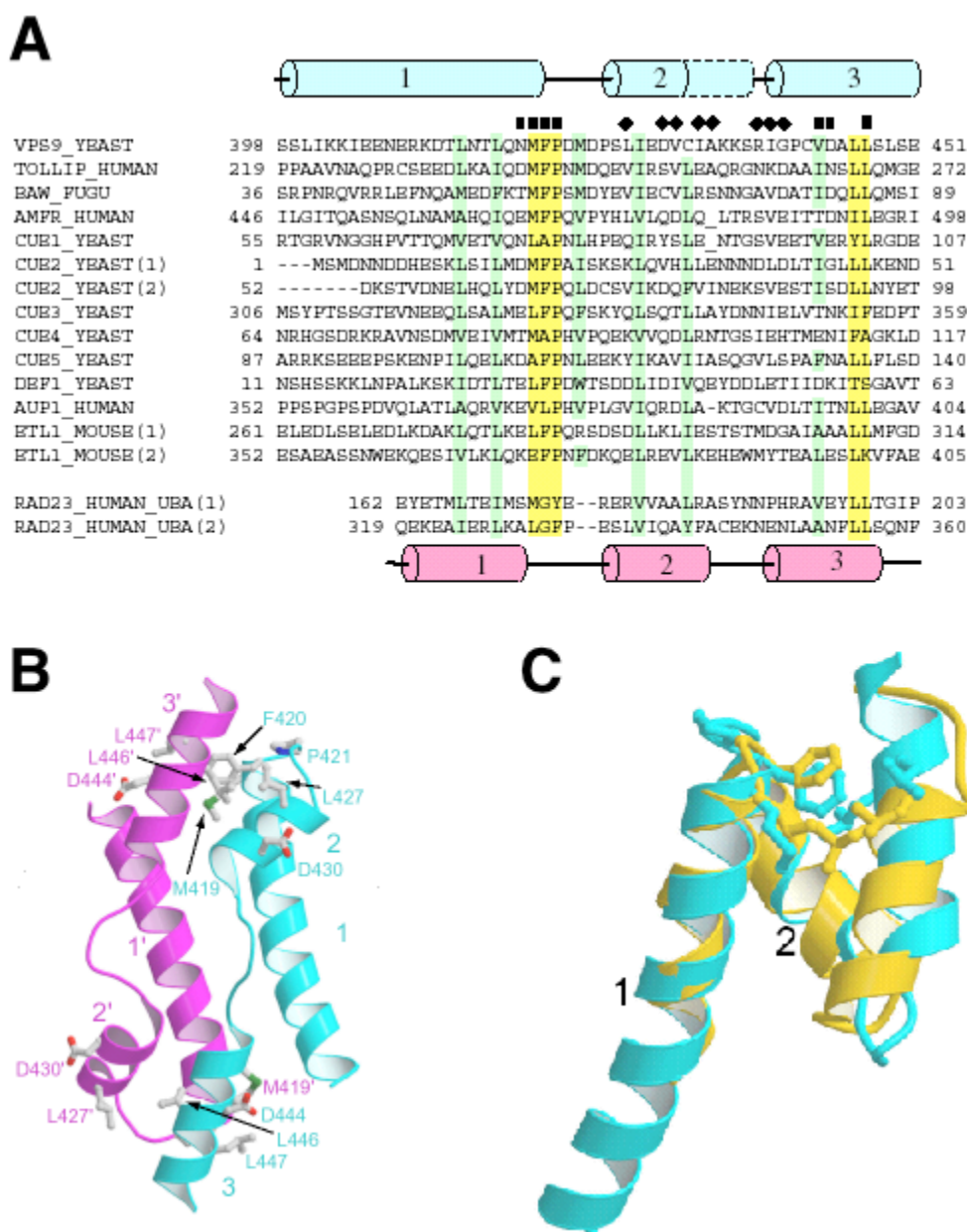


Figure 26. CUE domain is related to UBA domain. (A) Alignment of representative CUE domains and the two UBA domains of human Rad23. Contact residues that interact in both the monomer and dimer are marked with rectangles above them; residues that only interact in the dimer, small diamonds. Core hydrophobic residues of the CUE domains are highlighted in green; conserved MFP and LL motifs that bind ubiquitin, in yellow. Sequences are as described, with the addition of BAW, the Fugu homolog of the neurofibromatosis-1 protein, and AUP1, the ancient ubiquitous protein-1 (Schultz *et al.*, 1998, Ponting, 2000). The terminology for CUE2-5 follows Shih *et al.* (2003). The secondary structures are derived from the apo structure. The α 2' helix of the complexed dimer is longer than α 2 in the apo structure, and the additional length of α 2' is shown in dashed lines. (B) The CUE domain fold. Residues mutated in the study are shown. (C) Superimposition of the closed monomer CUE model and the hRad23-UBA(2) domain. [Figure generated by Gali Prag.]

loops; residues 394-397 are disordered. The first helix (α 1) is the longest feature (S398-

F420) and terminates at the conserved MFP sequence. Following a short loop (P421-

P425), helix $\alpha 2$ (S426-V431) runs antiparallel to $\alpha 1$. A larger loop (C432-P441) then precedes helix $\alpha 3$ (C442-E451), which runs still antiparallel to $\alpha 1$.

The Vps9p CUE domain forms extensive contacts across the crystallographic two-fold axis, and sedimentation equilibrium centrifugation analysis (performed by Rodolfo Ghirlando) is consistent with a reversible monomer-dimer equilibrium with a K_d (dimerization) of 1 mM (data not shown). In the CUE dimer, the second $\alpha 3$ ($\alpha 3'$) nestles between $\alpha 1$ and $\alpha 2$ of the first subunit and runs parallel to $\alpha 1$. The $\alpha 1$ and $\alpha 2$ helices of the Vps9p CUE domain can be superimposed on the first two helices of the human Rad23 UBA domain 2 (r.m.s.d. for 22C α positions is 1.8 Å) (Dieckmann, Withers-Ward et al. 1998; Mueller and Feigon 2002), with the Vps9p MFP coinciding with the LGF motif at the end of the first Rad23 helix, which has been implicated in ubiquitin binding through mutational analysis (Bertolaet, Clarke et al. 2001). The third UBA helix interacts with helices 1 and 2 in a manner equivalent to the interactions between Vps9p CUE helix $\alpha 3'$ and helices $\alpha 1$ and $\alpha 2$. The Vps9p CUE domain exists in equilibrium between monomer and dimer states, so $\alpha 3$ of the CUE monomer is assumed to adopt the position inhabited by $\alpha 3'$ in the dimer structure. This CUE monomer conformation (constructed by Gali Prag using Swiss-Pdb Viewer; (Guex and Peitsch 1997)) is modeled in Figure 26C and is superimposable with all three helices of the Rad23 UBA. Thus, both CUE and UBA can be grouped into a superfamily of three helical ubiquitin binding domains.

Structure of the Vps9p CUE domain binding ubiquitin.

Crystallization of the wild-type Vps9p CUE domain in complex with bovine ubiquitin failed; however, mutation of lysines 435 and 436 to alanine enabled crystallization of the CUE-ubiquitin complex. The structure was determined by MAD phasing using the SeMet signals, and refined to a resolution of 1.7 Å (Table 2; structure determined by Gali Prag). The crystallized complex contains two ubiquitin molecules and two CUE domains per asymmetric unit; however, the primary interactions between the CUE domain and ubiquitin are comprised of a single ubiquitin molecule interacting with an asymmetric CUE dimer (Figure 27B).

The structure of ubiquitin in the complex is largely unchanged from the free form (r.m.s.d. values 1.1 and 0.9 Å for all C α positions; pdb entry 1ubq; (Vijay-Kumar, Bugg et al. 1987)); however, the CUE dimer undergoes substantial conformational changes. In the apo CUE structure, residues 398-451 were apparent for both chains of the symmetric domain swapped dimer; by contrast, in the ubiquitin-CUE complex, the first CUE monomer (depicted in cyan) is ordered from residues 408-437 (α 1, α 2) and partially ordered in residues 440-444 (α 3), and the second chain (depicted in magenta) is ordered from 416'-451' (end of α 1', complete α 2', α 3'). As presented in Figure 27A, the right half of the CUE dimer is formed by first chain residues 398-431 (α 1, α 2) and second chain residues 437'-451' (α 3'). This region is similar to the apo form with shifts of only 1.2 Å r.m.s.d. (C α positions). In contrast, V444 of α 3 and amino-terminus of α 2' (D424) are shifted by 28 Å and 21 Å, respectively, from positions in the apo CUE dimer (α 1, α 2, and α 3' as positional reference). The first chain is repositioned by a pivot in the extended coil formed by residues 434-437; and the second chain α 1' and α 2' are rotated

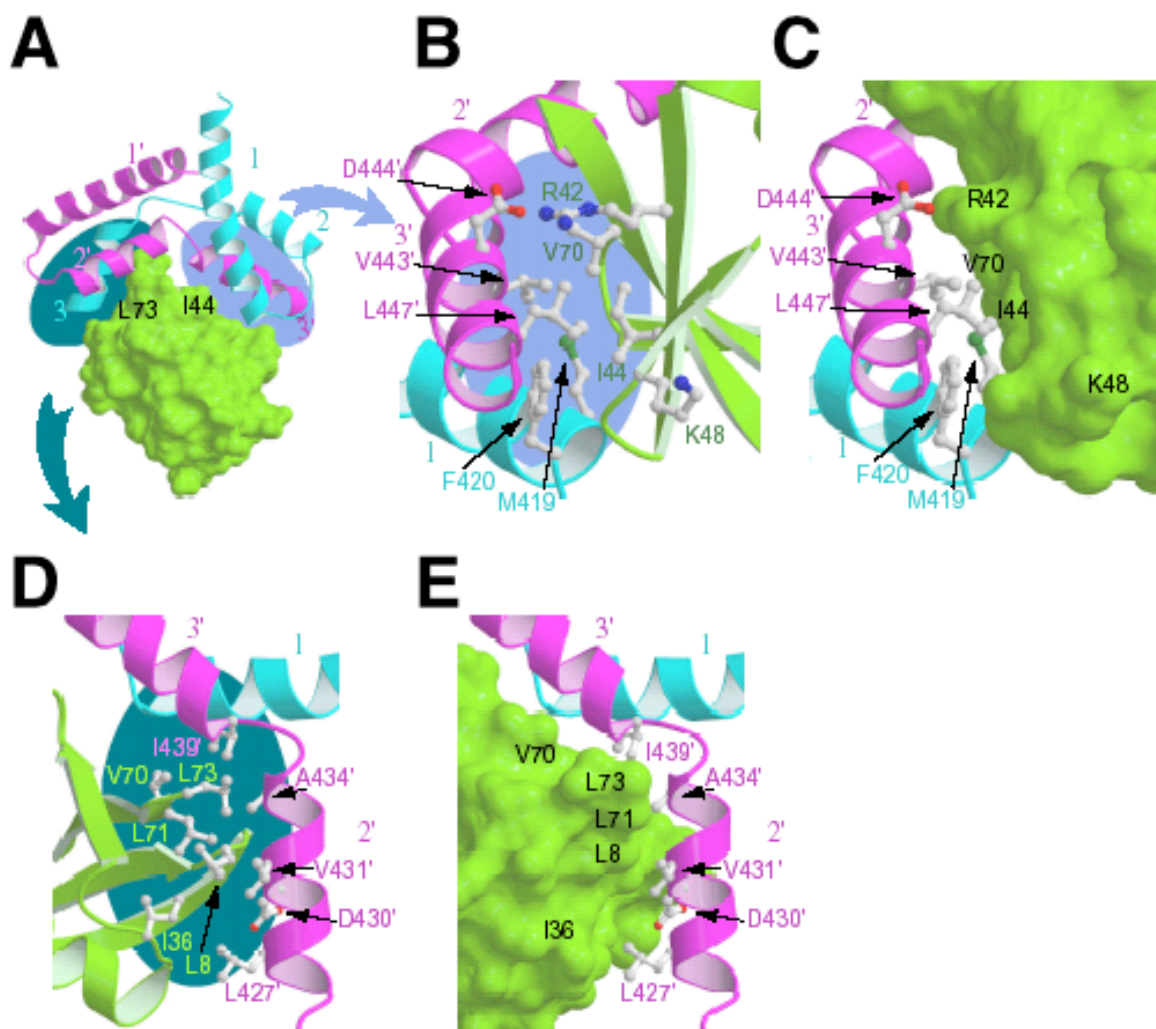


Figure 27. Structure of the CUE Dimer:ubiquitin complex. Only the ubiquitin making functionally relevant contacts with the CUE dimer is shown (green). (A) Ribbon drawing of a model of the complex. The disordered regions of the CUE dimer in the complex were modeled by overlaying the separate chains of the apo CUE dimer on the complex conformation of the CUE dimer. Closeup of the interaction between CUE and ubiquitin in the $\alpha 1/\alpha 3'$ interface (B, C) and the $\alpha 2'$ interface (D, E), with selected side chains shown, and backbones and surfaces colored as in part A. [Figure generated by Saurav Misra and Gali Prag.]

together roughly 180° relative to orientation in the apo structure, bringing the amino-termini of both subunits of the dimer into proximity of each other. These conformational changes generate a basket-like binding pocket with an opening 36 \AA across, 16 \AA wide and 8 \AA deep.

This binding pocket formed by the CUE dimer sits down onto ubiquitin (depicted in yellow) with the ubiquitin carboxy-terminus, the site of covalent attachment to

substrates, protruding from the backside (Figure 27A). The CUE interaction surface can be divided into the right (light blue, Figure 27B,C) and left (dark blue, Figure 27D,E) sides of this binding pocket, denoted as sites 1 and 2, respectively. Site 1 is formed by the conserved MFP residues (419-421) at the end of $\alpha 1$ and the $\Phi_{xx}LL$ residues (V443'-L447') of $\alpha 3'$. M419 and F420 directly bind to I44, A46, G47, H68, L69 and V70 of ubiquitin, while P421 serves both as the helix breaker and contacts A46 and G47. V443' and L447' interact with ubiquitin residues R42-I44-V70 and R42-G47-L48-Q49, respectively; and D444' forms a salt bridge to ubiquitin R42. Thus, M419, F420, V443', D444' and L447' appear to be the important site 1 residues for binding the ubiquitin surface surrounding I44.

The reorientated portion of the CUE dimer forms site 2 and binds the opposite surface of ubiquitin (Figure 27D,E). In particular, helix $\alpha 2'$ residues L427', D430' and V431' mediate the interaction. L427' and V431' form hydrophobic interactions between ubiquitin E34-G35-I36 and L71, respectively; and D430' interacts with T9. In site 1, the corresponding residues in $\alpha 2$ are orientated away from the ubiquitin interface, highlighting the asymmetry of the binding surface. The more conserved (I/L/V) $_{xxx}L$ residues of the CUE domain helix 2 alignment (Figure 26A, Vps9p residues 428'-432') appears to be involved in helix packing rather than ubiquitin binding.

A third contact region is formed in the $\alpha 2'$ - $\alpha 3'$ linker with residues R438' approaching the carboxy-terminus of the ordered ubiquitin (L73), I439' making hydrophobic contacts with V70, and G440' contacting R42 and V70. Thus, the CUE dimer with swapped $\alpha 3$ helices allows a linker region that wraps around the carboxy-terminal portion of ubiquitin without blocking the potential site of ubiquitin covalent

attachment to substrates. The combination of ubiquitin interactions with site 2 and the linker region in addition to site 1 suggest that dimerization of the Vps9p CUE domain is essential in formation of the high affinity ubiquitin binding surface.

Vps9p forms a dimer in vitro and in vivo.

To directly examine the Vps9p CUE-ubiquitin interaction in solution, sedimentation equilibrium centrifugation was performed with ubiquitin and the Vps9p CUE domain (Figure 28A; Rodolfo Ghirlando). Two simplified models were examined in analyzing the collected data. In the first model, interactions with the CUE dimer (CUE₂) and ubiquitin are cooperative, such that the free energy of association is greater than the CUE monomer (CUE₁)-ubiquitin complex formation. In the second model, the interactions are non-cooperative with the formation of the CUE₂-ubiquitin complex (from CUE₂ and free ubiquitin) energetically identical to the 1:1 complex. Analysis of the residuals observed between the analytical centrifugation data and the non-cooperative model suggest that this second model does not adequately describe the interaction (Figure 28A, Column 1). The data corresponds more closely to the model including cooperativity (Column 2), and the fit to the data yield a CUE₂-ubiquitin K_d of 1.2 μ M (within error, 0.5-3.0 μ M) and a CUE₁-ubiquitin K_d of 1.1 mM (within error, 0.7-1.9 mM). These results in solution support the validity of the obtained Vps9p CUE dimer-ubiquitin complex crystal structure.

To examine if Vps9p could form a dimer in vivo, a yeast two hybrid analysis was performed using combinations of Vps9p LexA DNA binding domain (bait) and Gal4 activation domain (prey) fusions, and interaction was scored using a β -galactosidase reporter system (Figure 28B). Prey fusions encoding full-length Vps9p (1-451) interacted with bait proteins containing the GEF domain and carboxy terminus (159-451) as well as the CUE domain baits (408-451); however, the full-length prey did not interact with the Vps9p amino-terminus bait (1-159) or the control LexA DNA binding domain (pVJL11). A similar interaction profile was obtained when Vps9p preys encoding the carboxy-terminus

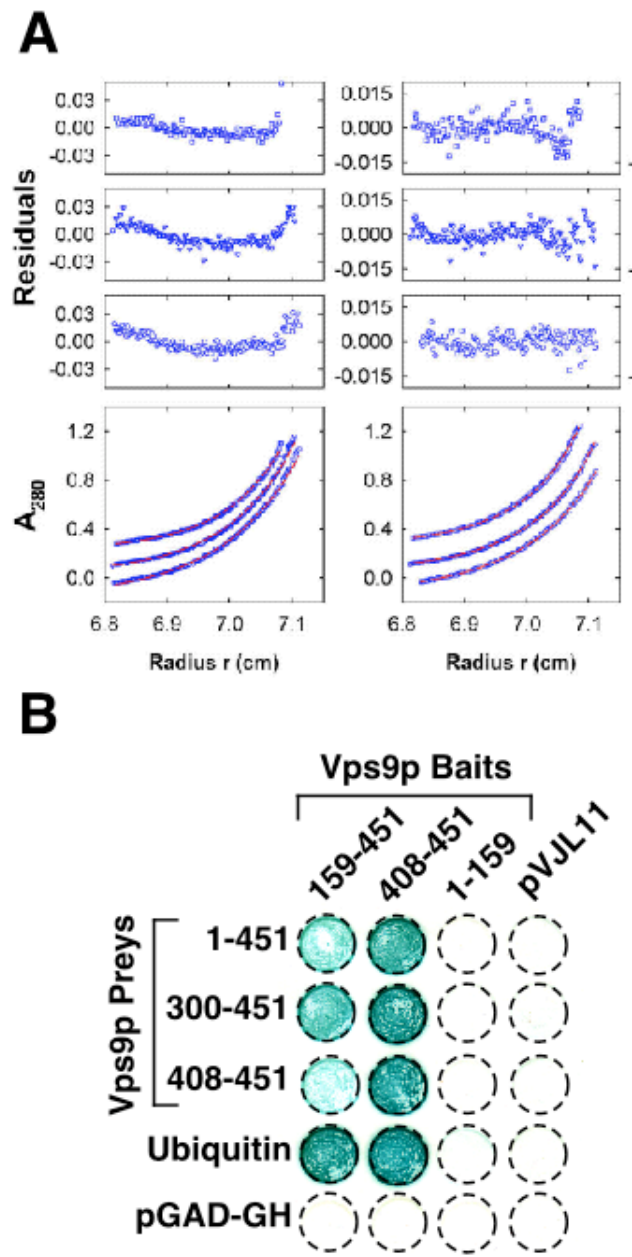


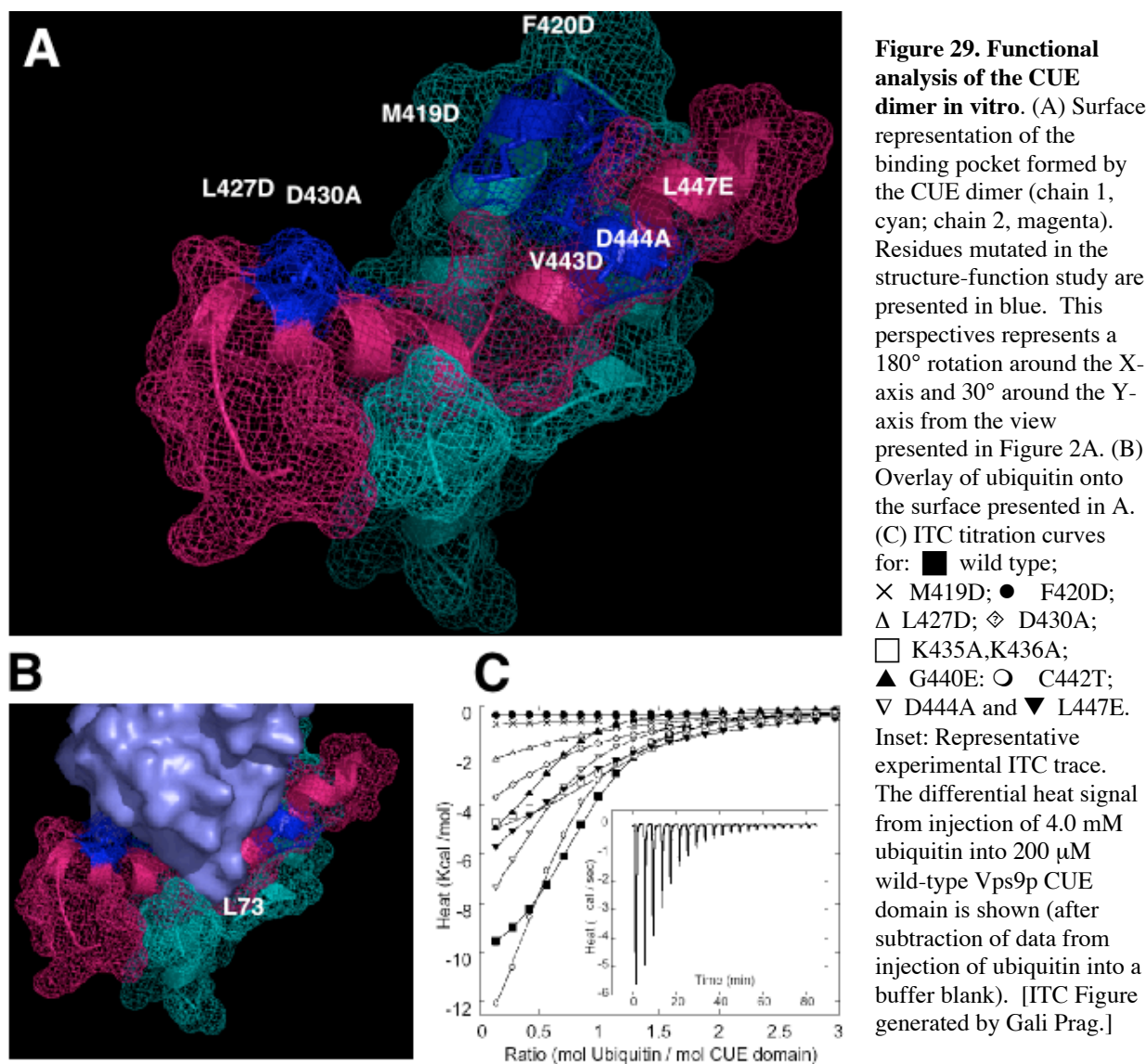
Figure 28. Dimerization of Vps9p in vitro and in vivo. (A) Sedimentation equilibrium profiles at 280 nm and 20.0°C. (Column 1) A 1:1 mixture of CUE and Ubiquitin fit to a non-cooperative interaction (equation [2]), illustrating that wild-type CUE is not properly fit by this model. (Column 2) A 2:1 mixture of CUE and Ubiquitin fit to a cooperative interaction (equation [1]). Symbols correspond to data collected at 24,000 (circles, shifted by -0.2 A₂₈₀), 26,000 (triangles) and 28,000 (squares, shifted by +0.2 A₂₈₀) rpm. [Figure generated by Rodolfo Ghirlando] (B) L40 yeast that were cotransformed with the indicated bait and prey plasmids were grown on selective media, transferred to a nitrocellulose, lysed, and the presence of β -galactosidase was determined using a colorimetric filter assay.

(300-451) or the CUE domain (408-451) were examined. These results suggest that Vps9p molecules interact via the carboxy-terminal region *in vivo* and that the CUE domain is sufficient for this interaction. This model is consistent with the crystal structure and the analytical centrifugation; however, the two hybrid analysis does not preclude indirect association or the presence of higher order CUE oligomers *in vivo*.

Site 1 and 2 contacts are required for high affinity ubiquitin binding *in vitro*.

To further validate the model of Vps9p dimer binding the ubiquitin monomer, a mutational analysis of the CUE binding surface was undertaken. As previously discussed and represented in Figure 29A (view from above; generated with PyMol, Delano Scientific, San Carlos, CA), the 2 chains (cyan and magenta) of the CUE dimer intertwine to form a basket-like binding surface; ubiquitin then fits into this basket with the carboxy-terminus (L73) protruding (Figure 29B). To address the importance of both the right and left portions of this pocket for ubiquitin binding, mutations were generated altering site 1 (M419D, F420D, V443D, D444A, L447E) and site 2 (L427D, D430A; affected residues indicated in blue). CUE domains harboring these mutations were expressed in *E. coli* and purified at levels similar to wild-type, suggesting that overall folding was unaffected.

The interaction between these alleles and ubiquitin was determined by isothermal titration calorimetry (ITC) (Figure 29C, Table 1; conducted by Gali Prag). The wild-type CUE domain binds ubiquitin with an apparent K_d of $20\mu\text{M}$. Mutation of the highly conserved M419 and F420 residues of site 1 ($\alpha 1$) resulted in complete loss of binding as



detectable by ITC, while the site 1 mutants in helix 3 (D444A and L447E) exhibited reduced, but still detectable, association with ubiquitin (61 μM and 133 μM, respectively). These results indicate that the binding site 1 of the CUE dimer formed by α1 and α3' helices is important for binding ubiquitin in vitro. However, this binding site could also be formed in the CUE monomer with α3' replaced by α3, as previously discussed; by contrast, binding site 2 is unique to the dimer structure. Mutation of site 2

Table 1. Mutational analysis of CUE function

| Sample | Interface ¹ | Apparent K_d (μ M) ² | Ubiquitination ³ | Puncta per cell ⁴ |
|--------------------|------------------------|--|-----------------------------|------------------------------|
| Vps9-CUE Wild Type | | 20 ± 1 | 100 | 3.0 ± 1.7 |
| M419D | mono/dimer | NB | 12 | 7.9 ± 2.3 |
| F420D | mono/dimer | NB | 11 | 8.0 ± 2.8 |
| L427D | dimer | 171 ± 14 | 8 | 8.9 ± 2.6 |
| D430A | dimer | 71 ± 8 | 64 | 4.8 ± 2.5 |
| K435A/K436A | dimer | 60 ± 6 | ND | ND |
| G440E | dimer | 26 ± 2 | ND | ND |
| C442T | none | 34 ± 1 | ND | ND |
| V443D | mono/dimer | ND | 9 | 8.3 ± 2.8 |
| D444A | mono/dimer | 61 ± 6 | 65 | 6.6 ± 2.4 |
| L447E | mono/dimer | 133 ± 8 | 29 | 8.1 ± 2.5 |

¹ “mono/dimer” indicates mutants that are in the $\alpha 1/\alpha 3'$ interface common to the monomer and dimer; “dimer” indicates mutants that are in the $\alpha 2'$ interface unique to the dimer; none, C442T is a control mutant for disulfide formation, and not directly part of an interface.

² ITC measurements. NB, no detectable binding within a limit of $\sim 500 \mu$ M; ND, not determined.

³ % wild type in vivo ubiquitination levels, quantified with a UVP Bioimaging System.

⁴ > 50 cells scored per data point.

[Table generated by Gali Prag and Brian Davies.]

residues L427 and D430 ($\alpha 2'$) also resulted in reduced binding with the L427D allele more strongly affected (171μ M and 71μ M). Ubiquitin binding to the L427D allele was further analyzed by sedimentation equilibrium centrifugation, and the resultant data was best fit by the non-cooperative model (K_d 3 mM; Rodolfo Ghirlando, data not shown). These results demonstrate that the site 2 interface and dimerization are required for high affinity ubiquitin binding in vitro.

Site 1 and 2 contacts are required for in vivo function.

In order to assess the role of the CUE binding surfaces in vivo, the site 1 and 2 mutants were incorporated into full-length Vps9p and expressed at genomic levels in yeast lacking endogenous Vps9p ($\Delta vps9$). Extracts were generated from yeast harboring the

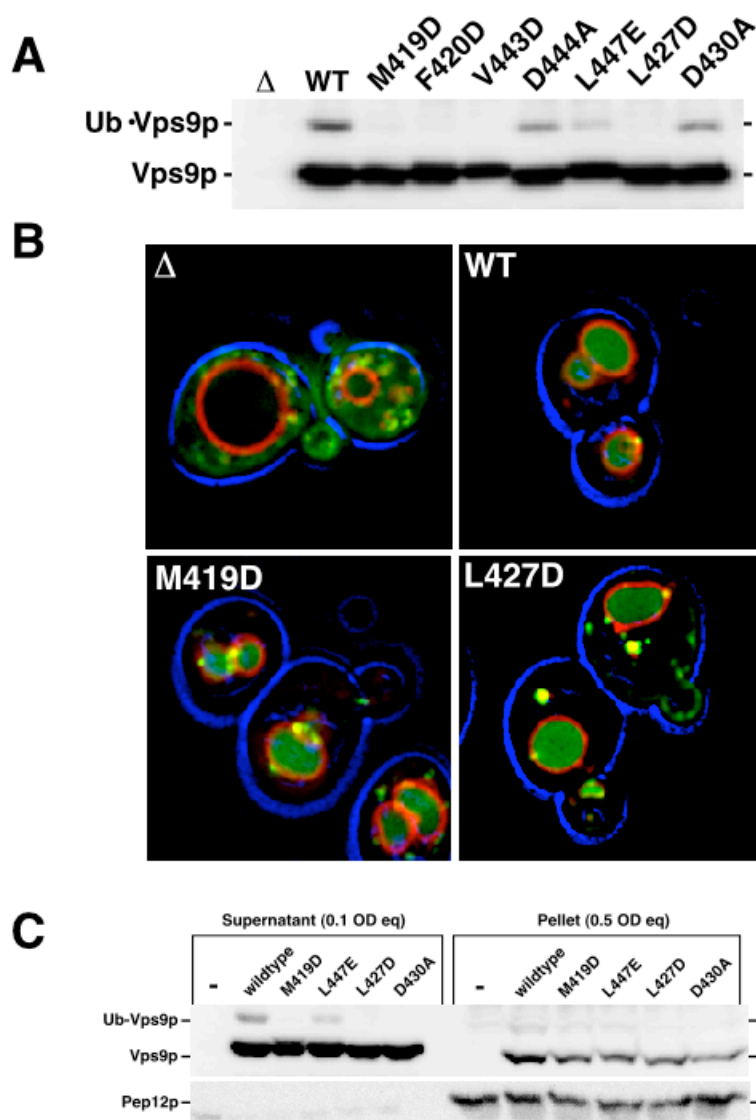


Figure 30. Functional analysis of the CUE dimer in vivo. (A) Lysates were generated from $\Delta vps9$ (lane 1) and $\Delta vps9$ yeast strains expressing wildtype and mutant alleles encoded on a plasmid. Western analysis with Vps9p antiserum was performed and the sizes of the unmodified and ubiquitinated forms of Vps9p are indicated. (B) Microscopic analysis of Ste3-GFP (green) in $\Delta vps9$ (Δ) and $\Delta vps9$ yeast strains expressing wildtype (WT), L427D or M419D alleles. The vacuolar limiting membrane is labeled with FM4-64 (red) and the perimeter of the cell was visualized with blue light. (C) Spheroplasts were generated from $\Delta vps9$ (lane 1) and $\Delta vps9$ yeast strains expressing wildtype and mutant alleles encoded on a plasmid, and cells were perforated by an osmotic lysis technique. Samples were then subjected to 13,000 x g centrifugation for 10 minutes, and the supernatant and pellet fractions were analyzed by SDS-PAGE. Western analysis was performed with Vps9p and Pep12p antisera.

mutant alleles, and the levels of Vps9p were examined by western analysis (Figure 30A). The total levels of Vps9p were equivalent for all the alleles examined, suggesting that the folding of the full length proteins are largely unaffected by the mutations. The presence of ubiquityl-Vps9p has been demonstrated to be dependent on CUE domain ubiquitin binding (discussed in Chapter 4, (Davies, Topp et al. 2003; Shih, Prag et al. 2003)), so ubiquitylation of the Vps9p alleles was analyzed. Approximately 10% of wild-type

Vps9p was present in the covalently modified form. Reduced levels of ubiquityl-Vps9p were present in strains expressing the alleles mutated in site 1 (M419D, F420D, V443D, D444A and L447E; Figure 30A). This result indicated that site 1, the binding surface common to the CUE monomer and dimer, is required for in vivo Vps9p ubiquitin binding. The L427D and D430A mutations in the $\alpha 2$ contacts, which are unique to the CUE dimer binding surface, were also defective in Vps9p ubiquitylation. This result supported the model that the Vps9p dimer is required for in vivo ubiquitin binding. In addition, quantitation of the ubiquitylation defects (Table 1) revealed a strong rank order correlation with in vitro ubiquitin binding defects. This correlation suggested that the in vitro ubiquitin binding, evaluated with the isolated CUE domain, recapitulates the in vivo Vps9p ubiquitin association.

The Vps9p CUE domain is required to potentiate Vps9p function in the endocytic pathway as indicated by defects in a-factor receptor (Ste3p) degradation (discussed in Chapter 4). Under basal condition, Ste3p undergoes constitutive endocytosis and delivery to the vacuole for degradation (Davis, Horecka et al. 1993; Roth and Davis 1996). To assess the functional requirement for CUE domain ubiquitin binding surfaces 1 and 2 in this process, the Vps9p alleles were expressed in a $\Delta vps9$ strain harboring a Ste3p-GFP fusion as a reporter for Ste3p trafficking. Strains harboring wild-type or mutant Vps9p alleles were labeled with FM4-64 to visualize the vacuole (red) (Vida and Emr 1995) and Ste3-GFP distribution was examined 45 minutes after the addition of cyclohexamide (to eliminate biosynthetic/secretory pathway distribution). Following this procedure, the reporter is predominantly localized to the vacuole with few perivacuolar puncta observed in wild-type cells (Figure 30B). In cells devoid of Vps9p (Δ), the

Ste3pGFP reporter is excluded from the vacuole, indicating that Vps9p is required following internalization but before delivery to the vacuole. Analysis of Ste3pGFP localization in both site 1 and site 2 mutants revealed partial defects in Ste3p trafficking. As shown in Figure 30B for cells harboring the M419D mutation (site 1) or the L427D mutation (site 2), the CUE domain mutants were characterized by the increased appearance of extravacuolar puncta. Quantitation of these structures was performed and is presented in Table 3. The increased occurrence of Ste3pGFP puncta in both site 1 and site 2 mutants indicated that ubiquitin interaction with both surfaces of the CUE dimer is required for potentiation of Vps9p activity in the endocytic pathway.

One mechanism by which the ubiquitin-CUE interaction may potentiate Vps9p function in the endocytic pathway is through facilitating membrane localization. To examine this possibility, membrane association of the CUE mutant alleles was examined in a crude fractionation procedure (see Materials and Methods). Spheroplasts were generated from cells expressing wildtype, L447E, L427D or D430A Vps9p alleles and gently perforated by an osmotic lysis procedure. The samples were then subjected to 13,000 x g centrifugation, and the presence of Vps9p in the supernatant and pellet fraction was determined by western analysis. Comparison of the wild-type supernatant (0.1 OD₆₀₀ equivalents) and pellet material (0.5 OD₆₀₀ equivalents) indicated that approximately 5% of Vps9p is membrane associated (Figure 30C). Alleles defective in ubiquitin binding either through mutation of site 1 (L447E) or site 2 (L427D, D430A) exhibited reduced association with the pelletable material (approximately 45% of wild-type levels; compare P13 lanes). While the nature of the association is unclear, this result

suggested that ubiquitin binding by the CUE domain may facilitate or stabilize Vps9p association with the membrane.

Vps9p Ubiquitylation is increased in Class D *vps* mutants.

Cells deficient in Vps9p ($\Delta vps9$) exhibit an enlarged vacuolar morphology characteristic of the Class D *vps* mutants (Burd, Mustol et al. 1996). This Class D phenotype is also present in *vps21*, *vps8*,

pep12/vps6, *vps45*,

vac1/vps19, *vps15*, *vps34*

and *vps3* mutants (Banta,

Robinson et al. 1988;

Raymond, Howald-

Stevenson et al. 1992).

Characterization of the proteins affected in these

mutants has suggested that

these gene products

function together to

mediate transport to the

endosome. To determine

if defects in transport to

endosome might alter the

level of Vps9p

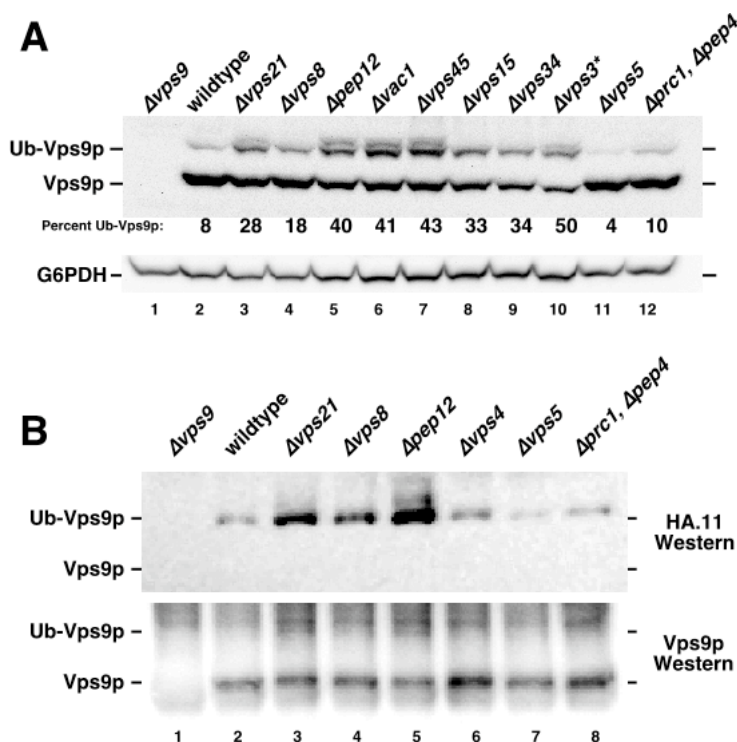


Figure 31. Vps9p ubiquitylation is increased in Class D *vps* mutants. (A) Lysates were generated from *vps9* (lane 1), wildtype (lane 2), Class D *vps* mutants (lanes 3-10), the Class B mutant *vps5* (lane 11) and a strain deficient for CPY, PrA and PrB proteolytic activity (lane 12). Western analysis with Vps9p antiserum was performed and the sizes of the unmodified and ubiquitinated forms of Vps9p are denoted. The proportion of Vps9p found in the ubiquitylated form is indicated. Western analysis with glucose-6-phosphate dehydrogenase antiserum was performed as a loading control. (B) An HA-ubiquitin fusion was expressed in *vps9* (lane 1), wildtype (lane 2), Class D mutants *vps21*, *vps8* and *pep12* (lanes 3-5), the Class E mutant *vps4* (lane 6), Class B mutant *vps5* (lane 7) and a strain deficient for CPY, PrA and PrB proteolytic activity (lane 8). Extracts were generated from these cells and subjected to immunoprecipitation with Vps9p antiserum. Western analyses with HA.11 monoclonal antibody and Vps9p antiserum were performed, and the sizes of the unmodified and ubiquitinated forms of Vps9p are indicated.

ubiquitylation, extracts were generated from the mutant strains, and the abundance of ubiquityl-Vps9p was assessed by western analysis (Figure 31A). Initial evaluation of the western analysis indicated that an upper band, consistent with the size of ubiquityl-Vps9p, is increased in the Class D *vps* mutants (lanes 3-10) but is not increased in an unrelated *vps* mutant (*vps5*, Class B; lane 11; *vps4*, Class E, data not shown) or in a strain defective in vacuolar proteases (TVY614, $\Delta prc1 \Delta pep4$; lane 12). Western analysis with glucose-6-phosphate dehydrogenase (G6PDH) antiserum was used as a loading control (lower panel).

To confirm that the upper band in the Vps9p western corresponds to the ubiquitylated form, *vps* mutant strains were transformed with the HA-ubiquitin construct, and extracts generated from these cells were subjected to immunoprecipitation with Vps9p antiserum. Western analysis with the HA.11 monoclonal antibody was then used to detect the covalently attached HA-ubiquitin in the immunoprecipitates. As shown in Figure 31B, HA-ubiquityl-Vps9p was enriched in extracts generated from the Class D mutants $\Delta vps21$, $\Delta vps8$ and $\Delta pep12$ (lanes 3-5) but was not enriched in extracts from the $\Delta vps4$ (lane 6) or $\Delta vps5$ strains (lane 7) or from TVY614 extracts (lane 8). These observations suggested that defects specifically in the Class D mutants result in increased Vps9p ubiquitylation.

Further inspection of the increased ubiquitylation in the Class D mutants indicated a correlation with site of action (Figure 31A). Examination of the loading control indicated that equivalent amounts of extract were analyzed; however, to compensate for differences in Vps9p expression levels in the different strains, the quantitation of ubiquitylation was determined as a proportion of total Vps9p present in the extract.

Under the culture conditions used in this experiment, approximately 8% of Vps9p was present in the ubiquityl form in the wild-type strain. The least affected mutants were $\Delta vps8$ (18%; E3 ubiquitin ligase, Andrew Friedberg, Bruce Horazdovsky, unpublished result) and $\Delta vps21$ (28%; rab5 homolog; (Horazdovsky, Busch et al. 1994)); and genetic evidence has suggested that Vps8p is a positive regulator of Vps21p (Pam Marshall, Andrew Friedberg, Bruce Horazdovsky, unpublished results). Vps15p and Vps34p form the phosphatidylinositol 3-kinase complex (Stack, Herman et al. 1993), and $\Delta vps15$ and $\Delta vps34$ mutants exhibit 33% and 34% ubiquitylation, respectively. Pep12p, a SNARE protein, associates physically with the Sec1p-homolog Vps45p and the Vps21p-effector Vac1p (Burd, Peterson et al. 1997; Peterson, Burd et al. 1999; Tall, Hama et al. 1999); in a corresponding manner, $\Delta pep12$, $\Delta vps45$ and $\Delta vac1$ mutants exhibited 40%, 41% and 43% ubiquityl-Vps9p. Cells deficient in Vps3p exhibited the greatest increase with 50% of Vps9p in the ubiquitylated form; however, comparison to the other Class D mutants is complicated by the apparent decrease in total Vps9p levels and subtle genetic differences in the parental strain. In tot, these results indicated that specific defects in the endosome delivery machinery differentially affect Vps9p ubiquitylation and suggested that ubiquitylation serves an important role in Vps9p function.

Lysines 402, 403, 435 and 436 are required for wild-type ubiquitylation.

To determine the site of ubiquitin conjugation to Vps9p, a scanning mutagenesis approach was undertaken. The amino-terminus has been demonstrated to be dispensible for Vps9p ubiquitylation, so residues 328-451 were analyzed as potential ubiquitylation sites. The ubiquitin carboxy-terminus is covalently attached to the substrate via a primary amine, typically the ϵ -amino group of lysine, so lysines were converted to arginines to maintain the character of the residue while eliminating the primary amine. Lysines 328, 334, 357, 369, 387, 393 and 410 were mutated individually, and lysine pairs at 402, 403 and 435, 436 were mutated in tandem. These nine alleles as well as the quadruple mutant K402, 3, 35, 36R were expressed in yeast lacking endogenous Vps9p, and the extent of Vps9p ubiquitylation was evaluated by western analysis (Figure 32). The expression levels for all alleles examined (lanes 3-12) were equivalent to wild-type (lane 2); in addition, Vps9p ubiquitylation levels in the K328R, K334R, K357R, K369R, K387R, K393R and K410R (lanes 3-8,10) alleles were equivalent to wild-type Vps9p levels (lane 2, 12% Ub-Vps9p). Mutation of lysine doublets present within the CUE domain (K402, 3, 12% Ub-Vps9p). Mutation of lysine doublets present within the CUE domain (K402,

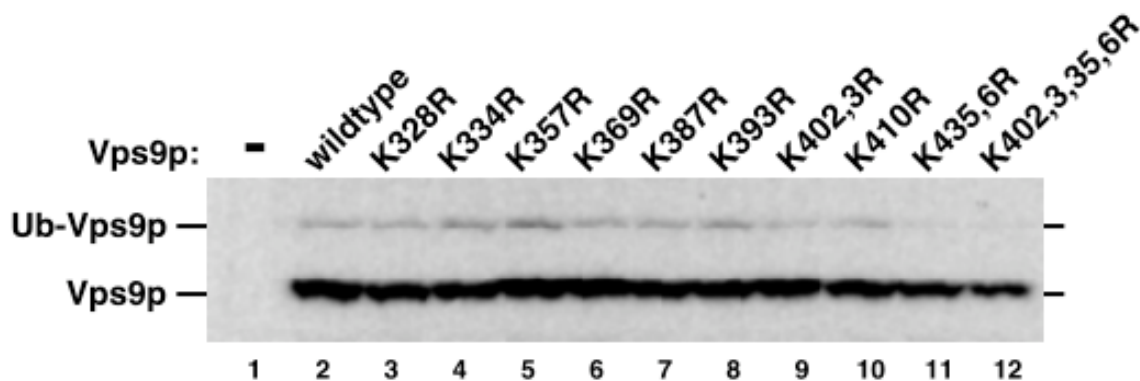


Figure 32. Lysine-arginine scanning of residues 328 to 451. Lysates were generated from $\Delta vps9$ (lane 1) and $\Delta vps9$ yeast strains expressing wildtype and mutant alleles encoded on a plasmid. Western analysis with Vps9p antiserum was performed and the sizes of the unmodified and ubiquitinated forms of Vps9p are indicated

3R and K435, 6R) resulted in 32% and 60% decreases in ubiquitylation (lanes 9 and 11), and the compound mutant (lane 12) exhibited a similar defect (64% reduction).

Examination of the ubiquitin-CUE domain complex suggests that these four conservative mutations would not significantly affect ubiquitin binding as lysines 402 and 403 are present in the amino-terminal portion of helix $\alpha 1$ distal to the ubiquitin interface and lysines 435 and 436 are present in the $\alpha 2$ - $\alpha 3$ linker region oriented away from ubiquitin. These observations suggested that lysines 402, 403, 435 and 436 within the CUE domain serve as potential sites for covalent modification with ubiquitin.

Discussion

Vps9p binds ubiquitin via the CUE domain, and this interaction both potentiates Vps9p function in the endocytic pathway and facilitates Vps9p monoubiquitylation. To gain insight into the mechanism by which the CUE domain binds ubiquitin and the effect of this interaction on Vps9p function, a structure function analysis was undertaken. The structure of the Vps9p CUE domain was determined to 2.3 Å resolution, and indicated that CUE can form a domain swapped dimer. Sedimentation equilibrium centrifugation demonstrated that this dimer forms in solution; however, the monomer is likely the relevant form as the K_d for dimerization is 1 mM. The modeled Vps9p CUE monomer exhibited similarity to the hRad23 UBA solution structure, indicating that the CUE and UBA motifs form a superfamily of three helical ubiquitin binding domains. The structure of the Vps9p CUE domain-ubiquitin complex was also determined to 1.7 Å resolution. The Vps9p CUE domain dimerizes to form a high affinity binding surface with K_d for ubiquitin of 1.2-20 μ M (determined by sedimentation equilibrium centrifugation and

isothermal titration calorimetry). Mutational analysis of two regions on this surface indicated that the dimer is required for high affinity ubiquitin binding in vitro and CUE domain function in vivo. Further characterization of the CUE domain mutants in vivo demonstrated that high affinity ubiquitin binding is required to maintain Vps9p association with pelleted material in a crude fractionation assay. These observations suggest that Vps9p forms a dimer to bind ubiquitin with high affinity and that this association stabilizes Vps9p membrane association to potentiate Vps9p function in the endocytic pathway. In addition, strains defective in transport to the endosome were found to exhibit increased Vps9p ubiquitylation, and four lysines within the CUE domain have been implicated as the site(s) of covalent modification by a site-directed mutagenesis approach. These results suggest that ubiquitylation of the Vps9p CUE domain is functionally linked to traffic into the endosome.

The crystal structure of the Vps9p CUE domain in complex with ligand demonstrates a mechanism by which small helical domains may bind ubiquitin with high affinity. Kang and colleagues recently determined the solution structure of a CUE domain of yeast Cue2p (CUE2-1³) in complex with ubiquitin (Kang, Daniels et al. 2003), and an interesting contrast is apparent. CUE2-1 binds ubiquitin as a monomer with residues in the αA ($\alpha 1$) and αC ($\alpha 3$) helices, but not the αB ($\alpha 2$) helix, contacting ubiquitin. These interactions are analogous to the contacts implicated in UBA ubiquitin binding and suggested to mediate low affinity binding between ubiquitin and the Vps9p CUE monomer, as in the L427D allele. Similarly, the CUE2-1 apparent K_d of 155 ± 9

³ Cue2p contains 2 CUE domains, both of which are capable of binding ubiquitin. The similarity to the Vps9p dimer is intriguing, however Kang et al. report that the two domains do not generate a cooperative binding effect in vitro.

μM (determined by NMR; (Kang, Daniels et al. 2003)) is comparable to the Vps9p L427D CUE K_d of $171 \pm 14 \mu\text{M}$ (determined by ITC); by contrast, the Vps9p CUE dimer binds cooperatively to ubiquitin with K_d of $1.2 \mu\text{M}$ (determined by sedimentation equilibrium centrifugation). These similarities and differences suggest that the CUE domain can bind ubiquitin either as a monomer with low affinity ($\sim 150 \mu\text{M}$) or, in some proteins such as Vps9p, as a dimer with high affinity ($1 \mu\text{M}$).

The Vps9p CUE dimer generates a concave surface with 2 primary contact sites that bind cooperatively to ubiquitin to generate this high affinity. However, additional interactions between the CUE dimer and ubiquitin are present in crystal lattice. As previously discussed, the primary ubiquitin binding surface is formed by $\alpha 1$ - $\alpha 3'$ (site 1), $\alpha 2'$ (site 2) and the $\alpha 2'$ - $\alpha 3'$ linker. Two additional hydrophobic surfaces are formed by $\alpha 1'$ - $\alpha 3$ (back of site 2) and $\alpha 2$ (back of site 1); and in the crystal lattice, these surfaces from neighboring CUE dimers contact the intervening ubiquitin in a manner equivalent to the primary binding site but lacking the $\alpha 2'$ - $\alpha 3'$ linker contacts. The *in vivo* relevance of these secondary binding sites is unclear, but they could contribute energy to stabilize Vps9p association with a receptor ubiquitylated at multiple sites or a polyubiquitin chain. Further experimentation will be needed to address these possibilities *in vivo*.

CUE domain mutations that diminish high affinity ubiquitin binding *in vitro* result in defective trafficking of Ste3p to vacuole, as previously demonstrated for the M419A allele in Chapter 4. Examination of the Vps9p fractionation pattern revealed a possible mechanism for this phenotype. Using a gentle and rapid fractionation procedure (suggested by David Katzmann), approximately 5% of Vps9p is associated with the membrane fraction (Figure 30C). This fractionation pattern is consistent with initial

analysis of a Vps9p-GFP fusion in which the majority of fluorescence is diffuse with a few discrete puncta apparent (data not shown). Analysis of the Vps9p CUE alleles revealed a decreased association with the pelleted material, suggesting that Vps9p localization is dependent on high affinity ubiquitin binding. How can ubiquitin binding by the CUE domain serve to localize Vps9p to the site of action if ubiquitin is present on multiple cellular targets? One possibility is that ubiquitin binding serves to stabilize localization that is initially determined through interactions mediated by the Vps9p amino-terminus (residues 1-159). The basal oligomeric state of Vps9p in the cell is unknown, but an intriguing possibility is that the monomer with low affinity for ubiquitin predominates in the cytosol. Vps9p residues 158-347 are sufficient to activate Vps21p *in vitro*, however residues 1-158 are also required to activate Vps21p *in vivo* (Greg Tall, Darren Carney, Bruce Horazdovsky, manuscript in preparation). This suggests that the amino terminus is sufficient to localize Vps9p to the membrane to activate Vps21p. The increase in local concentration upon membrane association might then favor transition to the dimeric form and the subsequent increase in ubiquitin affinity. In the presence of ubiquitylated-cargo, this dimeric form could then bind ubiquitin, undergo stabilization at the site of action and thereby potentiate guanine nucleotide exchange activity. One of the appealing features of this model is that a dynamic, localized concentration of Vps9p is generated, and this may be important to activate Vps21p at the appropriate site as kinetic analysis of Vps9p binding with Vps21•GDP in solution suggests weak association (K_d 23 μ M) (Esters, Alexandrov et al. 2001). Alternatively, ubiquitin induced Vps9p dimerization may directly affect the catalytic activity; however, no effect has been observed in the Vps21p GDP release assay with 20 or 40 μ M ubiquitin addition (data not

shown). More detailed analyses of Vps9p localization, the dimer/monomer equilibrium in vivo and biochemical activity in vitro may provide insights into the role of ubiquitin binding in Vps9p function.

The role of Vps9p ubiquitylation in transport to the endosome is also unclear. Mutations that block high affinity ubiquitin binding result in decreased ubiquitylation. One possibility is that localization or complex formation stabilized by the CUE-ubiquitin association is a prerequisite for interaction with the E3 ligase, thus suggesting a defect in generation of the ubiquitylated form. Alternatively, the CUE domain could form an intramolecular association with the Vps9p ubiquityl moiety that stabilizes the covalent modification, suggesting that CUE mutants exhibit less ubiquityl-Vps9p through increased deubiquitylation. These two possibilities may be distinguishable through in vitro ubiquitylation analysis and will be examined along with the CUE domain lysine-arginine mutants implicated as the conjugation site(s). Interestingly, increased levels of ubiquityl-Vps9p are observed when transport to the endosome is compromised (Class D mutants). This proliferation could result from an increase in formation or a decrease in turnover of the modified form (or a combination of both). An intriguing possibility is that defects in transport to the endosome result in the accumulation of intermediary protein complexes in which the Vps9p ubiquityl moiety is protected; this model would explain the discrete ubiquitylation phenotypes exhibited by different groups of Class D mutants if distinct complexes were stabilized. Ubiquitylation might also potentiate Vps9p catalytic activity. The increased proportion of Vps9p present in the Class D mutants suggests that these strains will serve as a good source of material for purification and biochemical characterization of ubiquityl-Vps9p.

Chapter 6. Discussion

Vacuolar protein sorting pathway

The transport of protein and lipid to the mammalian lysosome is required to maintain cellular homeostasis. Defects in the mannose-6-phosphate targeting system that populates the lysosome give rise to I-cell disease, with the syndrome progressing to lethality between 5 to 8 years of age (reviewed in (Kornfeld and Sly 2001)).

Interestingly, defects in the mammalian counterparts of the yeast VPS components have been observed to exhibit defects both more and less severe. The yeast protein Vps26p is required to maintain recycling of the vacuolar protein sorting receptor in association with the Vps5p•Vps17p sorting nexin complex and the Vps29p•Vps35p complex (Seaman, McCaffery et al. 1998); yet, the $\Delta vps26$ yeast are viable with no apparent growth defects (Bachhawat, Suhan et al. 1994). By contrast, disruption of the Vps26p murine homolog H β -58 (isolated in an insertional mutagenesis screen) results in embryonic lethality (Radice, Lee et al. 1991; Lee, Radice et al. 1992), a phenotype considerably more severe than I-cell disease. The counter example is seen with Vps23p. The yeast Vps23p protein is a component of the ESCRT-I complex involved in an early stage of multivesicular body formation (Babst, Odorizzi et al. 2000; Katzmann, Babst et al. 2001). The mammalian homolog is the product of the tumor suppressor gene, Tsg101. Functional inactivation of Tsg101 in mouse fibroblasts leads to increased recycling of the EGF-R, and Tsg101-mutant cells exhibit prolonged EGF-stimulated signaling (Babst, Odorizzi et al. 2000). These two examples highlight the importance of the mammalian VPS homologs in maintaining cellular homeostasis to sustain viability and retard

hyperproliferation. The contrast between the H β -58 and Tsg101 phenotypes suggests that inhibition of H β -58/hVps26p-mediated recycling could present a mechanism to restore the appropriate receptor levels to human Tsg101-tumors.

The beauty of the VPS system is the powerful genetics and relative simplicity of yeast that have enabled the pathway to be explored. The power of yeast genetics speaks for itself with the number of components that were identified through the genetic approaches of Jones, Stevens and Emr (Jones 1977; Bankaitis, Johnson et al. 1986; Rothman and Stevens 1986). But the simplicity of yeast in its ability to both grow in the absence of a functional sorting pathway and to possess little redundancy proved invaluable in the genetic study that was undertaken. A point in case is the rab5/Vps21p exchange factor Vps9p (Hama, Tall et al. 1999). In yeast, there is a single predicted protein (encoded by YPL070w⁴) that resembles Vps9p; by contrast, the human genome contains 7 identified VPS9 domain containing proteins (Schultz, Copley et al. 2000; Letunic, Goodstadt et al. 2002) and 3 additional possible open reading frames that contain the VPS9 domain (Darren Carney, personal communication). In the yeast system, a single *vps9* mutation can eliminate Vps21p activation; yet, the yeast are still viable (Burd, Mustol et al. 1996). The viability of the *vps* mutants has also enabled the genome-wide screening for defects in the transport system via high-throughput assays of the genome deletion library (4,653 viable strains) (Winzeler, Shoemaker et al. 1999), and the results are staggering. Whereas ~50 genetic loci were implicated in the *VPS* pathway though studies initiated in 1977 and reported through 2002, Bonifacino and colleagues

⁴ Sequence analysis of the YPL070w VPS9 domain reveals that multiple residues highly conserved among the active rab5/Vps21p GEF as absent; thus, YPL070w is anticipated to lack GEF activity (Bruce Horazdovsky, personal communication).

reported in a single publication close to 100 additional components that may contribute to the transport system (Bonangelino, Chavez et al. 2002). While individual analysis will be required to further validate the identified genes and begin to address their roles in the *VPS* pathway, these results demonstrate that the yeast system has not yet become obsolete.

Role of the sorting nexins in Vps10p trafficking

The study of the yeast sorting nexins Vps5p and Vps17p has greatly enhanced our knowledge of sorting nexin-mediated receptor trafficking from yeast to humans through identification of the Vps5p, Vps17p, Vps26p, Vps29p, Vps35p complex (Chapter 2,3 and (Horazdovsky, Davies et al. 1997; Seaman, McCaffery et al. 1998; Reddy and Seaman 2001; Seaman and Williams 2002)). SNX1 was identified as an EGF receptor tail binding partner using the two-hybrid screen (Kurten, Cadena et al. 1996); and a role for SNX1 in EGF-R trafficking was demonstrated by examining receptor localization upon SNX1 over-expression. Analysis of the sorting nexin knockout phenotype was initially performed in yeast, as described in Chapter 2 (Kohrer and Emr 1993; Horazdovsky, Davies et al. 1997; Nothwehr and Hinds 1997). Recently, the generation of the SNX1 as well as SNX2 knockout mice has been reported, and the individual homozygous mice are viable (Schwarz, Griffin et al. 2002). SNX1 and SNX2 are very closely related (~60% identity) (Haft, de la Luz Sierra et al. 1998), and have been demonstrated to heterodimerize, in a manner equivalent to Vps5p•Vps17p complex formation, or to homodimerize. The SNX1^{-/-} SNX2^{-/-} double mutant was generated and found to be inviable; thus the viability in the single knockouts suggests that SNX1 and SNX2 can

each homodimerize and have redundant functions. Schwarz et al. report that the arrested embryos resemble the H β -58 (Vps26) mutant phenotype (Radice, Lee et al. 1991; Lee, Radice et al. 1992; Schwarz, Griffin et al. 2002). Thus the phenotypic similarities observed between $\Delta vps5$ and $\Delta vps26$ with respect to Vps10p trafficking in yeast are reflected in the mammalian knockout phenotypes; in addition, SNX1, SNX2 and hVps26 have been demonstrated to form a protein complex (Haft, de la Luz Sierra et al. 2000).

The redundant nature of SNX1 and SNX2 indicate a distinction from the obligate Vps5p•Vps17p heterodimers. One possibility is that both the mammalian and yeast proteins represent evolutionary divergences. In sequence similarity searches (Altschul, Gish et al. 1990), Vps5p and Vps17p bear closer resemblance to the mammalian SNX1 and SNX2 than they do to each other, although Vps5p is more similar to SNX1 and SNX2 than is Vps17p. In the case of the mammalian system, an evolutionary progenitor in common with the single SNX1 apparent in worms and flies might have undergone gene duplication, and the resultant gene products have retained the ability to function as homodimers or heterodimers; however, in the fungal divergence, the two subunits have evolved into an obligate heterodimers with Vps17p exhibiting more divergence from the common ancestor. These possible distinctions between the mammalian SNX1 proteins and the Vps5p and Vps17p proteins may prove important in translating future yeast and mammalian studies.

In both systems, the SNX1/SNX2/Vps5p/Vps17p proteins form dimers that interact with the Vps26p, Vps29p and Vps35p subunits, and work in the yeast system implicate the Vps29p•Vps35p complex in binding the receptor tail (Nothwehr, Bruinsma et al. 1999; Nothwehr, Ha et al. 2000), possibly as an adaptor. However the ability of

Vps5p and Vps17p to bind membranes in the absence of Vps26p, Vps29p or Vps35p (Chapter 3) as well as distinct vacuolar morphologies in the Class A (*vps29*, *vps35*) and Class B (*vps5*, *vps17*) mutants (Banta, Robinson et al. 1988; Raymond, Howald-Stevenson et al. 1992) indicate that Vps5p•Vps17p exhibits a function, and membrane association, independent of the other subunits. Determination of this membrane association in terms of the binding target as well as morphological analysis of the compartment may be valuable in understanding how Vps5p and Vps17p mediate recycling. To address this issue, a purification procedure utilizing differential sedimentation, density and size (gel filtration chromatography) will be utilized to enrich for the Vps5p compartment, using western analysis with Vps5p antiserum to follow fractionation of the compartment.

Another approach that may provide valuable insights, but is beyond the scope of my time frame, is the biophysical characterization of complex formation. The Vps5p, Vps17p, Vps26p, Vps29p, Vps35p complex can exist as cytosolic form, but the membrane associated complex seems to be the functionally important form. PtdIns(3)P is also important for function of the complex, but in a manner that is unclear. One possibility is that PtdIns(3)P binding by the PX domains of Vps5p and Vps17p might modulate the interactions in the complex. Consistent with this idea, Vps5 Δ PXp appears to exhibit a slightly reduced association with Vps29p and Vps35p in crosslinking analysis of the complex (Figure 16), although such distinctions may be outside the experimental limitations. Reconstitution of the protein complex in vitro in the presence or absence of liposomes and determination of binding constants either through isothermal titration calorimetry or development of a kinetic spectroscopic assay would be ideal to address the

role of PtdIns(3)P in complex formation and sorting nexin function. However, I have not been able to generate large amounts of recombinant subunits for development of these assays to this point.

Role of ubiquitin in Vps9p function

Determining the role of ubiquitin in Vps9p function is an equally interesting task. Vps9p binds ubiquitin via the formation of the CUE dimer, as revealed by determination of the crystal structure and subsequent analysis in vitro and in vivo (Chapter 5). Three general models exist for how this ubiquitin binding may potentiate Vps9p functions. The first model suggests that the CUE domain may target Vps9p to ubiquitylated transmembrane proteins, such as endocytosed receptors. A second model is that the CUE domain mediates interaction with another ubiquitylated component of the trafficking pathway, including possible components of the ubiquitylation machinery. And third is the model in which the CUE domain forms an intramolecular association with the Vps9p-ubiquityl group.

Preliminary analysis of subcellular fractionation suggests that the CUE domain is involved in membrane association; however, these results must be expanded by a more complete examination of subcellular fractionation. The difficulty in these experiments is that potent de-ubiquitylating activity is present in the yeast lysate and may compromise membrane association. NEM is included in the buffer to inhibit this activity, but subcellular localization must also be examined by in vivo fluorescence for confirmation.

The formation of ubiquitin-dependent protein complexes (model 2) is interesting with respect to the increased Vps9p ubiquitylation apparent in the Class D *vps* mutants

(Figure 31). One possibility is that defects in the endosome fusion machinery result in the accumulation of Vps9p protein complexes with the ubiquityl moiety protected, and the Vps9p ubiquitylation variation in different sets within the Class D may represent distinct stabilized complexes. The Class D *vps* mutants with enhanced ubiquitylation also appear to be a good source for beginning purification of the ubiquitylated form. This procedure will be undertaken to both identify copurifying peptides and determine guanine nucleotide exchange activity of the ubiquitylated form. In addition, I would like to use mass spectrometry to determine the Vps9p ubiquitylation site, suggested by mutagenesis scanning to fall within the CUE domain.

The third model incorporates an intramolecular interaction to regulate Vps9p activity. Donaldson et al. favor a model in which the CUE domain folds back to inhibit GEF activity, and ubiquitin binding releases this autoinhibition (Donaldson, Yin et al. 2003). Preliminary analysis of Vps9p amino- and carboxy-terminal truncations support this model with removal of the carboxy-terminus resulting in a more active peptide (Greg Tall, Darren Carney, Bruce Horazdovsky, manuscript in preparation); however, a more detailed analysis is required (apparent K_m , k_{cat}) to control for protein stability artifacts. The corresponding experiment is to determine the effect of ubiquitin addition on wild-type Vps9p GEF activity, and initial experiments (20, 40 μ M ubiquitin addition, K_d 1-20 μ M for CUE₂:ubiquitin) do not indicate an effect (data not shown). The monomer-dimer equilibrium for full-length Vps9p in solution may be an important factor in these GEF assays and will need to be addressed in vitro and in vivo.

The determination of the VPS9 domain catalytic mechanism has been an objective of the Horazdovsky lab for the past 4 or 5 years in collaboration with members

of the Sprang lab (UT Southwestern). Initial attempts focused on complex formation between full-length Vps9p and Vps21p and subsequent crystal trials; however, the complex was fairly unstable. Crystal trials were also initiated using the VPS9 domain of human Rabex5 in combination with Vps21p; although this generates a more stable complex, suitable crystals were not achieved. Currently, Darren Carney is utilizing NMR approaches to define the solution structure of the Rabex5 VPS9 domain and the binding site on Vps21p. The observation that ubiquitin binds to the Vps9p CUE dimer with high affinity and forms lattice contacts suggests that revisiting Vps9p crystallization may be productive. It is possible that by stabilizing the CUE domain, promoting dimerization and generating a ubiquitin lattice the VPS9 domain crystallization may be facilitated. If so and if a structure can be obtained, further insight into the role of ubiquitin binding in Vps9p function could be gained by comparing the crystal structure to the solution structure of the isolated VPS9 domain Darren Carney will be determining.

.

Appendix 1.

| Strains and plasmids | Description | Source |
|-------------------------|--|--------------------------------------|
| Yeast Strains | | |
| SEY6210 | MAT α <i>leu2-3,112 ura3-52 his3-Δ200 trp1-Δ901 lys2-801 suc2-Δ9</i> | (Robinson, Klionsky et al. 1988) |
| TVY614 | SEY6210; Δ <i>pep4::LEU2 Δprc1::HIS3 Δprb1::HISG</i> | (Gerhardt, Kordas et al. 1998) |
| BHY152 | SEY6210; Δ <i>vps5::HIS3</i> | Chapter 2 |
| KKY10 | SEY6210; <i>vps17Δ1</i> | (Kohrer and Emr 1993) |
| BDY261 | SEY6210; Δ <i>vps26::NEO</i> | Chapter 3 |
| PSY129 | SEY6210; Δ <i>vps29::HIS3</i> | (Seaman, Marcusson et al. 1997) |
| PHY102 | SEY6210; <i>vps34Δ1::TRP1</i> | (Herman and Emr 1990) |
| DDY3477 | SEY6210; <i>vps34^{ts}</i> | (Tall, Hama et al. 1999) |
| EMY18 | SEY6210; Δ <i>vps35::HIS3</i> | (Cereghino, Marcusson et al. 1995) |
| BDY517 | SEY6210; Δ <i>vps5::HIS3</i> , Δ <i>vps17::NEO</i> | Chapter 3 |
| E. coli strains | | |
| DH5a | F ['] / <i>endA1 hsdR17 (r_K-m_K+) glnV44 thi-1 recA1 gyrA (NaI^r) relA1 Δ(lacIZYA-argF)U169 deoR (ϕ80dlacΔ(lacZ)M15)</i> | Invitrogen |
| Plasmids | | |
| pBS | pBluescript II | Stratagene |
| pRS414 | yeast CEN TRP1 expression vector | (Christianson, Sikorski et al. 1992) |
| pRS416 | yeast CEN URA3 expression vector | (Christianson, Sikorski et al. 1992) |
| pRS414 Vps5 Δ PX | <i>vps5</i> lacking residues 313 to 385, in pRS414 | Chapter 3 |
| pRS414 Vps5 | <i>VPS5</i> residues 313 to 385 restored to pRS414 Vps5 Δ PX | Chapter 3 |
| pRS414 Vps5 R319Q | <i>vps5</i> encoding the R319Q allele in pRS414 | Chapter 3 |
| pRS416 Vps17 | <i>VPS17</i> wild-type in pRS416 | Chapter 3 |
| pRS416 Vps17 KK150,1QQ | <i>vps17</i> encoding the KK150,1QQ allele in pRS416 | Chapter 3 |
| pBS NEO | kanMX4 module in pBS | (Hama, Tall et al. 1999) |
| pBS Vps26::NEO | <i>vps26Δ1::NEO</i> in pBS | Chapter 3 |
| pBS Vps17::NEO | <i>vps17::NEO</i> in pBS | Chapter 3 |

Appendix 2. Crystallographic data, phasing and refinement statistics.

| Data collection and phasing: | | | |
|--|--------------------------------|--------------------|--------------------|
| | apo | Complex set 1 | Complex set 2 |
| Space group | P6 ₅ 22 | C2 | C2 |
| Unit cell (Å) | a=b=70.49, | a=102.31 | a=101.61 |
| | | b=46.69 | b=45.89 |
| | c=61.38 | c=58.36 | c=57.80 |
| | $\alpha=\beta=90^\circ$ | $\alpha=\gamma=90$ | $\alpha=\gamma=90$ |
| | $\gamma=120^\circ$ | $\beta=97.33$ | $\beta=96.53$ |
| Wavelength (Å) ^a | 0.97910 | 0.9792 | 0.9564 |
| Resolution (Å) | 50-2.3 (2.38-2.3) ^b | 50-2.2 (2.28-2.2) | 50-1.7 (1.76-1.7) |
| Unique reflections | 4327 (415) | 13877 (1272) | 28955 (2626) |
| Completeness (%) | 99.8 (99.8) | 98.7 (92.0) | 98.4 (89.6) |
| Redundancy | 23.5 | 6.8 | 3.5 |
| $\langle I \rangle / \langle \sigma \rangle$ | 35.6 (6.2) | 26.1 (5.9) | 29.5 (2.3) |
| R _{merge} ^c (%) | 8.6 (40.8) | 7.2 (28.5) | 4.0 (36.7) |
| Anom. differences (%) | 4.3 - 5.9 | 3.2 - 4.7 | |
| Disp. differences (%) | 2.3 - 4.8 | 1.6 - 2.8 | |
| FOM - SOLVE | 0.43 (0.13) | 0.42 (0.31) | |
| FOM - RESOLVE | 0.57 (0.17) | 0.49 (0.32) | |

| Refinement | apo | complex |
|---|-----------|---------|
| Resolution range (Å) | 43.4-2.30 | 50-1.7 |
| No. of reflections | 7325 | 55378 |
| R ^d (%) | 24.4 | 26.0 |
| R _{free} ^e (%) | 26.6 | 27.7 |
| Cross-validated Luzatti error | 0.39 | 0.27 |
| Rms deviations: | | |
| Bond length (Å) | 0.006 | 0.01 |
| Bond angle (°) | 1.10 | 1.50 |
| Improper angle (°) | 0.86 | 1.06 |
| Dihedral (°) | 18.4 | 23.8 |
| Average B factor (Å ²) | 42.2 | 29.1 |
| Protein atoms | 425 | 1771 |
| Solvent atoms | 31 | 180 |
| Residues in core Φ - Ψ region | 100% | 99.5 |

^a Statistics are shown for the peak wavelength of the Selenomethionine MAD datasets. Statistics for the inflection wavelength (0.97924 Å for apo and 0.97931 for complex) and remote wavelength (0.95645 Å for apo and complex) were very similar.

^bStatistics in parentheses are for the highest resolution shell (Å).

$$^cR_{\text{merge}} = \sum |I(k) - \langle I(k) \rangle| / \sum I(k)$$

$$^dR = \sum |F_{\text{obs}} - kF_{\text{calc}}| / \sum F_{\text{obs}}$$

^e R_{free} is the R value calculated for a test set of reflections, comprising a randomly selected 10% of the data, not used during refinement.

[Table generated by Gali Prag and Saurav Misra.]

Bibliography

- Albert, S. and D. Gallwitz (1999). "Two new members of a family of Ypt/Rab GTPase activating proteins. Promiscuity of substrate recognition." J Biol Chem **274**(47): 33186-9.
- Altschul, S. F., W. Gish, et al. (1990). "Basic local alignment search tool." J Mol Biol **215**(3): 403-10.
- Babst, M., D. J. Katzmann, et al. (2002). "Escrt-III: an endosome-associated heterooligomeric protein complex required for mvb sorting." Dev Cell **3**(2): 271-82.
- Babst, M., D. J. Katzmann, et al. (2002). "Endosome-associated complex, ESCRT-II, recruits transport machinery for protein sorting at the multivesicular body." Dev Cell **3**(2): 283-9.
- Babst, M., G. Odorizzi, et al. (2000). "Mammalian tumor susceptibility gene 101 (TSG101) and the yeast homologue, Vps23p, both function in late endosomal trafficking." Traffic **1**(3): 248-58.
- Babst, M., T. K. Sato, et al. (1997). "Endosomal transport function in yeast requires a novel AAA-type ATPase, Vps4p." Embo J **16**(8): 1820-31.
- Babst, M., B. Wendland, et al. (1998). "The Vps4p AAA ATPase regulates membrane association of a Vps protein complex required for normal endosome function." Embo J **17**(11): 2982-93.
- Bach, G. (2001). "Mucopolidosis type IV." Mol Genet Metab **73**(3): 197-203.
- Bachhawat, A. K., J. Suhan, et al. (1994). "The yeast homolog of H < beta > 58, a mouse gene essential for embryogenesis, performs a role in the delivery of proteins to the vacuole." Genes & Development **8**(12): 1379-87.
- Bankaitis, V. A., L. M. Johnson, et al. (1986). "Isolation of yeast mutants defective in protein targeting to the vacuole." Proc Natl Acad Sci U S A **83**(23): 9075-9.
- Banroques, J., A. Delahodde, et al. (1986). "A mitochondrial RNA maturase gene transferred to the yeast nucleus can control mitochondrial mRNA splicing." Cell **46**: 837-44.

- Banta, L. M., J. S. Robinson, et al. (1988). "Organelle assembly in yeast: characterization of yeast mutants defective in vacuolar biogenesis and protein sorting." The Journal of Cell Biology **107**(4): 1369-83.
- Barr, V. A., S. A. Phillips, et al. (2000). "Overexpression of a novel sorting nexin, SNX15, affects endosome morphology and protein trafficking." **1**(11): 904-16.
- Bateman, A., E. Birney, et al. (2002). "The Pfam protein families database." Nucleic Acids Res **30**(1): 276-80.
- Becherer, K. A., S. E. Rieder, et al. (1996). "Novel syntaxin homologue, Pep12p, required for the sorting of luminal hydrolases to the lysosome-like vacuole in yeast." Mol Biol Cell **7**(4): 579-94.
- Bensen, E. S., B. G. Yeung, et al. (2001). "Ric1p and the Ypt6p GTPase function in a common pathway required for localization of trans-Golgi network membrane proteins." Mol Biol Cell **12**(1): 13-26.
- Bertolaet, B. L., D. J. Clarke, et al. (2001). "UBA domains of DNA damage-inducible proteins interact with ubiquitin." Nat Struct Biol **8**(5): 417-22.
- Biederer, T., C. Volkwein, et al. (1997). "Role of Cue1p in ubiquitination and degradation at the ER surface." Science **278**(5344): 1806-9.
- Bilodeau, P. S., J. L. Urbanowski, et al. (2002). "The Vps27p Hse1p complex binds ubiquitin and mediates endosomal protein sorting." Nat Cell Biol **4**(7): 534-9.
- Bonangelino, C. J., E. M. Chavez, et al. (2002). "Genomic Screen for Vacuolar Protein Sorting Genes in *Saccharomyces cerevisiae*." Mol Biol Cell **13**(7): 2486-501.
- Bowers, K., B. P. Levi, et al. (2000). "The sodium/proton exchanger Nhx1p is required for endosomal protein trafficking in the yeast *Saccharomyces cerevisiae*." Mol Biol Cell **11**(12): 4277-94.
- Bravo, J., D. Karathanassis, et al. (2001). "The crystal structure of the PX domain from p40(phox) bound to phosphatidylinositol 3-phosphate." Molecular Cell **8**(4): 829-39.
- Brickner, J. H. and R. S. Fuller (1997). "SOI1 encodes a novel, conserved protein that promotes TGN-endosomal cycling of Kex2p and other membrane proteins by modulating the function of two TGN localization signals." Journal of Cell Biology **139**(1): 23-36.

- Brunger, A. T., P. D. Adams, et al. (1998). "Crystallography & NMR system: A new software suite for macromolecular structure determination." Acta Crystallogr D Biol Crystallogr **54** (Pt 5): 905-21.
- Bryant, N. J. and T. H. Stevens (1998). "Vacuole biogenesis in *Saccharomyces cerevisiae*: protein transport pathways to the yeast vacuole." Microbiology and Molecular Biology Reviews **62**(1): 230-47.
- Bucci, C., R. G. Parton, et al. (1992). "The small GTPase rab5 functions as a regulatory factor in the early endocytic pathway." Cell **70**(5): 715-28.
- Buchberger, A. (2002). "From UBA to UBX: new words in the ubiquitin vocabulary." Trends Cell Biol **12**(5): 216-21.
- Burd, C. G., P. A. Mustol, et al. (1996). "A yeast protein related to a mammalian Ras-binding protein, Vps9p, is required for localization of vacuolar proteins." Mol Cell Biol **16**(5): 2369-77.
- Burd, C. G., M. Peterson, et al. (1997). "A novel Sec18p/NSF-dependent complex required for Golgi-to-endosome transport in yeast." Mol Biol Cell **8**(6): 1089-104.
- Burda, P., S. M. Padilla, et al. (2002). "Retromer function in endosome-to-Golgi retrograde transport is regulated by the yeast Vps34 PtdIns 3-kinase." J Cell Sci **115**(Pt 20): 3889-900.
- Cereghino, J. L., E. G. Marcusson, et al. (1995). "The cytoplasmic tail domain of the vacuolar protein sorting receptor Vps10p and a subset of VPS gene products regulate receptor stability, function, and localization." Molecular Biology of the Cell **6**(9): 1089-102.
- Chant, J., K. Corrado, et al. (1991). "Yeast BUD5, encoding a putative GDP-GTP exchange factor, is necessary for bud site selection and interacts with bud formation gene BEM1." Cell **65**(7): 1213-24.
- Cheever, M. L., T. K. Sato, et al. (2001). "Phox domain interaction with PtdIns(3)P targets the Vam7 t-SNARE to vacuole membranes." Nature Cell Biology **3**(7): 613-8.
- Chen, Y. A. and R. H. Scheller (2001). "SNARE-mediated membrane fusion." Nat Rev Mol Cell Biol **2**(2): 98-106.

- Chen, Y. J. and T. H. Stevens (1996). "The VPS8 gene is required for localization and trafficking of the CPY sorting receptor in *Saccharomyces cerevisiae*." Eur J Cell Biol **70**(4): 289-97.
- Christianson, T. W., R. S. Sikorski, et al. (1992). "Multifunctional yeast high-copy-number shuttle vectors." Gene **110**(1): 119-22.
- Conibear, E., J. N. Cleck, et al. (2003). "Vps51p Mediates the Association of the GARP (Vps52/53/54) Complex with the Late Golgi t-SNARE Tlg1p." Mol Biol Cell **14**(4): 1610-23.
- Cooper, A. A. and T. H. Stevens (1996). "Vps10p cycles between the late-Golgi and prevacuolar compartments in its function as the sorting receptor for multiple yeast vacuolar hydrolases." Journal of Cell Biology **133**(3): 529-41.
- Cowles, C. R., S. D. Emr, et al. (1994). "Mutations in the VPS45 gene, a SEC1 homologue, result in vacuolar protein sorting defects and accumulation of membrane vesicles." Journal of Cell Science **107** (Pt 12): 3449-59.
- Cowles, C. R., G. Odorizzi, et al. (1997). "The AP-3 adaptor complex is essential for cargo-selective transport to the yeast vacuole." Cell **91**(1): 109-18.
- Cowles, C. R., W. B. Snyder, et al. (1997). "Novel Golgi to vacuole delivery pathway in yeast: identification of a sorting determinant and required transport component." Embo J **16**(10): 2769-82.
- Davies, B. A., J. D. Topp, et al. (2003). "Vps9p CUE Domain Ubiquitin Binding Is Required for Efficient Endocytic Protein Traffic." J Biol Chem **278**(22): 19826-33.
- Davis, N. G., J. L. Horecka, et al. (1993). "Cis- and trans-acting functions required for endocytosis of the yeast pheromone receptors." J Cell Biol **122**(1): 53-65.
- Deloche, O. and R. W. Schekman (2002). "Vps10p Cycles between the TGN and the Late Endosome via the Plasma Membrane in Clathrin Mutants." Mol Biol Cell **13**(12): 4296-307.
- Deloche, O., B. G. Yeung, et al. (2001). "Vps10p transport from the trans-Golgi network to the endosome is mediated by clathrin-coated vesicles." Molecular Biology of the Cell **12**(2): 475-85.

- Dieckmann, C. L. and A. Tzagoloff (1985). "Assembly of the mitochondrial membrane system. CBP6, a yeast nuclear gene necessary for synthesis of cytochrome b." J Biol Chem **260**(3): 1513-20.
- Dieckmann, T., E. S. Withers-Ward, et al. (1998). "Structure of a human DNA repair protein UBA domain that interacts with HIV-1 Vpr." Nat Struct Biol **5**(12): 1042-7.
- Donaldson, K. M., H. Yin, et al. (2003). "Ubiquitin Signals Protein Trafficking via Interaction with a Novel Ubiquitin Binding Domain in the Membrane Fusion Regulator, Vps9p." Curr Biol **13**(3): 258-62.
- Doray, B., K. Bruns, et al. (2002). "Interaction of the cation-dependent mannose 6-phosphate receptor with GGA proteins." J Biol Chem **277**(21): 18477-82.
- Doray, B., P. Ghosh, et al. (2002). "Cooperation of GGAs and AP-1 in packaging MPRs at the trans-Golgi network." Science **297**(5587): 1700-3.
- Du, L. L., R. N. Collins, et al. (1998). "Identification of a Sec4p GTPase-activating protein (GAP) as a novel member of a Rab GAP family." J Biol Chem **273**(6): 3253-6.
- Dunn, R. and L. Hicke (2001). "Multiple roles for Rsp5p-dependent ubiquitination at the internalization step of endocytosis." J Biol Chem **276**(28): 25974-81.
- Ekena, K. and T. H. Stevens (1995). "The *Saccharomyces cerevisiae* MVP1 gene interacts with VPS1 and is required for vacuolar protein sorting." Molecular and Cellular Biology **15**(3): 1671-8.
- Ekena, K., C. A. Vater, et al. (1993). "The VPS1 protein is a dynamin-like GTPase required for sorting proteins to the yeast vacuole." Ciba Foundation Symposium **176**: 198-211; discussion 211-4.
- Ellson, C. D., S. Andrews, et al. (2002). "The PX domain: a new phosphoinositide-binding module." Journal of Cell Science **115**(Pt 6): 1099-105.
- Ellson, C. D., S. Gobert-Gosse, et al. (2001). "PtdIns(3)P regulates the neutrophil oxidase complex by binding to the PX domain of p40phox." Nature Cell Biology **3**(7): 679-82.

- Esters, H., K. Alexandrov, et al. (2001). "Vps9, Rabex-5 and DSS4: proteins with weak but distinct nucleotide-exchange activities for Rab proteins." J Mol Biol **310**(1): 141-56.
- Eymard-Pierre, E., G. Lesca, et al. (2002). "Infantile-onset ascending hereditary spastic paralysis is associated with mutations in the alsin gene." Am J Hum Genet **71**(3): 518-27.
- Fisk, H. A. and M. P. Yaffe (1997). "Mutational analysis of Mdm1p function in nuclear and mitochondrial inheritance." J Cell Biol **138**(3): 485-94.
- Fisk, H. A. and M. P. Yaffe (1999). "A role for ubiquitination in mitochondrial inheritance in *Saccharomyces cerevisiae*." J Cell Biol **145**(6): 1199-208.
- Gerhardt, B., T. J. Kordas, et al. (1998). "The vesicle transport protein Vps33p is an ATP-binding protein that localizes to the cytosol in an energy-dependent manner." Journal of Biological Chemistry **273**(25): 15818-29.
- Gerrard, S. R., N. J. Bryant, et al. (2000). "VPS21 controls entry of endocytosed and biosynthetic proteins into the yeast prevacuolar compartment." Mol Biol Cell **11**(2): 613-26.
- Ghosh, P., N. M. Dahms, et al. (2003). "Mannose 6-phosphate receptors: new twists in the tale." Nat Rev Mol Cell Biol **4**(3): 202-12.
- Gorvel, J. P., P. Chavrier, et al. (1991). "rab5 controls early endosome fusion in vitro." Cell **64**(5): 915-25.
- Graham, T. R. and S. D. Emr (1991). "Compartmental organization of Golgi-specific protein modification and vacuolar protein sorting events defined in a yeast sec18 (NSF) mutant." The Journal of Cell Biology **114**(2): 207-18.
- Gravel, R. A., K. M.K., et al. (2001). The G_{M2} gangliosidoses. The Metabolic and Molecular Basis of Inherited Disease. C. R. Scriver, A. L. Beaudet, W. S. Sly and D. Valle. New York, McGraw-Hill Medical Publishing Division. **3**: 3827-76.
- Guex, N. and M. C. Peitsch (1997). "SWISS-MODEL and the Swiss-PdbViewer: an environment for comparative protein modeling." Electrophoresis **18**(15): 2714-23.
- Guthrie, C. and G. R. Fink (1991). Guide to Yeast Genetics and Molecular Biology. New York, NY, Academic Press.

- Hadano, S., C. K. Hand, et al. (2001). "A gene encoding a putative GTPase regulator is mutated in familial amyotrophic lateral sclerosis 2." Nat Genet **29**(2): 166-73.
- Haft, C. R., M. de la Luz Sierra, et al. (2000). "Human orthologs of yeast vacuolar protein sorting proteins Vps26, 29, and 35: assembly into multimeric complexes." Mol Biol Cell **11**(12): 4105-16.
- Haft, C. R., M. de la Luz Sierra, et al. (2000). "Human orthologs of yeast vacuolar protein sorting proteins Vps26, 29, and 35: assembly into multimeric complexes." Molecular Biology of the Cell **11**(12): 4105-16.
- Haft, C. R., M. de la Luz Sierra, et al. (1998). "Identification of a family of sorting nexin molecules and characterization of their association with receptors." Molecular and Cellular Biology **18**(12): 7278-87.
- Hama, H., G. G. Tall, et al. (1999). "Vps9p is a guanine nucleotide exchange factor involved in vesicle-mediated vacuolar protein transport." Journal of Biological Chemistry **274**(21): 15284-91.
- Hanahan, D. (1983). "Studies on transformation of Escherichia coli with plasmids." J Mol Biol **166**(4): 557-80.
- Herman, P. K. and S. D. Emr (1990). "Characterization of VPS34, a gene required for vacuolar protein sorting and vacuole segregation in Saccharomyces cerevisiae." Molecular and Cellular Biology **10**(12): 6742-54.
- Herman, P. K., J. H. Stack, et al. (1991). "A novel protein kinase homolog essential for protein sorting to the yeast lysosome-like vacuole." Cell **64**(2): 425-37.
- Herman, P. K., J. H. Stack, et al. (1991). "A genetic and structural analysis of the yeast Vps15 protein kinase: evidence for a direct role of Vps15p in vacuolar protein delivery." Embo Journal **10**(13): 4049-60.
- Hettema, E. H., M. J. Lewis, et al. (2003). "Retromer and the sorting nexins Snx4/41/42 mediate distinct retrieval pathways from yeast endosomes." Embo J **22**(3): 548-57.
- Hicke, L. (1999). "Gettin' down with ubiquitin: turning off cell-surface receptors, transporters and channels." Trends Cell Biol **9**(3): 107-12.
- Hicke, L. (2001). "Protein regulation by monoubiquitin." Nat Rev Mol Cell Biol **2**(3): 195-201.

- Hiroaki, H., T. Ago, et al. (2001). "Solution structure of the PX domain, a target of the SH3 domain." Nature Structural Biology **8**(6): 526-30.
- Hirst, J., W. W. Lui, et al. (2000). "A family of proteins with gamma-adaptin and VHS domains that facilitate trafficking between the trans-Golgi network and the vacuole/lysosome." J Cell Biol **149**(1): 67-80.
- Hofmann, K. and P. Bucher (1996). "The UBA domain: a sequence motif present in multiple enzyme classes of the ubiquitination pathway." Trends Biochem Sci **21**(5): 172-3.
- Hofmann, K. and L. Falquet (2001). "A ubiquitin-interacting motif conserved in components of the proteasomal and lysosomal protein degradation systems." Trends Biochem Sci **26**(6): 347-50.
- Horazdovsky, B. F., G. R. Busch, et al. (1994). "VPS21 encodes a rab5-like GTP binding protein that is required for the sorting of yeast vacuolar proteins." Embo Journal **13**(6): 1297-309.
- Horazdovsky, B. F., C. R. Cowles, et al. (1996). "A novel RING finger protein, Vps8p, functionally interacts with the small GTPase, Vps21p, to facilitate soluble vacuolar protein localization." Journal of Biological Chemistry **271**(52): 33607-15.
- Horazdovsky, B. F., B. A. Davies, et al. (1997). "A sorting nexin-1 homologue, Vps5p, forms a complex with Vps17p and is required for recycling the vacuolar protein-sorting receptor." Molecular Biology of the Cell **8**(8): 1529-41.
- Horazdovsky, B. F., D. B. DeWald, et al. (1995). "Protein transport to the yeast vacuole." Current Opinion in Cell Biology **7**(4): 544-51.
- Horazdovsky, B. F. and S. D. Emr (1993). "The VPS16 gene product associates with a sedimentable protein complex and is essential for vacuolar protein sorting in yeast." The Journal of Biological Chemistry **268**(7): 4953-62.
- Horiuchi, H., R. Lippe, et al. (1997). "A novel Rab5 GDP/GTP exchange factor complexed to Rabaptin-5 links nucleotide exchange to effector recruitment and function." Cell **90**(6): 1149-59.

- Huibregtse, J. M., J. C. Yang, et al. (1997). "The large subunit of RNA polymerase II is a substrate of the Rsp5 ubiquitin-protein ligase." Proc Natl Acad Sci U S A **94**(8): 3656-61.
- Ito, H., Y. Fukuda, et al. (1983). "Transformation of intact yeast cells treated with alkali cations." Journal of Bacteriology **153**(1): 163-8.
- Joazeiro, C. A. and A. M. Weissman (2000). "RING finger proteins: mediators of ubiquitin ligase activity." Cell **102**(5): 549-52.
- Johnson, L. M., V. A. Bankaitis, et al. (1987). "Distinct sequence determinants direct intracellular sorting and modification of a yeast vacuolar protease." Cell **48**(5): 875-85.
- Jones, E. W. (1977). "Proteinase mutants of *saccharomyces cerevisiae*." Genetics **85**: 23-33.
- Jones, E. W. (1984). "The synthesis and function of proteases in *Saccharomyces*: genetic approaches." Annual Review of Genetics **18**: 233-70.
- Jones, T. A., J. Y. Zou, et al. (1991). "Improved methods for building protein models in electron density maps and the location of errors in these models." Acta Crystallogr A **47** (Pt 2): 110-9.
- Jorgensen, M. U., S. D. Emr, et al. (1999). "Ligand recognition and domain structure of Vps10p, a vacuolar protein sorting receptor in *Saccharomyces cerevisiae*." European Journal of Biochemistry **260**(2): 461-9.
- Jullien-Flores, V., O. Dorseuil, et al. (1995). "Bridging Ral GTPase to Rho pathways. RLIP76, a Ral effector with CDC42/Rac GTPase-activating protein activity." J Biol Chem **270**(38): 22473-7.
- Kaminska, J., B. Gajewska, et al. (2002). "Rsp5p, a New Link between the Actin Cytoskeleton and Endocytosis in the Yeast *Saccharomyces cerevisiae*." Mol Cell Biol **22**(20): 6946-8.
- Kanai, F., H. Liu, et al. (2001). "The PX domains of p47phox and p40phox bind to lipid products of PI(3)K." Nature Cell Biology **3**(7): 675-8.
- Kang, R. S., C. M. Daniels, et al. (2003). "Solution Structure of a CUE-Ubiquitin complex reveals a conserved mode of ubiquitin binding." Cell **113**: 621-30.

- Katzmann, D. J., M. Babst, et al. (2001). "Ubiquitin-dependent sorting into the multivesicular body pathway requires the function of a conserved endosomal protein sorting complex, ESCRT-I." Cell **106**(2): 145-55.
- Katzmann, D. J., G. Odorizzi, et al. (2002). "Receptor downregulation and multivesicular-body sorting." Nat Rev Mol Cell Biol **3**(12): 893-905.
- Kihara, A., T. Noda, et al. (2001). "Two distinct Vps34 phosphatidylinositol 3-kinase complexes function in autophagy and carboxypeptidase Y sorting in *Saccharomyces cerevisiae*." Journal of Cell Biology **152**(3): 519-30.
- Kim, J. and D. J. Klionsky (2000). "Autophagy, cytoplasm-to-vacuole targeting pathway, and pexophagy in yeast and mammalian cells." Annu Rev Biochem **69**: 303-42.
- Kleid, D. G., D. Yansura, et al. (1981). "Cloned viral protein vaccine for foot-and-mouth disease: responses in cattle and swine." Science **214**(4525): 1125-9.
- Klionsky, D. J., L. M. Banta, et al. (1988). "Intracellular sorting and processing of a yeast vacuolar hydrolase: proteinase A propeptide contains vacuolar targeting information." Molecular and Cellular Biology **8**(5): 2105-16.
- Klionsky, D. J. and S. D. Emr (1989). "Membrane protein sorting: biosynthesis, transport and processing of yeast vacuolar alkaline phosphatase." The Embo Journal **8**(8): 2241-50.
- Klionsky, D. J., P. K. Herman, et al. (1990). "The fungal vacuole: composition, function, and biogenesis." Microbiological Reviews **54**(3): 266-92.
- Kohrer, K. and S. D. Emr (1993). "The yeast VPS17 gene encodes a membrane-associated protein required for the sorting of soluble vacuolar hydrolases." Journal of Biological Chemistry **268**(1): 559-69.
- Kornfeld, S. (1992). "Structure and function of the mannose 6-phosphate/insulinlike growth factor II receptors." Annu Rev Biochem **61**: 307-30.
- Kornfeld, S. and I. Mellman (1989). "The biogenesis of lysosomes." Annu Rev Cell Biol **5**: 483-525.
- Kornfeld, S. and W. S. Sly (2001). I-cell disease and psuedo-Hurler polydystrophy: disorders of lysosomal enzyme phosphorylation and localization. The Metabolic and Molecular Basis of Inherited Disease. C. R. Scriver, A. L. Beaudet, W. S. Sly and D. Valle. New York, McGraw-Hill Medical Publishing Division. **3**: 3469-82.

- Kurten, R. C., D. L. Cadena, et al. (1996). "Enhanced degradation of EGF receptors by a sorting nexin, SNX1." Science **272**(5264): 1008-10.
- Lee, J. J., G. Radice, et al. (1992). "Identification and characterization of a novel, evolutionarily conserved gene disrupted by the murine H beta 58 embryonic lethal transgene insertion." Development **115**(1): 277-88.
- Lemmon, S. K. and L. M. Traub (2000). "Sorting in the endosomal system in yeast and animal cells." Current Opinion in Cell Biology **12**(4): 457-66.
- Letunic, I., L. Goodstadt, et al. (2002). "Recent improvements to the SMART domain-based sequence annotation resource." Nucleic Acids Research (Online) **30**(1): 242-4.
- Lin, Q., C. G. Lo, et al. (2002). "The Cdc42 target ACK2 interacts with sorting nexin 9 (SH3PX1) to regulate epidermal growth factor receptor degradation." The Journal of Biological Chemistry **277**(12): 10134-8.
- Luo, Z. and D. Gallwitz (2003). "Biochemical and genetic evidence for the involvement of yeast Ypt6-GTPase in protein retrieval to different Golgi compartments." J Biol Chem **278**(2): 791-9.
- Lupas, A., M. Van Dyke, et al. (1991). "Predicting coiled coils from protein sequences." Science **252**(5010): 1162-4.
- Marcusson, E. G., B. F. Horazdovsky, et al. (1994). "The sorting receptor for yeast vacuolar carboxypeptidase Y is encoded by the VPS10 gene." Cell **77**(4): 579-86.
- McConnell, S. J., L. C. Stewart, et al. (1990). "Temperature-sensitive yeast mutants defective in mitochondrial inheritance." J Cell Biol **111**(3): 967-76.
- Miller, E. A., M. C. Lee, et al. (1999). "Identification and characterization of a prevacuolar compartment in stigmas of *nicotiana glauca*." Plant Cell **11**(8): 1499-508.
- Miller, J. (1972). Experiments in molecular genetics. Cold Spring Harbor, NY, Cold Spring Harbor Laboratory.
- Misra, S., G. J. Miller, et al. (2001). "Recognizing phosphatidylinositol 3-phosphate." Cell **107**(5): 559-62.

- Mueller, T. D. and J. Feigon (2002). "Solution structures of UBA domains reveal a conserved hydrophobic surface for protein-protein interactions." J Mol Biol **319**(5): 1243-55.
- Mumberg, D., R. Muller, et al. (1995). "Yeast vectors for the controlled expression of heterologous proteins in different genetic backgrounds." Gene **156**(1): 119-22.
- Nagase, T., R. Kikuno, et al. (2000). "Prediction of the coding sequences of unidentified human genes. XVIII. The complete sequence of 100 new cDNA clones from brain which code for large proteins in vitro." DNA Res **7**: 271-81.
- Nakamura, N., G. H. Sun-Wada, et al. (2001). "Association of mouse sorting nexin 1 with early endosomes." J Biochem (Tokyo) **130**(6): 765-71.
- Nakamura, N., G. H. Sun_Wada, et al. (2001). "Association of mouse sorting nexin 1 with early endosomes." **130**(6): 765-71.
- Nass, R. and R. Rao (1998). "Novel localization of a Na⁺/H⁺ exchanger in a late endosomal compartment of yeast. Implications for vacuole biogenesis." J Biol Chem **273**(33): 21054-60.
- Nice, D. C., T. K. Sato, et al. (2002). "Cooperative binding of the cytoplasm to vacuole targeting pathway proteins, Cvt13 and Cvt20, to phosphatidylinositol 3-phosphate at the pre-autophagosomal structure is required for selective autophagy." J Biol Chem **277**(33): 30198-207.
- Nothwehr, S. F., P. Bruinsma, et al. (1999). "Distinct domains within Vps35p mediate the retrieval of two different cargo proteins from the yeast prevacuolar/endosomal compartment." Molecular Biology of the Cell **10**(4): 875-90.
- Nothwehr, S. F., N. J. Bryant, et al. (1996). "The newly identified yeast GRD genes are required for retention of late-Golgi membrane proteins." Molecular and Cellular Biology **16**(6): 2700-7.
- Nothwehr, S. F., E. Conibear, et al. (1995). "Golgi and vacuolar membrane proteins reach the vacuole in vps1 mutant yeast cells via the plasma membrane." Journal of Cell Biology **129**(1): 35-46.
- Nothwehr, S. F., S. A. Ha, et al. (2000). "Sorting of yeast membrane proteins into an endosome-to-Golgi pathway involves direct interaction of their cytosolic domains with Vps35p." Journal of Cell Biology **151**(2): 297-310.

- Nothwehr, S. F. and A. E. Hindes (1997). "The yeast VPS5/GRD2 gene encodes a sorting nexin-1-like protein required for localizing membrane proteins to the late Golgi." Journal of Cell Science **110** (Pt 9): 1063-72.
- Odorizzi, G., M. Babst, et al. (1998). "Fab1p PtdIns(3)P 5-kinase function essential for protein sorting in the multivesicular body." Cell **95**(6): 847-58.
- Otsuki, T., S. Kajigaya, et al. (1999). "SNX5, a new member of the sorting nexin family, binds to the Fanconi anemia complementation group A protein." Biochemical and Biophysical Research Communications **265**(3): 630-5.
- Otwinowski, Z. and W. Minor (1997). "Processing of X-ray diffraction data collected in oscillation mode." Methods in Enzymology **276**: 307-326.
- Paravicini, G., B. F. Horazdovsky, et al. (1992). "Alternative pathways for the sorting of soluble vacuolar proteins in yeast: a vps35 null mutant missorts and secretes only a subset of vacuolar hydrolases." Molecular Biology of the Cell **3**(4): 415-27.
- Parks, W. T., D. B. Frank, et al. (2001). "Sorting nexin 6, a novel SNX, interacts with the transforming growth factor-beta family of receptor serine-threonine kinases." Journal of Biological Chemistry **276**(22): 19332-9.
- Patterson, M. C., M. T. Vanier, et al. (2001). Niemann-Pick Disease Type C: A Lipid Trafficking Disorder,. The Metabolic and Molecular Basis of Inherited Disease. C. R. Scriver, A. L. Beaudet, W. S. Sly and D. Valle. New York, McGraw-Hill Medical Publishing Division. **3**: 3611-33.
- Peterson, M. R., C. G. Burd, et al. (1999). "Vac1p coordinates Rab and phosphatidylinositol 3-kinase signaling in Vps45p-dependent vesicle docking/fusion at the endosome." Current Biology **9**(3): 159-62.
- Pfeffer, S. R. (1999). "Transport-vesicle targeting: tethers before SNAREs." Nat Cell Biol **1**(1): e17-22.
- Pfeffer, S. R. (2001). "Membrane transport: retromer to the rescue." Current Biology **11**: R109-111.
- Phillips, S. A., V. A. Barr, et al. (2001). "Identification and characterization of SNX15, a novel sorting nexin involved in protein trafficking." Journal of Biological Chemistry **276**(7): 5074-84.

- Piper, R. C., E. A. Whitters, et al. (1994). "Yeast Vps45p is a Sec1p-like protein required for the consumption of vacuole-targeted, post-Golgi transport vesicles." European Journal of Cell Biology **65**(2): 305-18.
- Ponting, C. P. (1996). "Novel domains in NADPH oxidase subunits, sorting nexins, and PtdIns 3-kinases: binding partners of SH3 domains?" Protein Science **5**(11): 2353-7.
- Ponting, C. P. (2000). "Proteins of the endoplasmic-reticulum-associated degradation pathway: domain detection and function prediction." Biochem J **351 Pt 2**: 527-35.
- Pornillos, O., S. L. Alam, et al. (2002). "Structure and functional interactions of the Tsg101 UEV domain." Embo J **21**(10): 2397-406.
- Prehoda, K. E. and W. A. Lim (2001). "The double life of PX domains." Nature Structural Biology **8**(7): 570-2.
- Radice, G., J. J. Lee, et al. (1991). "H beta 58, an insertional mutation affecting early postimplantation development of the mouse embryo." Development **111**(3): 801-11.
- Raymond, C. K., I. Howald-Stevenson, et al. (1992). "Morphological classification of the yeast vacuolar protein sorting mutants: evidence for a prevacuolar compartment in class E vps mutants." Mol Biol Cell **3**(12): 1389-402.
- Raymond, C. K., P. J. O'Hara, et al. (1990). "Molecular analysis of the yeast VPS3 gene and the role of its product in vacuolar protein sorting and vacuolar segregation during the cell cycle." J Cell Biol **111**(3): 877-92.
- Reddy, J. V. and M. N. Seaman (2001). "Vps26p, a component of retromer, directs the interactions of Vps35p in endosome-to-Golgi retrieval." Molecular Biology of the Cell **12**(10): 3242-56.
- Reggiori, F., C. W. Wang, et al. (2003). "Vps51 is part of the yeast Vps fifty-three tethering complex essential for retrograde traffic from the early endosome and Cvt vesicle completion." J Biol Chem **278**(7): 5009-20.
- Rieder, S. E. and S. D. Emr (1997). "A novel RING finger protein complex essential for a late step in protein transport to the yeast vacuole." Mol Biol Cell **8**(11): 2307-27.

- Roberts, C. J., C. K. Raymond, et al. (1991). Methods for Studying the Yeast Vacuole. Guide to Yeast Genetics and Molecular Biology. C. Guthrie and G. R. Fink. New York, Academic Press. **194**: 644-61.
- Robinson, J. S., D. J. Klionsky, et al. (1988). "Protein sorting in *Saccharomyces cerevisiae*: isolation of mutants defective in the delivery and processing of multiple vacuolar hydrolases." Molecular and Cellular Biology **8**(11): 4936-48.
- Roth, A. F. and N. G. Davis (1996). "Ubiquitination of the yeast α -factor receptor." J Cell Biol **134**(3): 661-74.
- Rothman, J. H., I. Howald, et al. (1989). "Characterization of genes required for protein sorting and vacuolar function in the yeast *Saccharomyces cerevisiae*." Embo J **8**(7): 2057-65.
- Rothman, J. H. and T. H. Stevens (1986). "Protein sorting in yeast: mutants defective in vacuole biogenesis mislocalize vacuolar proteins into the late secretory pathway." Cell **47**(6): 1041-51.
- Rotin, D., O. Staub, et al. (2000). "Ubiquitination and endocytosis of plasma membrane proteins: role of Nedd4/Rsp5p family of ubiquitin-protein ligases." J Membr Biol **176**(1): 1-17.
- Saito, K., J. Murai, et al. (2002). "A novel binding protein composed of homophilic tetramer exhibits unique properties for the small GTPase Rab5." J Biol Chem **277**(5): 3412-8.
- Sambrook, J., E. F. Fritsch, et al. (1989). Molecular Cloning: A Laboratory Manual. Cold Spring Harbor, NY, Cold Spring Harbor Laboratory Press.
- Sato, T. K., T. Darsow, et al. (1998). "Vam7p, a SNAP-25-like molecule, and Vam3p, a syntaxin homolog, function together in yeast vacuolar protein trafficking." Molecular and Cellular Biology **18**(9): 5308-19.
- Sato, T. K., M. Overduin, et al. (2001). "Location, location, location: membrane targeting directed by PX domains." Science **294**(5548): 1881-5.
- Scheffzek, K., M. R. Ahmadian, et al. (1998). "GTPase-activating proteins: helping hands to complement an active site." Trends Biochem Sci **23**(7): 257-62.
- Schu, P. V., K. Takegawa, et al. (1993). "Phosphatidylinositol 3-kinase encoded by yeast VPS34 gene essential for protein sorting." Science **260**(5104): 88-91.

- Schultz, J., R. R. Copley, et al. (2000). "SMART: a web-based tool for the study of genetically mobile domains." Nucleic Acids Research (Online) **28**(1): 231-4.
- Schwarz, D. G., C. T. Griffin, et al. (2002). "Genetic analysis of sorting nexins 1 and 2 reveals a redundant and essential function in mice." Mol Biol Cell **13**(10): 3588-600.
- Seals, D. F., G. Eitzen, et al. (2000). "A Ypt/Rab effector complex containing the Sec1 homolog Vps33p is required for homotypic vacuole fusion." Proc Natl Acad Sci U S A **97**(17): 9402-7.
- Seaman, M. N., E. G. Marcusson, et al. (1997). "Endosome to Golgi retrieval of the vacuolar protein sorting receptor, Vps10p, requires the function of the VPS29, VPS30, and VPS35 gene products." Journal of Cell Biology **137**(1): 79-92.
- Seaman, M. N., J. M. McCaffery, et al. (1998). "A membrane coat complex essential for endosome-to-Golgi retrograde transport in yeast." Journal of Cell Biology **142**(3): 665-81.
- Seaman, M. N. and H. P. Williams (2002). "Identification of the functional domains of yeast sorting nexins Vps5p and Vps17p." Mol Biol Cell **13**(8): 2826-40.
- Seeger, M. and G. S. Payne (1992). "A role for clathrin in the sorting of vacuolar proteins in the Golgi complex of yeast." Embo J **11**(8): 2811-8.
- Segev, N. (2001). "Ypt/rab gtpases: regulators of protein trafficking." Sci STKE **2001**(100): RE11.
- Serafini, T., G. Stenbeck, et al. (1991). "A coat subunit of Golgi-derived non-clathrin-coated vesicles with homology to the clathrin-coated vesicle coat protein beta-adaptin." Nature **349**(6306): 215-20.
- Sheffield, P., S. Garrard, et al. (1999). "Overcoming expression and purification problems of RhoGDI using a family of "parallel" expression vectors." Protein Expr Purif **15**(1): 34-9.
- Sherman, F., G. R. Fink, et al. (1979). Methods in yeast genetics: a laboratory manual. Cold Spring Harbor, NY, Cold Spring Harbor Laboratory.
- Shih, S. C., D. J. Katzmann, et al. (2002). "Epsins and Vps27p/Hrs contain ubiquitin-binding domains that function in receptor endocytosis." Nat Cell Biol **4**(5): 389-93.

- Shih, S. C., G. Prag, et al. (2003). "A ubiquitin-binding motif required for intramolecular monoubiquitylation, the CUE domain." Embo J **22**(6): 1273-81.
- Shih, S. C., K. E. Sloper-Mould, et al. (2000). "Monoubiquitin carries a novel internalization signal that is appended to activated receptors." Embo J **19**(2): 187-98.
- Sikorski, R. S. and P. Hieter (1989). "A system of shuttle vectors and yeast host strains designed for efficient manipulation of DNA in *Saccharomyces cerevisiae*." Genetics **122**(1): 19-27.
- Siniossoglou, S., S. Y. Peak-Chew, et al. (2000). "Ric1p and Rgp1p form a complex that catalyses nucleotide exchange on Ypt6p." Embo J **19**(18): 4885-94.
- Siniossoglou, S. and H. R. Pelham (2001). "An effector of Ypt6p binds the SNARE Tlg1p and mediates selective fusion of vesicles with late Golgi membranes." Embo J **20**(21): 5991-8.
- Smith, B. J. and M. P. Yaffe (1991). "A mutation in the yeast heat-shock factor gene causes temperature-sensitive defects in both mitochondrial protein import and the cell cycle." Mol Cell Biol **11**(5): 2647-55.
- Stack, J. H., P. K. Herman, et al. (1993). "A membrane-associated complex containing the Vps15 protein kinase and the Vps34 PI 3-kinase is essential for protein sorting to the yeast lysosome-like vacuole." Embo Journal **12**(5): 2195-204.
- Stepp, J. D., K. Huang, et al. (1997). "The yeast adaptor protein complex, AP-3, is essential for the efficient delivery of alkaline phosphatase by the alternate pathway to the vacuole." J Cell Biol **139**(7): 1761-74.
- Stevens, T., B. Esmon, et al. (1982). "Early stages in the yeast secretory pathway are required for transport of carboxypeptidase Y to the vacuole." Cell **30**(2): 439-48.
- Tall, G. G., M. A. Barbieri, et al. (2001). "Ras-activated endocytosis is mediated by the Rab5 guanine nucleotide exchange activity of RIN1." **1**(1): 73-82.
- Tall, G. G., H. Hama, et al. (1999). "The Phosphatidylinositol 3-Phosphate Binding Protein Vac1p Interacts with a Rab GTPase and a Sec1p Homologue to Facilitate Vesicle-mediated Vacuolar Protein Sorting." Molecular Biology of the Cell **10**: 1873-89.

- Terwilliger, T. C. (2000). "Maximum-likelihood density modification." Acta Crystallogr D Biol Crystallogr **56** (Pt 8): 965-72.
- Terwilliger, T. C. and J. Berendzen (1999). "Automated MAD and MIR structure solution." Acta Crystallogr D Biol Crystallogr **55** (Pt 4): 849-61.
- Valls, L. A., C. P. Hunter, et al. (1987). "Protein sorting in yeast: the localization determinant of yeast vacuolar carboxypeptidase Y resides in the propeptide." Cell **48**(5): 887-97.
- Valls, L. A., J. R. Winther, et al. (1990). "Yeast carboxypeptidase Y vacuolar targeting signal is defined by four propeptide amino acids." J Cell Biol **111**(2): 361-8.
- van der Bliek, A. M. and E. M. Meyerowitz (1991). "Dynamin-like protein encoded by the *Drosophila shibire* gene associated with vesicular traffic." Nature **351**(6325): 411-4.
- Vater, C. A., C. K. Raymond, et al. (1992). "The VPS1 protein, a homolog of dynamin required for vacuolar protein sorting in *Saccharomyces cerevisiae*, is a GTPase with two functionally separable domains." Journal of Cell Biology **119**(4): 773-86.
- Vida, T. A. and S. D. Emr (1995). "A new vital stain for visualizing vacuolar membrane dynamics and endocytosis in yeast." J Cell Biol **128**(5): 779-92.
- Vida, T. A., T. R. Graham, et al. (1990). "In vitro reconstitution of intercompartmental protein transport to the yeast vacuole." J Cell Biol **111**(6 Pt 2): 2871-84.
- Vida, T. A., G. Huyer, et al. (1993). "Yeast vacuolar proenzymes are sorted in the late Golgi complex and transported to the vacuole via a prevacuolar endosome-like compartment." The Journal of Cell Biology **121**(6): 1245-56.
- Vijay-Kumar, S., C. E. Bugg, et al. (1987). "Structure of ubiquitin refined at 1.8 Å resolution." J Mol Biol **194**(3): 531-44.
- Vogelstein, B. and D. Gillespie (1979). "Preparative and analytical purification of DNA from agarose." Proc Natl Acad Sci U S A **76**(2): 615-9.
- Vojtek, A. B., S. M. Hollenberg, et al. (1993). "Mammalian Ras interacts directly with the serine/threonine kinase Raf." Cell **74**(1): 205-14.

- von Mollard, G. F., S. F. Nothwehr, et al. (1997). "The yeast v-SNARE Vti1p mediates two vesicle transport pathways through interactions with the t-SNAREs Sed5p and Pep12p." J Cell Biol **137**(7): 1511-24.
- Voos, W. and T. H. Stevens (1998). "Retrieval of resident late-Golgi membrane proteins from the prevacuolar compartment of *Saccharomyces cerevisiae* is dependent on the function of Grd19p." Journal of Cell Biology **140**(3): 577-90.
- Wada, Y. and Y. Anraku (1992). "Genes for directing vacuolar morphogenesis in *Saccharomyces cerevisiae*. II. VAM7, a gene for regulating morphogenic assembly of the vacuoles." J Biol Chem **267**(26): 18671-5.
- Waksman, M., Y. Eli, et al. (1996). "Identification and characterization of a gene encoding phospholipase D activity in yeast." J Biol Chem **271**(5): 2361-4.
- Wang, G., J. M. McCaffery, et al. (2001). "Localization of the Rsp5p ubiquitin-protein ligase at multiple sites within the endocytic pathway." Mol Cell Biol **21**(10): 3564-75.
- Weissman, A. M. (2001). "Themes and variations on ubiquitylation." Nat Rev Mol Cell Biol **2**(3): 169-78.
- Wendland, B. (2002). "Epsins: adaptors in endocytosis?" Nat Rev Mol Cell Biol **3**(12): 971-7.
- Wendland, B., S. D. Emr, et al. (1998). "Protein traffic in the yeast endocytic and vacuolar protein sorting pathways." Current Opinion in Cell Biology **10**(4): 513-22.
- Wichmann, H., L. Hengst, et al. (1992). "Endocytosis in yeast: evidence for the involvement of a small GTP-binding protein (Ypt7p)." Cell **71**(7): 1131-42.
- Wickner, W. and A. Haas (2000). "Yeast homotypic vacuole fusion: a window on organelle trafficking mechanisms." Annu Rev Biochem **69**: 247-75.
- Wiemann, S., B. Weil, et al. (2001). "Toward a catalog of human genes and proteins: sequencing and analysis of 500 novel complete protein coding human cDNAs." Genome Res **11**(3): 422-35.
- Winzeler, E. A., D. D. Shoemaker, et al. (1999). "Functional characterization of the *S. cerevisiae* genome by gene deletion and parallel analysis." Science **285**(5429): 901-6.

- Withers-Ward, E. S., T. D. Mueller, et al. (2000). "Biochemical and structural analysis of the interaction between the UBA(2) domain of the DNA repair protein HHR23A and HIV-1 Vpr." Biochemistry **39**(46): 14103-12.
- Worby, C. A. and J. E. Dixon (2002). "Sorting out the cellular functions of sorting nexins." Nat Rev Mol Cell Biol **3**(12): 919-31.
- Wurmser, A. E., T. K. Sato, et al. (2000). "New component of the vacuolar class C-Vps complex couples nucleotide exchange on the Ypt7 GTPase to SNARE-dependent docking and fusion." J Cell Biol **151**(3): 551-62.
- Xu, Y., H. Hortsman, et al. (2001). "SNX3 regulates endosomal function through its PX-domain-mediated interaction with PtdIns(3)P." Nature Cell Biology **3**(7): 658-66.
- Xu, Y., L. F. Seet, et al. (2001). "The Phox homology (PX) domain, a new player in phosphoinositide signalling." The Biochemical Journal **360**(Pt 3): 513-30.
- Yang, Y., A. Hentati, et al. (2001). "The gene encoding alsin, a protein with three guanine-nucleotide exchange factor domains, is mutated in a form of recessive amyotrophic lateral sclerosis." Nat Genet **29**(2): 160-5.
- Yu, J. W. and M. A. Lemmon (2001). "All phox homology (PX) domains from *Saccharomyces cerevisiae* specifically recognize phosphatidylinositol 3-phosphate." The Journal of Biological Chemistry **276**(47): 44179-84.
- Zerial, M. and H. M. McBride (2001). "Rab proteins as membrane organizers." Nat Rev Mol Cell Biol **2**: 107-119.
- Zheng, B., Y. C. Ma, et al. (2001). "RGS-PX1, a GAP for GalphaS and sorting nexin in vesicular trafficking." Science **294**(5548): 1939-42.
- Zheng, Y., A. Bender, et al. (1995). "Interactions among proteins involved in bud-site selection and bud-site assembly in *Saccharomyces cerevisiae*." J Biol Chem **270**(2): 626-30.
- Zheng, Y., R. Cerione, et al. (1994). "Control of the yeast bud-site assembly GTPase Cdc42. Catalysis of guanine nucleotide exchange by Cdc24 and stimulation of GTPase activity by Bem3." J Biol Chem **269**(4): 2369-72.
- Zheng, Y., M. J. Hart, et al. (1993). "Biochemical comparisons of the *Saccharomyces cerevisiae* Bem2 and Bem3 proteins. Delineation of a limit Cdc42 GTPase-activating protein domain." J Biol Chem **268**(33): 24629-34.

Zhu, Y., B. Doray, et al. (2001). "Binding of GGA2 to the lysosomal enzyme sorting motif of the mannose 6-phosphate receptor." Science **292**(5522): 1716-8.

VITAE

Brian Andrew Davies was born in Miami, Florida, on April 29, 1973, the second of three sons of Dr. Peter John Arwyn Davies, M.D., Ph.D. and Dr. Dana Ruth Kessler Davies, Ph.D. After completing his degree at Bellaire High School, Bellaire, Texas in 1991, he enrolled at the Massachusetts Institute of Technology in Cambridge, Massachusetts. During the summer of 1992, he participated in the Baylor College of Medicine SMART program under the guidance of Dr. Craig Chinault, Ph.D. From January, 1993 through December, 1994, he participated in the MIT UROP program under the guidance of Dr. H. Robert Horvitz, Ph.D. He was awarded the Scientifica Bacularia degree in February 1995. From January, 1995 through July, 1995, he worked as a research technician in the Howard Hughes Medical Institute in the laboratory of Dr. H. Robert Horvitz. In August, 1995 he entered the Graduate School of the Biomedical Sciences at the University of Texas Southwestern Medical Center at Dallas and worked under the guidance of Dr. Bruce Horazdovsky, Ph.D. He received the Jonnson Scholarship in August, 1995, the Howard Hughes Predoctoral Fellowship in May, 1996, and a Haberecht-Wildehare Award in June, 1999. He will hopefully be awarded a Doctorate of Philosophy in June, 2003.

Permanent Address: 5503 Cheltenham Drive
Houston, Texas 77096